UNIVERSITÀ DEGLI STUDI DI MILANO
FACOLTÀ DI SCIENZE AGRARIE E ALIMENTARI
Department of Food, Environmental and Nutritional Sciences (DeFENS)

Graduate School in Molecular Sciences and Plant, Food and Environmental Biotechnology

PhD programme in Food Science, Technology and Biotechnology

XXVI cycle

NANOFIBERS: TAILOR-MADE APPLICATIONS FOR THE FOOD AND BEVERAGE INDUSTRY

Scientific field AGR/15

CARLOS ALBERTO FUENMAYOR BOBADILLA

Tutor: Prof. Maria Stella Cosio

Co-tutor: Prof. Alberto Schiraldi

PhD Coordinator: Prof. Maria Grazia Fortina

2014

The thesis is dedicated to all of them who devote their lives to science, those who share their knowledge and wisdom with generosity, in love, and in the sincere hope it will change the world for better.

Contents

CONTENTS

Contents

Contents

Contents

LIST OF FIGURES

Contents

Contents

Contents

LIST OF TABLES

ABSTRACT

The increasing demand for food that are more nutritious, safe, affordable, pleasant and healthy is the driving force of product and process innovation in the food and beverage industry. Nanotechnology offers a way to meet such demands through the design of materials that are able to improve the performance in some of the most relevant operations of this industry (such as filtration, preservation and quality control), as well as some important characteristics of the products (such as stability, flavour, nutritional quality, etc.). Among the nanomaterials developed for practical purposes, electrospun nanofibrous materials, produced from synthetic and bio- polymers have received great attention by virtue of their fabrication simplicity through the electrospinning technique and their special nano-related features that include large surface-to-mass ratio, very high porosity, enhanced mechanical resistance and improved responsive capacity to changes in the surrounding atmosphere compared to conventional configurations of the same polymer or polymer blend.

Nanofibrous materials can combine the advantages of particulate nanomaterials like nanoparticles with the advantages of polymeric laminate materials like films or membranes.

In this thesis, we will demonstrate the potentialities of nanofibers in three spheres of food-related applications: (i) sensors aimed at food quality control, (ii) as encapsulation/release systems for active ingredients or packaging materials and (iii) as separation membranes for beverage filtration. The methodological strategy that will be followed, intends to be as close as possible to the *ready-to-use* approach, rather than to the *proof-of-concept* study, by using more realistic samples, materials and testing conditions.

The thesis is thus structured in three chapters, each one devoted to the above mentioned technological sphere. In particular, *chapter 1* will investigate the application of polyamidic nanofibrous membranes for increasing selectivity and specificity in electrochemical sensing of complex foodstuffs. *Chapter 2* will explore the use of nanofibers for encapsulation and controlled release of bioactive chemical species (such as antioxidant phenolic compounds and antimicrobial volatiles). Finally, *chapter 3* will descrive the use of nanostructured membranes for the filtration of beverages (in particular of apple juice) and for selectively removing bitter polyphenols.

Every tailor-made application developed represents a separate scientific contribution and is an individual deliverable of the thesis.

RIASSUNTO

Attualmente, l'industria alimentare, per meglio rispondere alle attese dei consumatori, diversifica l'offerta con nuovi prodotti alimentari, risultato della continua ricerca e dell'innovazione tecnologica. L'applicazione di nuovi processi di produzione e l'impiego di materiali innovativi, hanno aumentato la varietà di alimenti disponibili e apportato dei miglioramenti rivelandosi molto promettenti per la futura produzione alimentare.

In particolare, le nanotecnologie forniscono materiali quali nanoparticelle, nanoemulsioni, membrane porose, ecc., capaci di migliorare alcune delle principali operazioni unitarie quali la filtrazione, il packaging, i sistemi di controllo analitico nonché alcune delle caratteristiche dei prodotti quali la stabilità, il sapore, l'aroma, ecc.

Tra le diverse forme di nanostrutture, particolare attenzione hanno ricevuto i materiali nanofibrosi, sviluppati mediante la tecnica di elettrofilatura (electrospinning). Questa tecnica, consente di produrre a partire da polimeri biologici e sintetici membrane nanostrutturate caratterizzate da un elevato rapporto superficie/massa, una elevata porosità e resistenza meccanica. I materiali nanofibrosi possono combinare i vantaggi dei nanomateriali particolati come le nanoparticelle, con quelli dei laminati polimerici come film o membrane.

In questa tesi si sono studiate le potenzialità delle nanofibre in tre campi di applicazioni alimentari: (i) sensori destinati al controllo di qualità degli alimenti, (ii) sistemi di incapsulamento/rilascio per la formulazione di ingredienti attivi o materiali di packaging e (iii) membrane di separazione per il filtraggio di bevande. La strategia metodologica seguita ha utilizzato un approccio ready-to-use e non proof-of-concept, con campioni, materiali e condizioni operative, il più possibile reali.

Di conseguenza la tesi è stata strutturata in tre capitoli, corrispondenti ai campi di applicazioni sopra elencati. In particolare il capitolo 1, descrive l'applicazione delle membrane nanofibrose poliammidiche per aumentare la selettività e specificità di sensori elettrochimici usati per l'analisi di matrici alimentari anche complesse. Il capitolo 2, esplora l'utilizzo delle nanofibre per incapsulare e rilasciare in modo controllato specie chimiche bioattive (quali composti fenolici antiossidanti e composti volatili antimicrobici). Infine, il capitolo 3 studia l'impiego delle membrane nanostrutturate per filtrare bevande (quali succo di mela) e per rimuovere selettivamente i suoi polifenoli amari.

Ognuna delle applicazioni specifiche rappresenta un contributo scientifico distinto ed è un singolo risultato della tesi.

PREFACE

Scientific considerations

The term *nanotechnology* refers to a group of emerging technologies, crossing transversally many science fields that share as a common approach the study, modification or application of extremely small objects, namely materials, structures and devices with at least one characteristic dimension in the nanometer scale (usually 100 nm or less). Nanotechnology is aimed at taking advantage of the special features or behaviors (mechanical, optical, electrical, magnetic, etc.) that materials often have when they are structured at the nano-scales due to quantum effects or other simpler physical effects of the size reduction.This set of technologies have been claimed to have a revolutionary potential for many industries pervading many aspects of the human being life experience.

For the agri-food sector, nanotechnology offers many possible solutions to problems at practically all the levels of the field (Kumari & Yadav, 2014): from agricultural productivity to food preservation, from detection of pathogens and contaminants to processing, from food additives to food analysis, from functional foods to food-related waste treatment, and so on.

Being agriculture and nutrition so critical for human sustenance and representing one of the biggest slices of the global economy cake, either government agencies or industries have identified the potential significance of nanotechnology in the agri-food sector. Nevertheless, for some nanotechnology applications there are potential health risks, and environmental and sociological concerns creating ambiguity about its use in food related applications (Siegrist *et al*., 2007; Gruère *et al*., 2011).

In any case, mainstream food and beverage companies, alongside a growing mass of small, freshly arrived nanotech start-ups, are investing, using or interested in nanotechnology applications for the innovation in products and processes (Pérez-Esteve *et al*., 2013; Chaudhry *et al*., 2008). The driving force for these industries is the constantly rising pressure to meet consumer demands for new products that are safe, convenient, affordable, pleasant and healthy. Nanotechnology offers a way to meet such demands, putting adjectives to the conventional devices. In other words, nanotechnology makes feasible to develop new *sustainable* processing aids for foodstuffs, *smart* or *active* food packaging materials, *functional* and *bioactive* ingredients and *nano*-biosensors, amongst others. These are good news for the food and beverage industry and the reason why there is so much interest on food-related nanomaterials.

The development of every particular novel nanotech material to be applied in food and beverage industry demands a strong knowledge-based support that comprehends a profound study of the material structure and of the innovative features that it proposes, accompanied by considerations on the way the material will interact with the environment and the consumers, whether consumers are food technologists, regulatory agencies or people buying an ice cream.

Among the nanostructures developed for practical purposes, electrospun nanofibrous materials produced from synthetic and bio- polymers have received great attention by virtue of their fabrication simplicity through the electrospinning technique and their special nano-related features.

These materials are polymeric “fabric-like” mats or membranes, that are macroscopically homogeneous, whereas microscopically composed by ultra-thin fibers, i.e., nanofibers, more commonly disposed in a random, non-woven arrangement. Their features include large surface-to-mass ratio, very high porosity, enhanced mechanical resistance and improved responsive capacity to changes in the surrounding atmosphere (Ramakrishna *et al*., 2005) compared to conventional configurations of the same polymer or polymer blend.

In a certain way, nanofibrous materials can combine the advantages of particulate nanomaterials like nanoparticles, carbon nanotubes, quantum dots, mesoporous silica or liposomes (e.g., surface areas, porosity, quantum-like properties), with the advantages of polymeric laminate materials like films or membranes (e.g., mechanical resistance, handling versatility, elasticity, permeability).

In consequence, non-woven nanofibers produced by the electrospinning technique are ideal materials for a number of food-related applications, in particular as (i) sensors aimed at food quality control, (ii) as encapsulation/release systems for active ingredients or packaging materials and (iii) as separation membranes for beverage filtration.

In this thesis, we will demonstrate the potentialities of nanofibers in the three above mentioned fields through the application or the design of novel nanofibrous materials, tailored to tackle very specific needs of the food and beverage industry in each scenarios.

The methodological strategy that will be followed, intends to be as close as possible to the *ready-to-use* approach, rather than to the *proof-of-concept* study, by using more realistic samples, materials and testing conditions.

The thesis is structured in three chapters, each one devoted to its corresponding technological sphere, as follows:

In *chapter 1* nanofibrous membranes are investigated in electrochemical sensing of foodstuffs as selective barriers against interfering compounds and as recognition systems nanobiosensors. In the first case-study (*section 1.2*) nylon-6 nanofibrous membranes are used as coating for transducers (carbon electrodes) enabling the direct determination of ascorbic acid in real samples (fruits and fruit juices). In the second case-study (*section 1.3*) the same kind of electrospun material is used for the covalent immobilization of xanthyne oxidase and the subsequent (preliminary) development of an amperometric sensor for xanthyne and hypoxanthine determination in foodstuffs.

In *chapter 2*, the use of nanofibrous mats as devices for encapsulation and controlled release of bioactive materials, with potential uses as functional ingredients or food active packaging devices, is explored. The first case-study (*section 2.2*) regards the use of blend electrospinning to produce edible nanofibers and nanofibrous composites –either fast disintegrating and not- for the encapsulation and pH-differentiated fast release of antioxidants, namely hydrophobic and hydrophilic phenolic compounds. The second case-study (*section 2.3*) consists in the production by electrospinning of nanofiber/mesoporous-silica- composites for the encapsulation of hydrophobic antioxidants; in this case, the MSP functionalization with molecular gates allows for a highly specific sustained release at neutral pH whereas entrapping the cargo in acid media. In the third case-study (*section 2.4*) the potential of electrospinning in the encapsulation of aroma volatile compounds with antimicrobial activity is explored; model aroma compounds are encapsulated in β-CD inclusion complexes and homogeneously dispersed in polysaccharide nanofibrous membranes in a single electrospinning step for pH-triggered release of the volatile compound, beyond a threshold of water activity ($aw \geq 0.9$) of the environment.

Finally, in *chapter 3*, polyamidic membranes as selective filtration devices are studied in connection with the clarification of apple juice and its bitter polyphenols-selective removal, achieved by a dead-end filtration system operating at different trans-membrane pressures. Relevant morphological, structural and transport characteristics of the membranes as potential filtration devices are explored and compared to those of commercial polyamidic filtration membranes.

Each chapter (and sub-chapter) is accompanied by a specific introduction with its own state-of-the art review that will serve to the reader for better understanding the advances that each case-study represents to the particular technological sphere of the food sector where it has place. Every tailor-made application developed represents a separate scientific contribution and is an individual deliverable of the thesis. To the date this document was written, some of the results had been published (see *Appendix 1*) and some were about to be published in peer-reviewed scientific journals.

Additionally, since this thesis is not an investigation of the electrospinning itself as a technique, but it did require a profound knowledge of this electrohydrodynamic process, we consider that a very short *separata* with the generalities of this technique might turn useful to the reader.

Preface

Personal considerations

The realization of this PhD was made possible by the full financial support of the Colombian government through the International PhD Training Program (*Generación del Bicentenario, Becas Francisco José de Caldas*) of the Administrative Department of Science, Technology and Innovation (*COLCIENCIAS*). I acknowledge this noble initiative of my country, aimed at the scientific formation of a generation of young researchers in top-level institutions of the world; a generation that, to my concern, is meant to return to the country and contribute, from science, in areas that are key for the sustainable development of the population and the territory. I expect that the scientific results obtained and the skill acquisition that they demanded will reflect somewhat, in the future, as a grain of sand, in improved possibilities for the food industry and in the strengthening of the scientific potential of Colombia in this important sector.

1. Chaudhry Q et al., 2008, Applications and implications of nanotechnologies for the food sector. Food Addit Contam 25: 241-258.
2. Gruère et al., 2011, Agricultural, food, and water nanotechnologies for the poor: opportunities, constraints, and the role of the consultative group on international agricultural research. Publication of the International Food Policy Research Institute.
3. Kumari A, Yadav SK, 2014, Nanotechnology in Agri-Food Sector. Crit Rev in Food Sci Nutr, 54:975-984.
4. Pérez-Esteve E et al., 2013, Nanotechnology in the development of novel functional foods or their package. An overview based in patent analysis. Recent Pat Food Nutr Agric 5:35-43.
5. Ramakrishna S et al, 2005, An introduction to electrospinning and nanofibers (Vol. 90). Singapore: World Scientific.
6. Siegrist M et al., 2007, Public acceptance of nanotechnology foods and food packaging: The influence of affect and trust. Appetite, 49:459-466.

Preface

BRIEF INTRODUCTION TO ELECTROSPINNING AND NANOFIBERS

As anticipated above, nanofibrous membranes, mats or scaffolds are fabric-like materials composed by ultra-thin fibers or nanofibers, more commonly disposed in a random, non-woven interconnected arrangement (See Figure P1).

For the sake of clarity, at this point of the document, it is worth to make some precisions: although the academic community has somewhat reached an agreement for the < 100 nm as a reference for the *nanotechnology* classification, some commercial, scientific and technological sectors have accepted a broader flexibility, for instance 300 nm or even 500 nm (Ramakrishna *et al*., 2005). Something that some academics would categorise as *sub-microtechnology*. Even though we acknowledge the validity and utility of the 100 nm standard, for practical reasons and for considering it more comprehensive with the regard to the special features observed in the case of this kind of materials, even well above the 100 nm "threshold", in this thesis we will embrace the wider approach and refer to nanofiber or nanofibrous materials, mat, membrane, structure, etc., when the fibers display characteristic diameters that are in the sub-micron scale below 500 nm. Furthermore, whilst the thesis document has been written following in general the British English rules, some concessions have been made, that include as the most important exception the word "fiber" that in the correct British English would be called "fibre". This concession has one simple practical reason that is rendering it more readily available in the cyberspace (the word "nanofiber" appears to be nearly 100 times more present than "nanofibre").

Polymeric nanofibers can be produced by several techniques that include drawing, template synthesis, phase separation, self-assembly, "forcespinning", melt-blown processes and electrospinning. Among these techniques though, electrospinning seems to be currently the most widespread one, and it is likely to be the simplest and most technologically feasible.

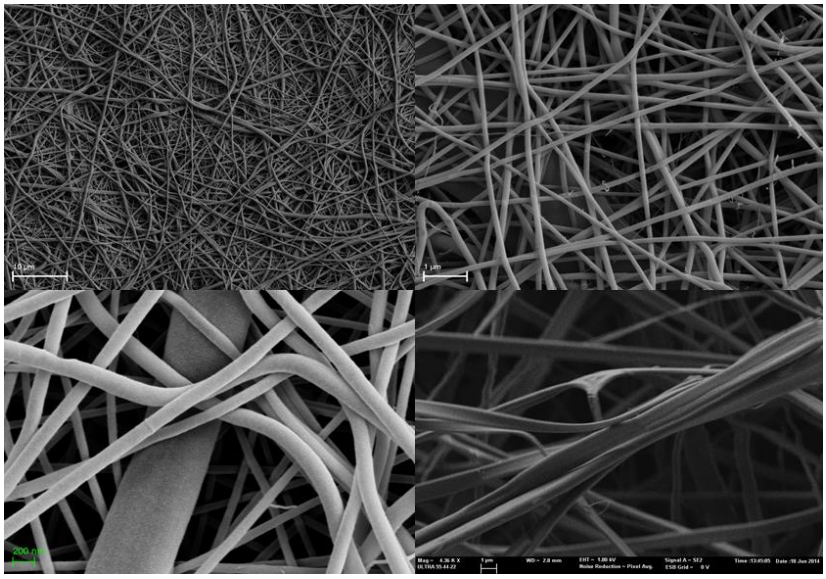

Figure P1. Micrographs of different elecrospun nanofibers and ultrathin fibers.Top: poly(lactic acid) (left) and pullulan (rigt). Bottom: PLA and nylon-6 (left) and zein (right).

Electrospinning, also called electrostatic spinning, is a electrohydrodynamic process that uses electric fields to spin polymer fibers with diameters ranging from hundreds to tens of nanometers, creating non-woven ''fabric-like'' mats Teo & Ramakrishna (2006), Greiner & Wendorff (2007),

Reneker & Yarin (2008) and Kriegel *et al.* (2008) amongst several other works, provide an exciting insight to the electrospinning process setup, mechanism, characteristics, transport phenomena, history, commercial and economic implications, etc.

The working principle of electrospinning is very straightforward: a high voltage is applied to a polymer fluid (usually a polymeric solution) such that charges are induced within the fluid. When these charges reached a critical value, a fluid jet erupts from the droplet at the tip of the needle, resulting in the formation of a Taylor cone. Then, fibers are collected as a non-woven mesh or membrane on a collector plate that acts as the counter electrode (Figure P2).

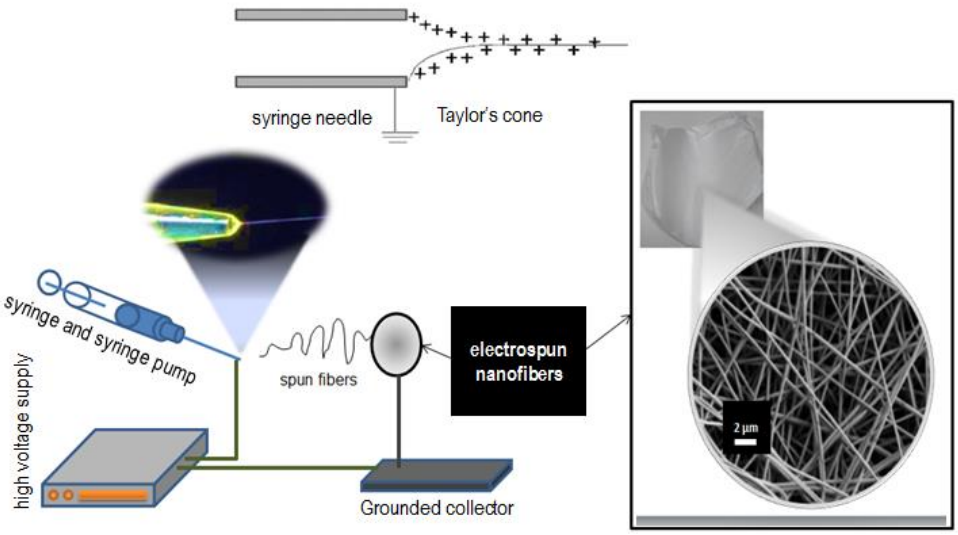

Figure P2. Schematic representation of an electrospinning setup.

The mechanism can be described as follows: in the needle tip, the capillary forms a drop that contains the polymer solution (i.e., polymer, possibly other components and a solvent); in the absence of electrical field, the drop is subjected to a balance of forces, namely gravitational forces and surface tension. When electrical field is applied and the drop becomes electrostically charged, it introduces additional forces into this complex force balance. As a result, the surface of the drop is distorted forming a conical shape (Figure P2) towards the position in the electrical field with the opposite charge (or to the grounded end). This phenomenon is called Taylor's cone. When the electrical field reaches a critical value, a charged jet of the polymer solution is ejected, or spun, towards a grounded collector. In order to maintain a hydrodynamic equilibrium, new solution needs to be fed to the needle tip at the same rate that it is spun. Depending on a number of factors related to the solution conditions and the process conditions (ranging from applied voltage, feed rate, electrical field intensity, distance from needle tip to collector, solution properties like viscosity and conductivity, environmental conditions like temperature and relative humidity and their multifactorial combination), the jet may not remain intact and instead break apart into droplets in which case not fibers but particles or beads are deposited on the collector plate.

Many modifications to the essential process has been made to achieve more specialized configuration of the nanofibers or the nanofibrous materials. The most relevant of these modifications are: multinozzle or multijet electrospinning (Figure P3), coaxial electrospinning (Figure P4) and electrospinning with rotating colectors (Figure P5). The first one consists in the use of several syringes in parallel alignment allowing for the fabrication of electrospun membranes containing different fiber

materials. The second one consists in the use of concentric needles transporting different electrospinning solutions. This configuration allow, at certain conditions, to obtain core-shell nanofibers. The third one consists in the use of rotating collectors that allow to obtain fibers that are arraged following a defined alignment or simply, depending on the rotation velocity, to obtain continuous materials.

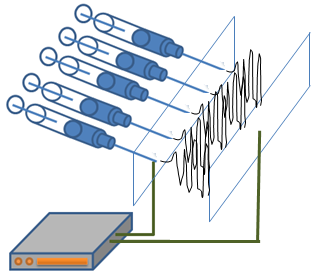

Figure P2. Schematic representation of an multijet electrospinning setup.

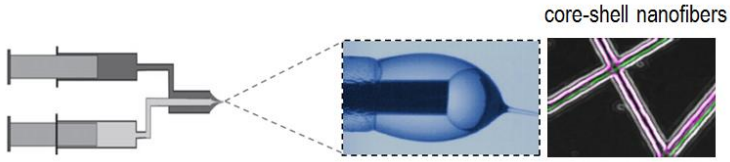

Figure P2. Schematic representation of coaxial electrospinning setup.

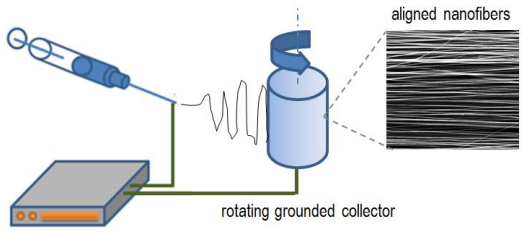

Figure P3. Schematic representation of electrospinning setup with rotating collector.

1. Greiner A, Wendorff JH, 2007, Electrospinning: a fascinating method for the preparation of ultrathin fibers. Angewandte 46: 5670-5703.
2. Kriegel C et al., 2008, Fabrication, functionalization, and application of electrospun biopolymer nanofibers. Crit Rev in Food Sci Nutr 48:775-797.
3. Ramakrishna S et al, 2005, An introduction to electrospinning and nanofibers (Vol. 90). Singapore: World Scientific.
4. Reneker DH, Yarin AL, 2008, Electrospinning jets and polymer nanofibers. Polymer 49:2387-2425
5. Teo W, Ramakrishna S, 2006, A review on electrospinning design and nanofibre assemblies. Nanotechnology 17: R89.

1
NANOFIBERS IN FOOD ELECTROCHEMICAL SENSING

1.1 INTRODUCTION

Analytical chemistry comprehends the study of both quantitative and qualitative chemical composition of a system of interest. Such analytical process can be divided in three main components: sample preparation, separation and detection, each of which offers a number of challenges depending on the compositional complexity of the studied system. In the particular case of food matrices, complexity and variability are inherent factors that can hinder both identification and quantification of analytes, especially when considering the relative unsteadiness of the compositional profiles of most of food or food-related systems.

Improving analyte selectivity and sensitivity as well as reducing time-demand and difficulty of the whole analytical processes are the driving forces of most research efforts in current analytical chemistry. In this context, the never-ending pursue for developing innovative materials, from biomaterials to inorganic materials to bio/synthetic hybrids, with novel or improved morphologies and functionalities, together with advances in electronics and computing, are expected to enable the continuous progress towards more exact, precise and inexpensive tools in food sensing.

Currently, nanostructured materials are likely to represent the richest source of innovation in this field. According to some researchers (Chigome & Torto, 2011) the advancements in nanomaterials are the key for a total control of the analytical processes. Nanomaterials are promising for the development of sensors mainly due to two reasons: (i) larger specific surface areas which provide an increased number of sites of interactions with the analytes or the signal transduction, and (ii) the special features or behaviours (optical, electrical, magnetical, etc.) that materials might exhibit when they are structured at nano-scales, compared to their conventional bulk equivalents, which widen the type of sensor/analyte interactions that can be utilized for separation, detection and quantification. An important amount of research has been conducted on the use of nanomaterials for different aspects of the analytical processes (Asefa *et al*., 2009; Vaseashta & Dimova-Malinovska, 2005; Lucena *et al*., 2011; Zhu *et al*., 2004; Valcárcel *et al*., 2008; Scida *et al*., 2011; Sykora *et al*., 2010; Duan *et al*., 2011; Zhang *et al*., 2006; Nilsson *et al*., 2007), including food sensing (Duncan, 2011).

Nanotechnology-base sensors include carbon nanotubes (O'Conell, 2012), arrays of nanoparticles (Kreno *et al.*, 2011), quantum dots (Shen *et al.*, 2012) and electrochemical and optical sensors constituted by -or modified with- a variety of nanostructures (Duncan, 2011). Nanobiosensors are particularly promising since they combine the advantages of nanostructured materials with the high selectivity of biological components (DNA markers, microorganisms, living eukaryotic cells, enzymes, etc.) for interacting specifically with a certain analyte (Pumera *et al.*, 2007).

One of the most interesting type of nanostructured materials that can be used for sensing applications are nonwoven nanofibrous membranes prepared by means of electrospinning. This kind of materials have shown to offer prospects in building more efficient interfaces with electronic components whose size is comparable to that of molecules. The extremely high surface-to-mass ratios and high porosities of electrospun nanomaterials, combined with their mechanical properties and versatility and their fabrication straightforwardness, have attracted significant attention in this field because such features meet the ideal requisites of analytical sensors (Duncan, 2011). In nanofibrous membranes, as in nanomaterials in general, molecular and surface forces (steric, hydrophobic, capillary and Van der Waals) become more relevant than bulky phenomena (Min *et al*., 2008). Besides, the morphology of electrospun nanofibrous membranes can be described as fibrous interconnected webs consisting mainly of empty space, such as pores and channels, with densities being above 95% lower than the corresponding thick material. Such a porous structure makes feasible an increased accessibility and a low resistance to diffusion of reactive agents, while offering also an enormous surface that can be "engineered" according to specific needs. All of these features are obvious advantages in developing sensing devices with improved resolution and sensitivity respect to conventional materials-based sensors, that are able to perform cheaper, faster and more accurate measurements (Ramakrishna *et al*., 2006).

There are already at least above a hundred types of electrospun nanomaterials-based sensors

relying on a wide variety of polymeric materials and sensing principles, for specific target substances (Wang & Lin, 2008; Arecchi, 2009; Ding *et al.*, 2010; Chigome & Torto, 2011; Scampicchio *et al.*, 2012). Nanofibrous membranes can be used in sensing application, mainly in three ways (including their combination) (Figure 1.1):

(i) As a passive or active coating for preventing attrition/fouling phenomena at the detector or for selectively avoiding the passage of interfering molecules to the detector. In this case nanofibrous membranes act as a component of the sensing unit, namely a selective barrier (Toghill & Compton, 2010).
(ii) If nanofibers are functionalized with sensitive components that can be biological/organic (Patel *et al*., 2006; Herricks *et al*., 2005) -enzymes, antibodies, cells-, or inorganic (Ji *et al*., 2006) -carbon nanotubes, metal nanoparticles, etc.-, the membranes act as highly efficient immobilization supports of the sensor recognition system. Also in this case nanofibrous membranes acts as an active or catalytic component of the sensing unit.
(iii) In some cases, nanofibrous membranes can act as detectors themselves (Drew *et al*., 2004; Lu *et al*., 2005). For instance, metal-coated nanofibers, including nanofibers coated with metal nanoparticles and metal oxides, can provide different detection approaches depending on the thermal conductivity, the piezoelectric properties, amongst the other special features of the deposited metal (Pinto *et al*., 2003;Wei *et al*., 2006; Liu W. *et al*., 2003). Also, conductive polymer or conductive polymer-coated nanofibers (Wang *et al*., 2007) and polyelectrolites nanofibers (Ding *et al*., 2004) have been used as sensing nanomaterials for analytes in both solid and gas/vapour phases. Furthermore, photoelectric detectors (Shi *et al*., 2009), quenching-based fluorescent optical detectors (Wang *et al*., 2002; Wang *et al*., 2004; Chae *et al*., 2007), Fourier transform infrared (FTIR) spectroscopy optical detectors (Luoh & Hahn, 2006) and simpler colour-changing fibers for colorimetric assays (Scampicchio *et al.*, 2009; Chigome & Torto, 2011) have been developed using electrospun nanomaterials.

The above-mentioned approaches are particularly useful in electrochemical sensing, in which the measurement of the electronic currents derived from the oxidation/reduction of chemical species in an electrolytic cell are used for assessing a particular compound directly or indirectly involved in the redox process. Determining electroactive biochemical species present in food matrices via solid electrodes is often restrained by the irreversible adsorption of chemical species on the surface of the working electrode, resulting in electrode deterioration and inactivation, and therefore in the loss of sensitivity (Kilmartin, 2001; Campuzano & Wang, 2011, Reneker & Chun, 1996; Lee *et al*., 2011; Wu *et al*., 2010; Vohra *et al*., 2011; Cucchi *et al.*, 2007; Wang *et al*., 2009a; Formo *et al*., 2008; Min *et al.*, 2008; Kriegel *et al*., 2008; Scampicchio *et al*., 2008; Gibson *et al*., 2001; Allred & McCreery, 1992). This problematic is more relevant in the case of biological-origin matrices, such as foodstuffs, in which a great assortment of electroactive substances is commonly present in the system. Electrodes coated with nanofibrous membranes have longer lifetimes than uncoated electrodes in contact with solutions that contain fouling species (Scampicchio *et al.*, 2012). Furthermore, the barrier effect of these membranes can be made selective towards interfering compounds when increasing their affinity with the polymer material. Scampicchio et al. take advantage of this effect for selectively determining a nutritionally-relevant compound (vitamin C) in standard solutions containing interfering polyphenols using nanofibrous-coated glassy carbon electrodes: at certain pH conditions (<7), the ionic form of ascorbic acid is able to diffuse through the polyamide nanofibrous membrane, whereas undissociated flavones, that would otherwise foul the electrode, remain adsorbed on the polymeric fibers (Scampicchio *et al*., 2008).

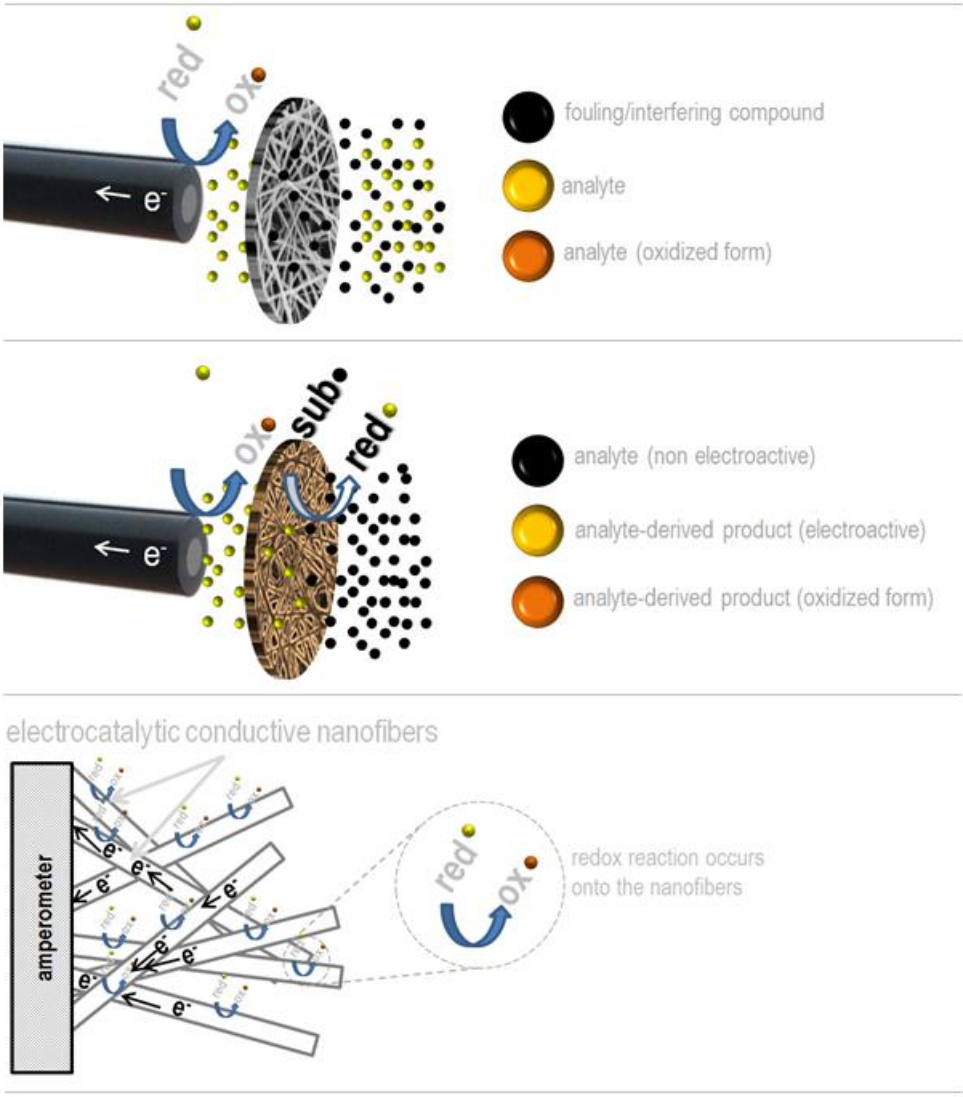

Figure 1.1. Schematic representation of different approaches on the use of nanofibers in electrochemical sensing. (i) top: membranes act as selective barrier against fouling or undesirable compounds while allowing the diffusion of the electroactive analyte towards the electrode; (ii) middle: catalysts, e.g., enzymes, nanoparticles or carbon nanotubes, are incorporated to the nanofibers producing an electrochemically detectable product that diffuses towards the electrode; (iii) bottom: nanofibers of metals or conductive polymers with catalytic features act as electrochemical detectors.

Electrochemical nanobiosensors based on electrospun nanofibers result very attractive in food sensing thanks to the high specificity that they can reach. Electrodes (in this case acting as the transducers) can be coated/modified with membranes that contain enzymes, antibodies or cells, that are able to react with -or catalyse the reaction of- the analyte; the biological element is immobilized, attached, or encapsulated in the nanofibrous membranes which act as a recognition system. High surface-to-mass ratios, together with the ultra-thin structure of the fibers, allow electrospun nanofibrous membranes to potentially load a superior amount of biological material per surface unit while enabling the collocation of the recognition system in close proximity to the electrode surface, resulting in a non-delayed

transduction signal. Most of this kind of devices have been employed in amperometric glucose detection (e.g. in biological fluids/tissues and foodstuffs) because of the low detection limits that they can easily achieve, and also probably because the first works in this field were proposed on enzymatic electrochemical sensors with the enzyme glucose oxidase bound to the transducer, channelling the subsequent research in that direction (Ding *et al.*, 2010). Glucose oxidase has been immobilized in nanofibrous membranes made of various materiales and coupled to different electrodes, such as carbon nanotube-filled poly(acrylonitrile-*co*-acrylic acid) (Wang *et al*., 2009b); PVA membranes coupled to gold electrodes (Ren *et al*., 2006); and nylon-6 coupled to glassy carbon electrodes (Scampicchio *et al*., 2010). Fu *et al.*, 2014 have immobilized laccase in carbon nanofibers and copper/carbon composite nanofibers for detecting catechol on glassy carbon electrodes at detection limits lower the 2 µm. (Mao *et al.*, 2013) immobilized horseradish peroxidase onto carbon nanofiber webs, at different densities of state, for detecting H_2O_2, below 2 µm. Electrospun PVP/urease composite nanofibers have also been demonstrated to be promising in the detection and quantification of urea (Sawicka *et al*., 2005). Polyamide/tyrosinase nanofibers coating a glassy carbon electrode surface has been used as a biosensor for the detection of phenolic compounds (Arecchi et al., 2010). Apart from these examples, other enzymes have been successfully immobilized in nanofibrous matrices maintaining the catalytic activity, including α-chymotrypsin, lipases and catalases (Wang *et al*., 2009c); although in most of these cases their use in food sensing has not been studied yet, it is possible to anticipate that such catalytic materials will have practical applications in developing very specific biosensors for foodstuffs. Ding *et al*., 2009, developed a nanobiosensor based on haemoglobin microbelts deposited by electrospinning as coatings of glassy carbon electrodes for the determination of H_2O_2 and nitrite. Another example of how a biological element attached to nanofibers can be used as an efficient recognition system is that illustrated by Senecal *et al*., 2008; in this study composite electrospun membranes made of polyamine/polyurethane with amine functional groups and carboxylated polyvinyl chloride with carboxyl as functional groups, are functionalized with covalently-attached antibodies and linked to a sensor unit, for capturing down to very low levels (1 ng) of *Staphylococcus* eneterotoxin B (SEB). The main drawbacks to be overcome with regard to this type of biosensors regard the inevitable problem of stability and at some extent, the question of how the enzyme activity is affected (not neccesarily diminished) by the protein/polymer interactions.

Other electrochemical sensors based on the use of electrospun nanofibers rely on the incorporation of inorganic materials that confer recognition ability or better sensitivity towards specific molecular targets. Such materials can be nanotubes, nanoparticles, nanorods, functionalized mesoporous silica materials, etc. Nanofibrous membranes functionalized with carbon nanotubes combine the catalytic properties of the nanotubes with the protective effect of the membranes and represent an interesting material to be used in electrochemical sensing (Hou & Reneker, 2004). Such systems has been used for measuring food relevant substances like sulfhydryl compounds (Li *et al*., 2011), gases (Ding *et al*., 2010), and even DNA and complex biomolecules (Yang *et al*., 2009; Dai *et al*., 2014).

As anticipated above, conductive polymeric nanofibers have been also used to develop electrochemical sensors. For instance, electrodes covered with electrospun nanofibrous membranes of conducting polymer blends (polystyrene, polyvinylpyrrrolidone and polyethylene oxide) have been used in developing an electronic nose, based on the fact that each polymer modifies the interacting surface to different tested analytes (Zampetti *et al*., 2011). Polyamide nanofibers doped with Fe(III) salts made conductive via their exposure to pyrrole vapours can be used to detect phosphate and carbonate anions (Granato *et al*., 2009; Granato *et al*., 2008). Furthermore, copper oxide nanofibers (Wang *et al*., 2009a), Pd(IV)-doped copper oxide composite nanofibers (Wang *et al*., 2009d), Ni nanoparticle-loaded carbon nanofibers (Liu *et al*., 2009), poly(vinylidene fluoride)/poly(aminophenylboronic acid) composite nanofibrous membranes (Manesh *et al*., 2007), amongst others, have been used as amperometric enzymeless sensors for glucose determination.

Although it falls outside the category of electrochemical sensing devices, Ding *et al*. (2010) provide an interesting detailed review on different materials that have been used in the fabrication of

metal-oxide semiconductors (MOS) using nanofibers, as resistive detectors for gases, organic vapours, amines and other volatile organic compounds, which can be promising in the developing of complex electronic nose-like arranges for food head-space analysis.

The combination of the above-mentioned approaches seem to be currently becoming the more important line of research. Numnuam et al. developed an amperometric sensor by immobilizing uricase on an electrospun nanocomposite of chitosan-carbon nanotubes nanofiber covering an electrodeposited layer of silver nanoparticles on a gold electrode (Numnuam *et al*., 2014). Ouyang et al., prepared polyurethane nanofibers filled with carbon nanotubes and silver nanoparticles and subsequently used them in a non-enzymatic amperometric biosensor for determination of H_2O_2 (Ouyang *et al.*, 2013). Uzun et al. modified the graphite rod electrodes surface with nylon 6,6/multiwalled carbon nanotubes nanofibers covered with a conducting polymer and incorporated with glucose oxidase for determining glucose in beverages (Demirci Uzun *et al.*, 2014). These examples are intended to illustrate the potential and versatility of electrospun nanomaterials in the fabrication of novel food sensing systems.

It seems that most of the works present in the literature on this particular subject regards glucose as a "model target molecule" which suggest that at least a significant part of these sensing units are still in the proof-of-concept phase, or are prototype devices not necessarily able to perform well in more realistic scenarios. Research on the subject of electrospun nanofibers as food sensing devices must be focused on their use for the efficient determination of nutrionally-relevant substances or food safety indicators, diversifying the target molecules with respect to the "main-stream" glucose, and, when possible, testing the systems in the assessment of real foodstuffs.

In this chapter, the use of a nanofibrous membranes in amperometric sensor development is addressed, both as selective barriers against interfering compounds and as recognition system of a biosensor. In the first case (section 1.2) nylon-6 nanofibrous membranes are used as coating for transducers (glassy and screen printed carbon electrodes) enabling the direct determination of ascorbic acid in real samples (fruits and fruit juices). In the second case (section 1.3) the same kind of electrospun material is used for the covalent immobilization of xanthyne oxidase and the subsequent (preliminary) development of an amperometric sensor for xanthyne and hypoxanthine determination.

1.2 NANOFIBER-MODIFIED CARBON SENSORS FOR IN SITU ASSESSMENT OF ASCORBIC ACID IN FRUITS

Vitamin C, one of the principal antioxidants present in fruits and vegetables, is important in human nutrition and health, and as a food processing additive (Szeto *et al.*, 2002; Smith J & Hong-Shum L, 2011). Its main biologically active form of is L-ascorbic acid (AA) or L-ascorbate (Asard H *et al.*, 2004). Its determination, which is of great significance, is rather simple due to the fact that is photometrically and electrochemically very active. Titration, spectrophotometry, spectroscopy, and their combination with separation techniques (Dürüst *et al.*, 1997; Speek *et al.*, 1984; Brause *et al.*, 2003; Nováková *et al.*, 2004) have been widely used for its evaluation. These methods can be relatively expensive and time consuming. Moreover, their accuracy in food products depends highly on the sample preparation and extraction procedures, that must avoid its oxidation and photodecompomposition.

Direct AA determination by conventional techniques is limited as they require an extraction protocol from the original matrix, followed by a proper sample dilution and the use of antioxidant agents such as metaphosphoric acid. Therefore, the assessment of AA with techniques that are rapid, straightforward, portable and that require a minor preparation, represents an important challenge (Terry L *et al.*, 2005).

Electrochemical analysis may enable the in-situ evaluation (Lau S, *et al.*, 1989; Guanghan *et al.*, 1994; Civit *et al.*, 2008; Bordonaba & Terry, 2009; Escarpa, 2012) of certain compounds, providing a valid tool in the fresh food produce industry, and for regulatory agencies. Regarding the electrochemical determination of AA with metal or carbon electrodes in food matrices, the main drawbacks are: (i) the high working potentials required for its electrochemical oxidation leading to

poor selectivity and (ii) the fouling caused mostly by oxidation byproducts that usually leads to poor reproducibility (Falat & Cheng, 1983). Attempts to overcome these issues by using active mediators or by modifying carbon or metal electrodes have been described (Akiylmaz & Dinçkaya, 1999; Florou *et al.*, 2000; Roy *et al.*, 2004; Pavan *et al.*, 2005; Ijeri *et al.*, 2004; Nassef *et al.*, 2007; Zare & Nasirizadeh, 2010; Satheesh Babu *et al.*, 2010; Manjunatha *et al.*, 2010; Kit-Anan *et al.*, 2012), but its determination in real food matrices has been not so widely investigated (Civit *et al.*, 2008; Guorong *et al.*, 2000; Tian *et al.*, 2006; Thangamuthu *et al.*, 2007; Barberis *et al.*, 2010; Barberis *et al.*, 2012; Zhang *et al.*, 2013).

In the particular case of screen-printed (SP) sensors, even though their effectiveness for quantification of AA and other vitamins in standard solutions or purified biological samples has been extensively studied and demonstrated (Hart & Wring, 1997; Hart *et al.*, 2005; Renedo *et al.*, 2007¸ Pakapongpan *et al.*, 2012; Sha *et al.*, 2013), they have rarely been applied to the evaluation of AA in real food samples (Civit *et al.*, 2008; Kulys & D'Costa, 1991; Milakin *et al.*, 2013).

As mentioned above, nanofibrous membranes are a valid alternative for sensor modification. In this chapter a rapid and simple system for estimating the content of AA of fruits, directly in the sample (in-situ) without any extraction/separation protocol, nor the use of antioxidant aids, by coating glassy carbon (GC) and screen printed (SP) carbon electrodes with electrospun nylon-6 nanofibrous membranes. The methodolgy is rapid, accurate and does not require expensive equipment nor skilled operator.

1.2.1 Materials and methods

1.2.1.1 Chemicals

All chemicals and solvents were of analytical reagent grade and were used without any further purification. Solutions were prepared with ultra-pure MilliQ water (Millipore, Inc.; Ω = 18 MΩ·cm-1). Sulfuric acid (97%), metaphosphoric acid, nylon-6 and standards of L-ascorbic acid, caffeic acid, epicatechin, ferulic acid, p-coumaric acid, quercetin, naringenin and tannic acid, were purchased from Sigma-Aldrich (Milan, Italy). Formic acid (98%) was purchased from Fluka, Sigma-Aldrich (Steinham, Germany). Standard solutions of AA were prepared in buffer citrate (0.1 M; pH from 2.5 to 4.0) from daily-prepared and degassed stock solutions.

1.2.1.2 Samples

The samples (apple, pear, lemon, kiwi, orange, tangerine and strawberry) were purchased from a local retailer and selected to show the wider applicability of the methodology.

1.2.1.3 Fabrication of nanofibrous membranes

Nylon-6 membranes were prepared as described by Scampicchio *et al.*, 2009, with some modifications. Briefly, a 23 % (w/w) solution of nylon-6 was prepared in formic acid. Plastic syringes (10 mL) fitted with a metallic needle (Hamilton) were filled with the polymeric solution and placed in a KDS100 syringe pump (KD-Scientific, New Hope, PA) at a flow rate of 0.15 mL h^{-1}. The needle of the syringe was linked to a Spellman SL150 high voltage power supply by an alligator clip. A foil-covered copper tray, positioned at 11 cm in front of the needle, was used as collector and grounded. For the electrospinning, the electrical potential was set at 25 kV. At the end of the electrospinning runs, the membranes were peeled-off. Membranes with different thicknesses were obtained by stopping the collection after different times (from 5 min to 60 min); at electrospinning conditions described above, membranes thickened at a rate of 2.3 μm min^{-1} (r^2 = 0.98), resulting in thickness between approximately 10 to 125 μm. These fibers exhibit randomly oriented and interconnected arrangement with diameters of 95 ± 25 nm, and are free of beads (Figure 1.2c). The average density and porosity of the membranes are 75 kg m^{-3} and 94%, respectively.

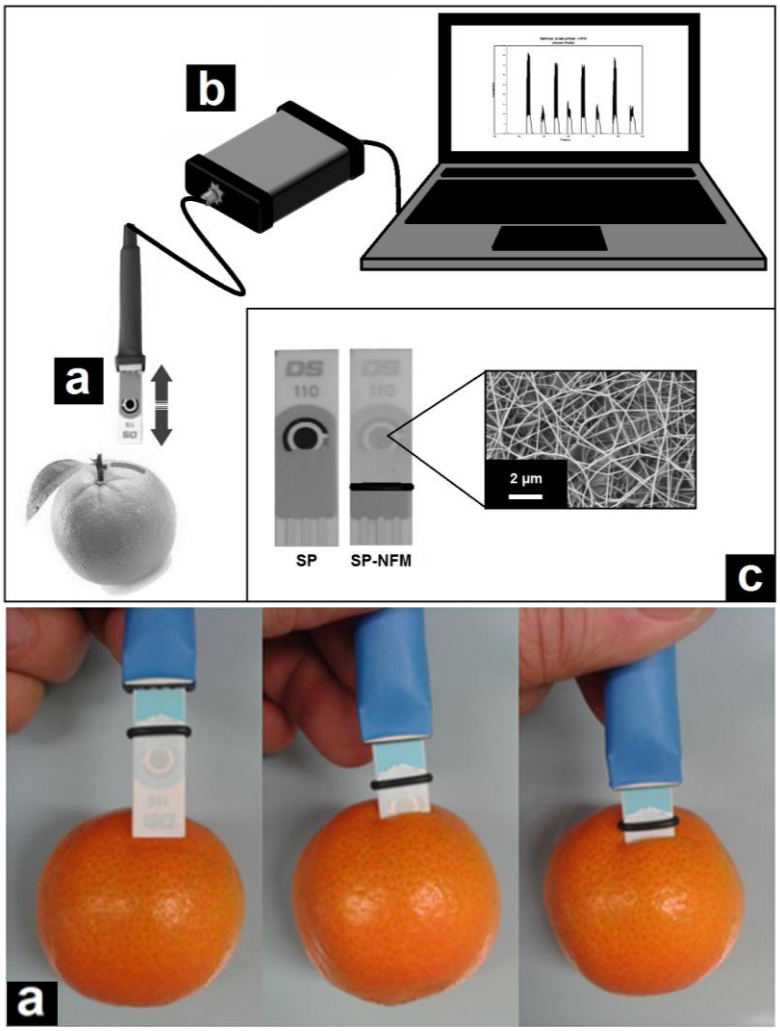

Figure 1.2. Schematic representation of the *in-situ* amperometric sensing unit: the sensor that is repeatedly taken in and out the fruit (a) is connected to a bi-potentiostat (b); in the box, a picture of the SP and SP-NFM electrodes with a SEM micrograph of the nylon-6 nanofibrous membrane (c)..

1.2.1.4 Electrochemical apparatus and electrode modification

Portable Bipotentiostat µstat 200 (DropSens, Spain) was used for the amperometric measurements. The system controlled the electrodes used in this work: SP electrodes were disposable screen-printed DS 110 (DropSens, Spain) formed by graphite electrodes as working and counter electrodes, and a silver electrode as pseudo-reference electrode; and conventional glassy carbon (GC) electrodes that were used together with a Ag/AgCl 3 M reference electrode and a Pt wire counter electrode. Modification of the electrodes was done by coating its surface with a wet NFM followed by drying at room temperature (~15 min). Membranes were held to the electrodes with a rubber o-ring (Figure 1.2a). It must be noticed that for SP sensors, the coated surface included the working, counter and reference electrodes.

1.2.1.5 Amperometric measurements

Amperometric batch measurements of standard solutions of AA and interfering compounds were performed in 10 mL stirred buffers, prepared as described above. The sensors were calibrated using AA standard solutions (50 – 1800 mg L^{-1}) at a fixed applied potential of 0.35 V. Amperometric measurements in real samples were performed according to the following four-steps sequence: (i) the electrode (or electrode arrange) was washed with distilled water; (ii) the electrode was immersed ~6 s in an AA standard solution several times (4 to 10) and the amperometric signal was recorded; (iii) the electrode was thoroughly washed with distilled water; (iv) the electrode was introduced ~6 s for several times (4 to10) in the real sample by directly pricking the fruit, and the amperometric signal was recorded (Figure 1a and 1b). In the case of fruits with hard peel or pulp (e.g., apple, orange, tangerine, lemon) a ~2 cm-deep knife cut was enough to facilitate the sensor penetration (Figure 1.2b). The AA concentration of the standard solutions was selected on the basis of the expected content of vitamin C reported in the literature. This sequence was repeated at least three times for each real sample analyzed.

1.2.1.6 Chromatographic apparatus

The HPLC system consisted of a Model 2080 plus PU pump and a UV-vis 2070 plus detector (Jasco, Japan). The chromatographic conditions were described by Mannino & Cosio, 1997, briefly: column, Fruit Quality Analysis (100 x 7.8 mm id) (Bio-Rad, CA, USA); eluting solution, 0.001 M sulfuric acid at a 0.7 mL min^{-1} flow rate; detection at 254 nm. The sample injection volume was 20 μL. Integration of peak areas and retention time was performed with Borwin v. 1.2. software (Jmbs Developments, France).

1.2.2 Results and discussion

1.2.2.1 Sensor performance in AA standard solutions

To evaluate the performance of the sensors for in-situ determination, preliminary experiments were performed by measuring the amperometric response of the SP and GC sensors operating in AA standard solutions at the applied potential of 0.35 V. This potential was chosen on the basis of preliminary experiments of cyclic voltammetry (data not shown): the oxidation peak was found between 0.3 and 0.5 V with the maximum intensity at ~0.43 V. The potential of 0.35 V was considered low enough for favoring an appropriate selectivity, yet offering a good signal. A dynamic range of AA concentrations from 10 to 1800 mg L^{-1} was selected considering that the AA concentration of fruit pulps and extracts varies from less than 10 mg L^{-1} to more than 1500 mg L^{-1}. Results are shown in Figure 1.3. Sensitivity of SP was greater about 25 times than that of GC sensor in the corresponding linearity range (up to 400 mg L^{-1}). Because of their higher sensitivity, smaller dimension and the fact that having all the three electrodes of the sensor array together represents an advantage in terms of manageability, screen printed sensors were selected for the successive analyses.

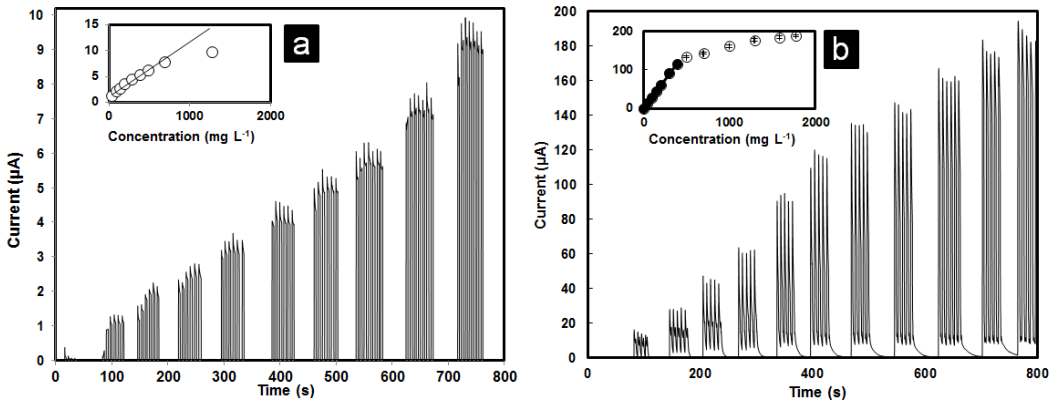

Figure 1.3. Comparisson between the amperometric response of GC (a) and SP (b) electrodes in standard AA (citrate buffer 0.1 M; pH 4.0) 10- 1800 mg·L^{-1} with the corresponding current versus concentration plots (in the box).

The sensitivity of SP sensors modified with nanofibrous membranes of various thickness (SP-NFM) was determined under the same described conditions. As expected the sensitivity changed with membrane thickness. Figure 1.4 shows the sensitivity of the SP-NFM when using different membrane thicknesses. The thinnest membranes (11 ± 2 μm) allowed higher values of sensitivity whereas no influence of membrane thickness was observed when it varied from 34 ± 3 μm to 50 ± 3 μm. On the other hand, thicker membranes (108 ± 4 μm) caused a significant signal reduction. This is due to the electrical resistance of the membrane that adds to the ohmic drop of the sensor, contributing to a slower electron transfer. However, it must be noticed that membranes are prone to breakage when the thickness is less than 30 μm. In order to have reasonable resistance and sensitivity for the samples under study, membranes of 34 μm (obtained after 15 min of electrospinning) were used in all subsequent analyses.

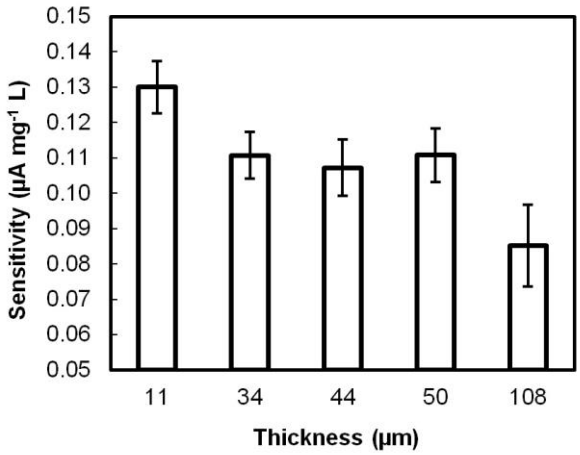

Figure 1.4 Effect of the membrane thickness on the sensitivity of SP-NFM electrode (AA from 10–1800 mg $L^{-1;}$ 0.1 M citrate buffer at pH 4.0). Vertical error bars correspond to standard deviations of n = 3 repetitions.

Figure 1.5 shows the amperometric responses obtained by using SP and SP-NFM sensors at increasing AA concentrations from 10 to 1800 mg L^{-1} at pH 4.0. Each peak array corresponds to

repetitive measurements of the solutions at the same concentration. Coating of the SP sensor with the nanofibrous membrane entailed a widening of the linearity range and a decrease of the sensitivity. Namely, linearity range of the SP electrode (Figure 1.5a) was 10-400 mg L-1 whereas that of the SP-NFM (Figure 1.5b) was 10-1300 mg L^{-1}. Sensitivity of the SP-NFM sensor was nearly 25% that of the SP sensor. These results are in agreement with the presence of a partial barrier-to-diffusion effect of the membrane. Since vitamin C can be present in high and different amount in fruits, and dilution in the proposed assay is not possible, the wider linearity range extends the applicability of this technique to a larger variety of fruits.

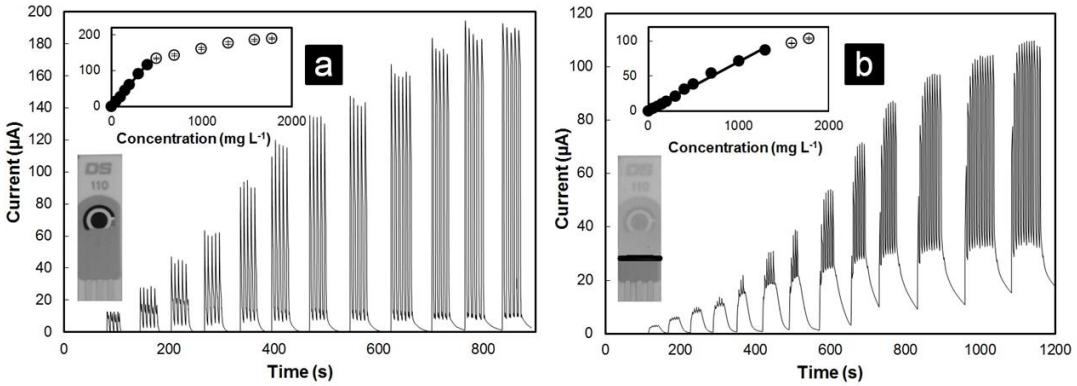

Figure 1.5. Examples of in-batch amperometric responses of SP (a) and SP-NFM (b) electrodes in 0.1 M citrate buffer at pH 4.0 to increasing concentrations of AA (10 – 1800 mg L^{-1}) with the corresponding current versus concentration plots (in the box).

SP-NFM electrode response was rapid (<1 s) even though it was covered with the membrane. The shape of the peak arrays obtained with the SP-NFM electrode appears different (Figure 1.5b). This is due to (i) the effect of membrane impregnation (Figure 1.5a), and (ii) the diffusion phenomenon, which causes a slight signal delay with respect to the SP electrode. The former refers to the elapsed time until the membrane is saturated with the solution, which results in a delay in the signal stabilization; in fact, the signal became stable after the third or fourth immersion in the solution, when the saturation condition is reached. In addition, until the membrane is thoroughly washed with water, it remains soaked with AA solution, which causes a noticeable background signal when the sensor is out of the liquid medium. As long as the measurement is repeated several times (at least 4 to 5), to guarantee a stable response, and the electrode is carefully washed between two different solutions (or samples), neither the repeatability nor the overall signal stability are compromised.

The time that the SP-NFM electrode remained immersed in the liquid medium, here named contact time, affected its sensitivity and repeatability. This effect was investigated and results are shown in Figure 1.6. As can be seen from the figure, contact times of 15 s or larger caused more than 20% of sensitivity loss, whereas no significant differences were found for contact times between 3 and 10 s. With regard to repeatability, contact times between 4 and 10 s were found optimal, with RSD < 2% (n = 30). Considering the high AA concentrations evaluated, the loss of sensitivity might be explained by an excessive accumulation/deposition of the oxidation product, namely dehydroascorbic acid, on the electrode surface, which is favoured by large contact times, causing a passivation-like effect and consequently a decrease in the measured faradaic current.

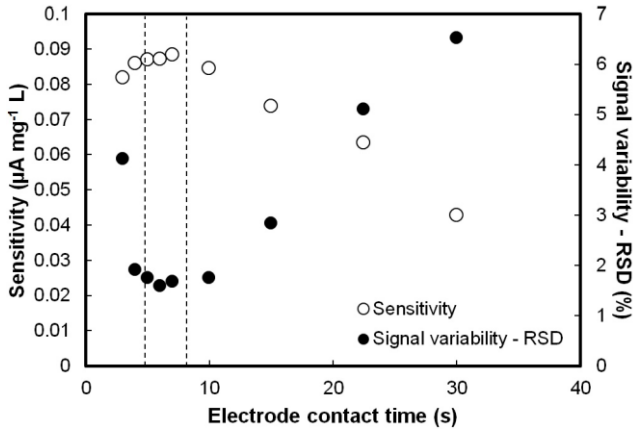

Figure 1.6. Sensitivity and signal variability (% RSD) of SP-NFM sensor as a function of the electrode contact time (extracted from current versus concentration plots: AA from 10 – 1800 mg L-1; 0.1 M citrate buffer at pH 4.0). Dashed lines indicate the optimal range of contact time.

The sensitivity of SP-NFM electrode was also evaluated at different pH values within the typical range of fruits. Figure 1.7 shows the current versus concentration plot from 50 to 1300 mg L^{-1} at pH 2.5, 3.0 and 4.0. There was no correlation ($p < 0.05$) between pH and current for the range evaluated, meaning that, in these conditions pH does not exert a significant effect on the amperometric response.

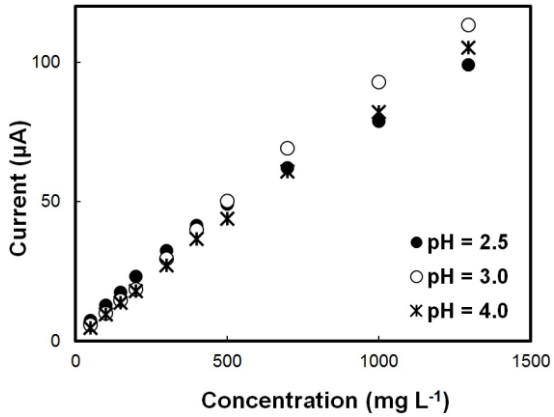

Figure 1.7 Current versus concentration plots obtained with SP-NFM electrode at different values of pH (AA from 10 – 1300 mg L^{-1}; 0.1 M citrate buffer)

1.2.2.2 Interference of phenolic compounds

In order to evaluate the effect of potential interferences, the response of SP and SP-NFM electrodes to standard solutions of different phenolic compounds (caffeic acid, epicatechin, ferulic acid, p-coumaric acid, naringenin, quercetin and tannic acid) that can be naturally found in the fruits, was analyzed. Figure 1.8 shows the characteristic reduction on the sensor response towards phenolics (in this case caffeic acid) caused by the NFM coating.

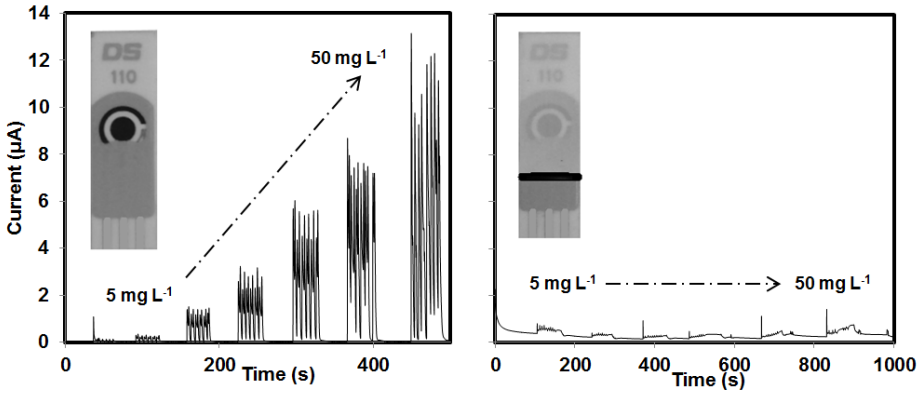

Figure 1.8. Amperometric response of SP (left) and SP-NFM (right) to increasing concentrations of caffeic acid (5 – 50 mg L^{-1}) at an operating applied potential of 0.35 V (0.1 M citrate buffer).

The coated sensor gave lower responses for all the interfering compounds evaluated, showing the efficiency of the membrane in reducing the effect of polyphenols present the fruits under study. Table 1.1 summarizes the amperometric response obtained at the maximum concentration evaluated (I_{max}) of both SP and SP-NFM electrodes, along with the sensitivity, for the different phenolics tested.

Table 1.1. Sensitivity, current at the maximum concentration (*Imax*) and response linearity (r^2) of SP and SP-NFM sensors to standard solutions (0.1 M citrate buffer at pH 4.0) of different phenolic compounds at a working potential of 0.35 V.

Phenolic	Tested range (mg L^{-1})	I_{max} (μA)		Sensitivity (μA mg^{-1} L)	
		SP	SP-NFM	SP	SP-NFM
p-coumaric acid	5 - 20	4.485	0.395	0.081 (r^2 = 0.77)	0.014 (r^2 = 0.65)
caffeic acid	5 - 50	11.804	0.920	0.239 (r^2 = 0.98)	0.017 (r^2 = 0.50)
ferulic acid	0.2 - 1	0.332	0.013	0.313 (r^2 = 0.98)	0.015 (r^2 = 0.73)
naringenin	1 - 10	3.179	0.245	-	-
epicatechin	1 - 10	0.905	0.068	0.099 (r^2 = 0.99)	0.010 (r^2 = 0.92)
quercetin	1 - 10	4.485	0.395	-	-
tannic acid	1 -10	0.427	0.029	0.043 (r^2 = 0.97)	0.004 (r^2 = 0.95)
ascorbic acid	10-1800	189.65	103.76	0.277 (r^2 = 0.99)	0.070 (r^2 = 1.00)

The decrease of the sensor sensitivity towards phenolic compounds cannot be fully explained by the decrease of diffusivity caused by the fibrous layer. As previously observed by Scampicchio *et al*., 2008, nylon nanofibrous membranes act as selective barriers against polyphenol oxidation on carbon electrode surfaces (Figure 1.9). In fact, the diminution of Imax varied from 85% for p-coumaric acid to 96% for ferulic acid. The membranes though, are more effective as barriers towards polyphenols that are highly undissociated (e.g. tannic acid and epicatechin) having more affinity to the NFM than to aqueous medium (Scampicchio *et al*., 2008). Instead, the hydrophobicity of the polyamidic membrane limits the adsorption of smaller phenolic compound (e.g. p-coumaric and caffeic acids) that are partially dissociated at the pH of fruits. These results demonstrate that the NFM-coating help to preserve the sensors from the amperometric response distortion caused by phenolic compounds.

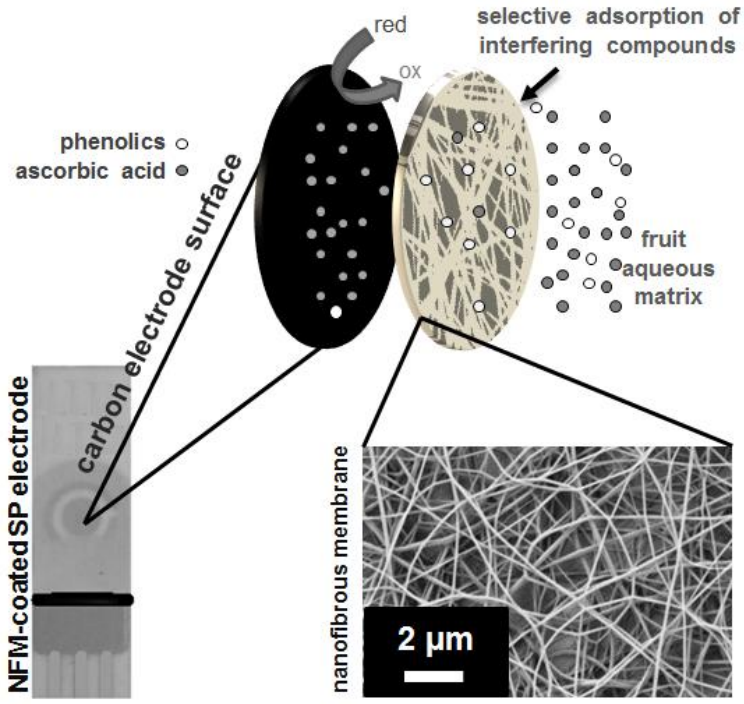

Figure 1.9. Schematic representation of the membrane role in the amperometric in-situ measurement device

1.2.2.3 Analysis of fruit samples

The proposed method was applied to different types of fruits containing between 30 and 600 mg of AA per kg of sample. Each sample was analyzed by directly "pricking" the fruits at least six times with the SP-NFM electrode in three different "slots" (i.e. in triplicate). Between each fruit measurement, the amperometric response for a standard solution was recorded (Figure 1.10). The signal variability of the in-situ measurements, when the fruit was pricked in the same slot, was maximum 7.1% (RSD) whereas it was higher when considered the different slots (RSD up to 11%).

In Table 2 the results obtained by the in-situ amperometric method are compared to those obtained with a standard method (HPLC-UV). The regression line was obtained by linear ordinary least squares, provided that the concentrations obtained by the more precise standard method are reported in abscissa axis. There is a good correlation between the two methods ($r = 0.98$) showing that the membrane is effective in preventing any interference to reach the electrode. In fact, the regression line is $y = 1.046x + 5$ and the confidence interval ($p = 95\%$) for the slope and the intercept are ± 0.091 and ± 38, respectively. The slope is not significantly different from 1 and the intercept is not significantly different from zero, even if its confidence interval is quite large.

As can be seen in Table 1.2, the amperometric determinations gave higher values of standard deviation in all cases respect to the HPLC-UV method, due to the fact that the former does not entail any homogenization protocol and therefore the natural variability related to a complex matrix (in this case the fruit) adds to the intrinsic variability of the method.

It is expected that fruits whose AA concentration is not in the range of the proposed method can still be analyzed by tuning thickness of the membrane and/or the operating potential. Namely,

thicker membranes allow an extended working range though with a reduced sensitivity, which in turn can be improved by increasing the working potential.

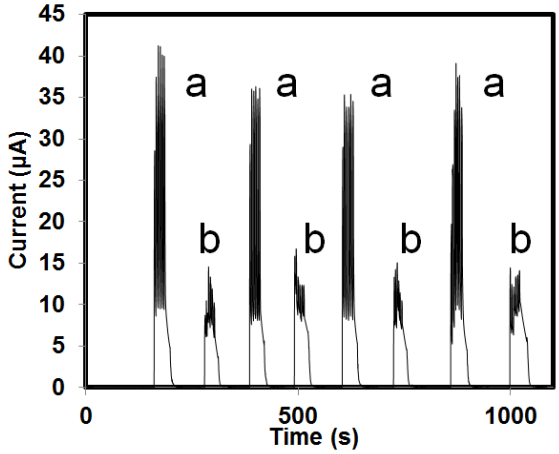

Figure 1.10. Typical plots of amperometric responses used for the quantification of the ascorbic acid content in fruit pulps. The peak arrays correspond to the sensor insertion in (a) standard solutions of AA (800 mg L^{-1}) and (b) lemon pulps.

Table 1.2. Determination of AA content in fresh fruits using SP-NFM electrode (in-situ) and a reference methodology (HPLC-UV) (*n*=3).

Sample	mg of AA kg^{-1}			
	amperometric detection (SP-NFM)		**reference method (HPLC-UV)**	
apple	37	± 8	32	± 1
pear (1)	43	± 5	39	± 0
pear (2)	66	± 6	56	± 1
lemon	390	± 22	432	± 8
kiwi	324	± 46	339	± 9
orange (1)	542	± 50	553	± 43
orange (2)	428	± 22	476	± 12
orange (3)	521	± 43	557	± 4
tangerine (1)	366	± 6	396	± 3
tangerine (2)	448	± 52	411	± 8
tangerine (3)	501	± 48	559	± 1
strawberry (1)	545	± 58	563	± 6
strawberry (2)	547	± 19	555	± 19
strawberry (3)	470	± 17	437	± 8

1.2.2.4 Sensor lifetime

The SP-NFM electrode showed very good operational stability at least after 22 measurements (Figure 1.11-left). However, considering the easiness of preparation and cost, it is recommendable to use a new membrane for each analytical session. Furthermore, the protective effect of the NFM coating against fouling and detrition is evident in Figure 1.11(right) that shows how the amperometric response at the fourth measurement of a real sample (in this case lemon juice) using uncoated electrode (SP) had decayed down to 20% the value of the first measurement, whereas for SP-NFM the response decay was much less dramatic.

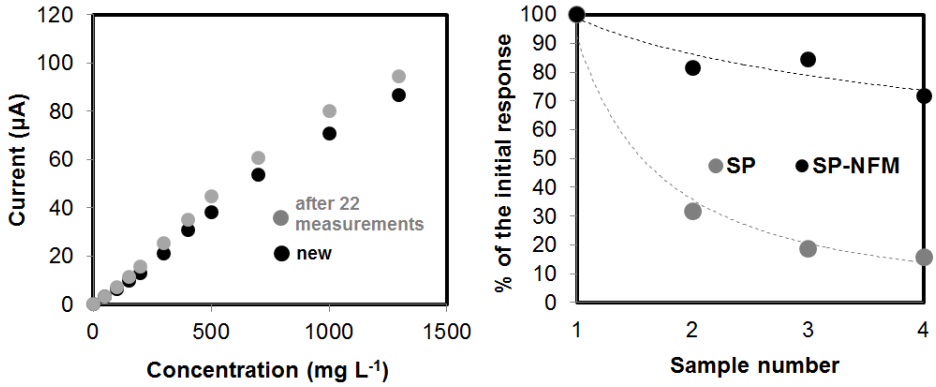

Figure 1.11 Standard curves of AA built using a new SP-NFM sensor and the same SP-NFM sensor after 22 measurements (left); decay of the amperometric reponse of SP and SP-NFM to the same sample (right).

In sum, the applicability of a novel sensing unit based on a disposable screen printed carbon electrode (SP) coated by a electrospun nylon-6 nanofibrous membrane was demonstrated for the in-situ determination of AA in both standard solution and real fruit samples. The sensor displays high sensitivity, reproducibility and selectivity towards AA with a good stability and a fast response. In short, the membrane in this sensing unit acts as a partial barrier-to-diffusion from the matrix to the electrode surface, especially towards phenolic compounds, protecting the electrochemical signal from the distortion caused by the oxidation of these chemical species. In addition, the membrane shields the electrode against the mechanical damage to which it is exposed when introduced in a complex solid matrix as a fruit pulp. Such kinf of methodology is straightforward, rapid and inexpensive for the assessment, especially when compared to traditional analytical determinations that require a sample pre-treatment. Moreover, due to the simplicity of the apparatus, it could be used like a portable device to be applied in the field.

1.3 IMMOBILIZATION OF XANTHINE OXIDASE IN ELECTROSPUN NANOFIBERS FOR SELECTIVE BIOSENSING OF XANTHINE AND HYPOXANTHINE

Purine derivatives play significant role in human metabolism, and hence they are of great biochemical and biomedical interest. Among them, xanthine, hypoxanthine and uric acid are intermediate metabolites of purine in human beings, which are useful biomarkers for several diseases such as perinatal asphyxia, hyperuricemia, cerebral ischemia and gout (Kalimuthu *et al.*, 2012). Inosine is a purine nucleoside composed of hypoxanthine and D-ribose, it is a major degradation product of adenosine with potent immunomodulatory and neuroprotective effects and it has been used to relieve the symptoms of many disease (Liu *et al*., 2006). Besides providing useful markers for clinical studies, purines are important in food quality control as index of the freshness of fish (Jones *et al*., 1964; Alasalvar *et al*., 2001). In fish meat, a large number of post-mortem reactions are initiated during storage. These deteriorative changes consist on the formation of nucleotide and nucleoside metabolities resulting from the ATP degradation.

Many analytical methods were developed for their determination in solution or for monitoring their concentration levels in biological fluids such as human blood, urine, or blood serum (Dutt & Mottola, 1974). Among them, a variety of methods namely HPLC, spectrophotometry, electrophoresis have been used for purines determination. These methods are found to be costly, time consuming and involve complex procedures (Mateos & Bravo, 2007). Most of these compounds are electrochemically active and can be determinate by electrochemical techniques using different conventional and nanostructured electrodes (Pham *et al.*, 2003). Oxidation of some biologically important xanthines was studied by cyclic voltammetry, differential pulse voltammetry (DPV) and stripping voltammetry (CSV), in connection with carbon paste electrode (CPE) (Aydoğdu *et al*., 2014), boron-doped diamond electrodes (Marselli *et al.*, 2003) or glassy carbon electrode (GC) (Luo *et al.*, 2001).

Electrochemical biosensors combine the advantages of the specificity of the enzyme for recognizing particular target molecules with the direct transduction of the rate of reaction into a current. Thus, these biosensors show effectiveness and selectivity for the detection of substrate. In the sensing process, electron acceptors have been used to shuttle electrons from catalytic site to electrode (Grieshaber *et al*., 2008; Vadgama & Crump, 1992). Xanthine oxidase (XAO) based electrochemical biosensors have been employed widely for diagnosis and medical management of xanthinuria, muscle disease, gout, liver disorders, kidney stone and also measurement of meat freshness in food industries (Pundir & Devi, 2014; Vanegas *et al*., 2014; Hu et al., 2000; BAş *et al.*, 2014) . In these biosensors, XAO has been immobilized onto various supports such as nafion membranes, nylon membranes, cellulose acetate membranes, polyvinyl chloride (PVC) membranes (Devi et al., 2011).

As anticipated, electrospun nanofibrous membranes offer prospects in building more efficient interfaces with electronic components whose size is comparable to that of molecules. The extremely high surface-to-mass ratios and high porosities of electrospun nanomaterials, combined with their mechanical properties and versatility and their fabrication straightforwardness. The high porosity especially, is critical to the efficient transport of the analytes through the supporting membrane to the transducer (Scampicchio *et al.*, 2010; Janshoff & Steinem, 2006).

In this part of the thesis we preliminarily explore the capability of XAO-immobilized on nylon-6 nanofibrous membranes to serve as recognition systems of xanthine, in a sensor configuration in which xanthine concentration is related to the faradaic current of its enzyme-catalized oxidation product (i.e., H_2O_2) with an appropriate transducer.

1.3.1 Materials and methods

1.3.1.1 Chemicals

Rodhium, xanthine, hydrogen peroxide, xanthine oxidase (XAO), bovine serum albumin (BSA), glutaraldehyde (GlA) and nylon-6 were obtained from Sigma Aldrich. Formic acid (98%) was purchased from Fluka. Stock solution was prepared by dissolving 0.01g in 10 mL of standard in buffer

phosphate 0.1M pH 7.0.

1.3.1.2 Electrochemical apparatus and transducer preparation

Amperometric measurements were made with a portable Potentiostat (DS-Drop Sens µSTAT 100). A three-electrode system, including working electrode (transducer), saturated Ag/AgCl reference electrode and a Pt counter electrode. As transducer rodhium-carbon paste (5%) was used, based on a serious o previous experiments as it will be discussed below. The transducer was prepared in the dry state by hand-mixing (with a spatula) using powders of rodhium and carbon paste with paraffin wax for 15 min. A portion of the resulting composite was packed firmly into a Teflon electrode cavity in which the electrical contact was established via a copper wire. The composite surface was smoothed on a weighing paper and rinsed carefully with double-distilled water prior to each measurement

1.3.1.3 Fabrication of nanofibrous membranes

As in section 1.2.1.3.

1.3.1.4 Enzyme immobilization

The enzyme xanthine oxidase (XAO) was immobilized on the nylon nanofibers by a drop coating procedure, following the approach given by Scampicchio et al. (2010). An enzyme solution was prepared containing 10 mg of XAO and 40 mg of BSA in 1 mL of buffer phosphate. To this solution, 10 µL of the cross-linking agent glutaraldehyde (GlA) (2,5 % v/v in water) was added. Briefly, 5 x 10-6 L of a 20 g/L xanthine oxidase solution (in PB 0.1 M, pH 7.0) was dropped into the coated electrode. The biosensor was left to dry for 10 min at RT. Next, this dropping procedure was repeated twice. Finally, the biosensor was immersed in a PB 0.1 M solution at pH 7.0.

1.3.2 Results and discussion

1.3.2.1 Selection of the transducer

A series of experiments were carried out in order to evaluate the electrocatalytic action of different modified and conventional electrodes towards hydrogen peroxide, product of reaction carried out by xanthine oxidase:

$$\text{Xanthine} + O_2 + H_2O \xrightarrow{\text{XAO}} \text{Uric acid} + H_2O_2 \quad (1)$$

Optimization of working conditions was accomplished by batch amperometric detection using hydrogen peroxide as a substrate. The selection of rhodium-carbon 5% as the transducer was done on the basis of the comparison of several metal-based electrodes. In order to compare modified electrode, amperometric tests were performed at different fixed potential in buffer phosphate (0.1 M, pH 7.0) on the different electrodes, namely rodhium-carbon 5%, cobalt oxide, platinum-carbon 5%, ruthenium oxide 10%. Results are shown in Figure 1.12.

At higher operating potentials (> 0.4 V), the best sensitivity (i.e., higher peak current) was obtained with ruthenium oxide working electrodes. It must be noticed that such high operating potentials though are not ideal, since at these conditions there is a high tendency to reveal interfering compounds, especially if the analyte must be detected in a food-derived matrix. Conversely, at lower operating potentials (< 0.0 V), hydrogen peroxide produced a reduction signal, for which the highest sensitivity is provided by the rodhium-carbon as working electrode. Therefore, the rhodium-carbon electrode was selected as the transducer for the biosensor device, operating at a potential of -200 mV, in order to minimize possible interferences.

1.3.2.2 Effect of electrode nanofibers-coating on H_2O_2 sensitivity

The second step of this work consisted in comparing the response of hydrogen peroxide using

(i) nude rodhium-carbon electrode, (ii) rodhium-carbon electrode coated with the nanofibrous membranes and (iii) rodhium-carbon electrode coated with the nanofibrous membranes, adding onto the membrane BSA and GlA. With the proposed approach, in the first place the analytes (in this case the purine) must be able to migrate from the bulk to the nanofibers surface (onto which the enzyme-oxidation occurs) and in the second place, the H_2O_2 produced must be able to "trespass" the fibrous network towards the electrode surface, where it is finally detected. Thus this comparison permitted to establish at which extent the membrane limits the H_2O_2 detection detecting a possible barrier-to-diffusion effect.

The results of in-batch amperometric detection of H_2O_2 (12 – 15 mg L^{-1}) experiments are showed in Figure 1.13. The results show that the electrochemical behavior of the three electrodes coated with membrane, BSA and GlA and uncoated are comparable.

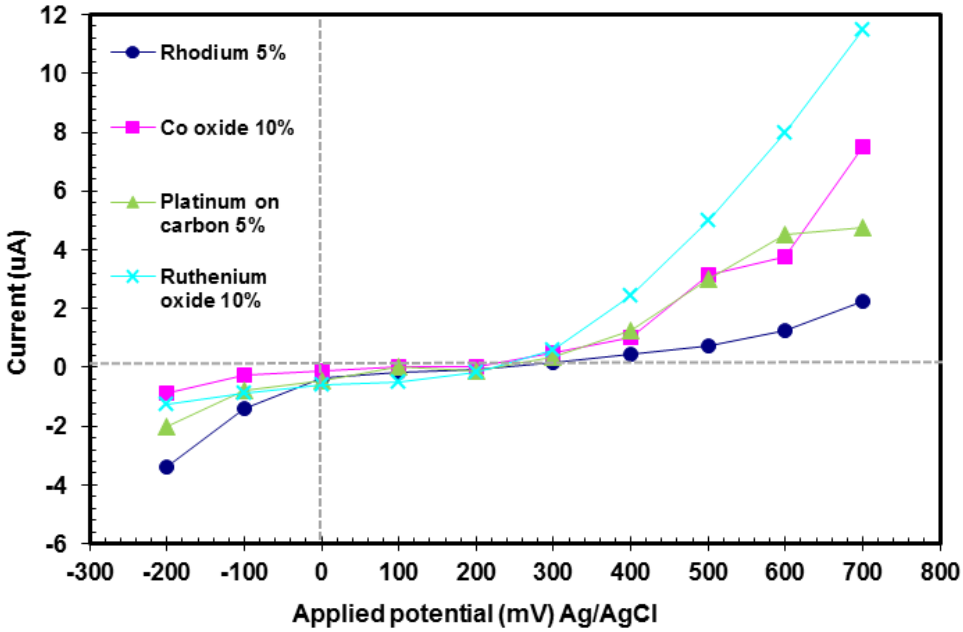

Figure 1.12. Amperometric response of various metallic electrochemical sensors to 50 mg L^{-1} solutions of H_2O_2 at variable applied potentials (phosphate buffer 0.1 M; pH 7.0).

Figure 1.13 (insert) shows also the corresponding calibration curves of the three electrodes (by plotting the concentration against the plateau current obtained after the addition of the analyte subtracting the baseline signal). The sensitivity of the uncoated electrode was 0.10 µA mg^{-1} L in the linear tract, 0.08 µA mg^{-1} L for the membrane-coated electrode and 0.09 µA mg^{-1} L for the electrode coated with membrane, BSA and GlA. This indicates that the redox characteristics of rodhium-carbon electrode are minimally affected by the nanofibrous membranes. The comparison of the electrode with and without coating reveals only a slight change due to a decrease in the mass transport of hydrogen peroxide towards the electrode surface.

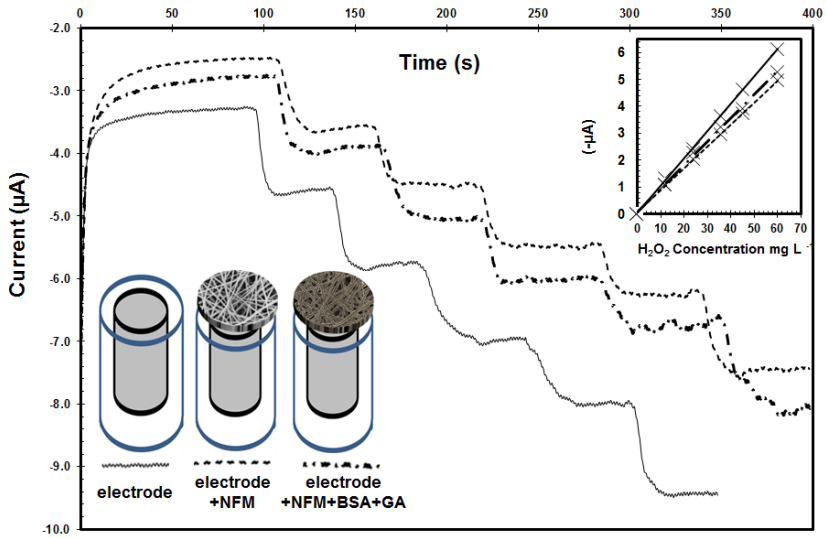

Figure 1.13. In-batch amperometric detection of H_2O_2 (12 – 15 mg L^{-1}) with rhodium-carbon electrodes (uncoated, coated with a nylon nanofibrous membrane and with a nylon nanofibrous membrane with BSA and GlA) at a constant -0.2 V fixed potential (phosphate buffer 0.1 M; pH 7.0). In the insert, the corresponding current-vs-concentration plots.

1.3.2.3 Xanthine biosensing

Finally, the immobilization of xanthine oxidase on the nylon-6 nanofibers and the response of the sensor coated with the recognition system towards the presence of different concentrations of xanthine was studied.

The immobilization technique consisted in a simple procedure. BSA works as a carrier protein and the presence of amine groups, which are bound to the carbonyl group of the glutaraldehyde, leave the active centres of the enzyme at liberty to interact with the substrate (Scampicchio *et al.*, 2010). The amperometric current, at an applied potential of -0.2 V, of XAO-coated sensors in solutions containing 0, 5, 8 and 10 mg L^{-1} was recorded for 2 hours. The resulting signal was xanthine concentration-dependent, showing a noisy-yet-stable trend after ca. 1 h. Subtracting the baseline current allowed to correlate the signal with the xanthine concentration: Figure 1.14 shows the current-vs-time plot for the further 1 h after the stabilization time. The increase in current is attributed to the reduction of hydrogen peroxide on the electrode surface, which is constantly regenerated by the enzyme through the oxidation of xanthine to uric acid. Under this consideration, the reduction current increase rate (-μA s^{-1}) can be considered as a measurement of the reaction rate. Albeit there were too few points for making a statistically-valid quantitative correlation, this variable was positively associated to the xanthine concentration (Figure 1.14-insert), as can be expected for an enzyme-catalysed reaction.

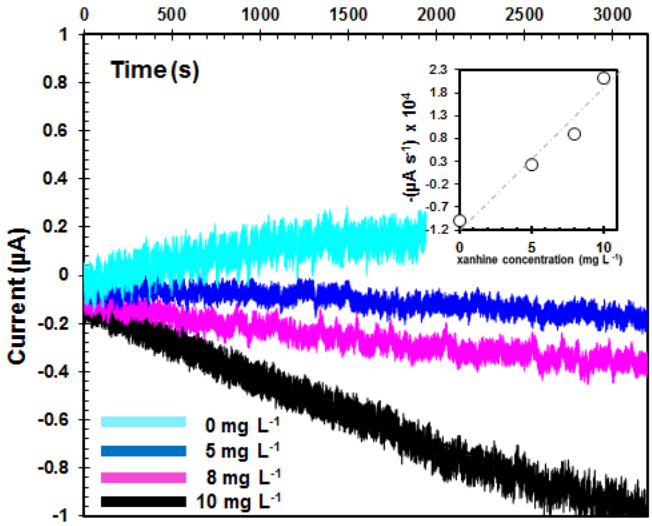

Figure 1.14. Amperometric responses of the XAO/nylon-6/rhodium carbon biosensor, after 1 h of stabilization at a fixed potential of -0.2 V, to different concentrations of xanthine (phosphate buffer 0.1 M; pH 7.0).

In order to produce a more ready-to-use system for xanthine quantitative assessment this kind of sensor can be prepared by using higher loads of enzyme, or enzymes with enhanced catalytic activity which would cope with the relatively long stabilization periods and further improve the overall sensitivity. Nevertheless the results indicate that this device can be a valid alternative for the selective biosensing of xanthine or other purines.

1.4 REFERENCES

1. Akiylmaz E, Dinçkaya E, 1999, A new enzyme electrode based on ascorbate oxidase immobilized in gelatin for specific determination of l-ascorbic acid. Talanta 50: 87-93.
2. Alasalvar C et al., 2001, Freshness assessment of cultured sea bream by chemical, physical and sensory methods. Food Chem 72: 33-40.
3. Allred C, McCreery R, 1992, Adsorption of catechols on fractured glassy carbon electrode surfaces. Anal Chem 64: 444-448.
4. Arecchi A, 2009, Electrospun nanofibrous membranes: novel materials for food technology applications. In 14th Workshop on the Developments in the Italian PhD Research on Food Science Technology and Biotechnology, Oristano, Italy.
5. Arecchi A et al., 2010, Nanofibrous membrane based tyrosinase-biosensor for the detection of phenolic compounds. Anal Chim Acta 659: 133-136.
6. Asard et al., Vitamin C Function and Biochemistry in Animals and Plants. Bios Scientific Publishers, London, 2004.
7. Asefa T et al., 2009, Recent advances in nanostructured chemosensors and biosensore. Analyst 134: 1980-1990.
8. Aydoğdu G et al., 2014, A novel electrochemical DNA biosensor based on poly-(5-amino-2-mercapto-1, 3, 4-thiadiazole) modified glassy carbon electrode for the determination of nitrofurantoin. Sens Actuat B-Chem 197 (2014): 211-219.
9. Barberis A et al., 2010, New Ultralow-Cost Telemetric System for a Rapid Electrochemical Detection of Vitamin C in Fresh Orange Juice. Anal Chem 82: 5134-5140.
10. Barberis A et al., 2012, Detection of postharvest changes of ascorbic acid in fresh-cut melon, kiwi, and pineapple, by using a low cost telemetric system. Food Chem 135: 1555-1562.
11. BAş S et al., 2014, Hypoxanthine Biosensor Based on Immobilization of Xanthine Oxidase on Modified Pt Electrode and Its Application for Fish Meat. Int J Polym Mater Polym Biomater 63: 476-485.
12. Bordonaba J, Terry L, 2009, Development of a glucose biosensor for rapid assessment of strawberry quality: relationship between biosensor response and fruit composition. J Agric Food Chem 57: 8220-8226.
13. Brause A et al., 2003, Determination of total vitamin C in fruit juices and related products by liquid chromatography: Interlaboratory study. J AOAC Int 86: 367-374.
14. Campuzano S, Wang J, 2011, Nanobioelectroanalysis based on carbon/inorganic hybrid nanoarchitectures. Electroanal 23: 1289-1300.
15. Chae S et al., 2007, Polydiacetylene supramolecules in electrospun microfibers: fabrication, micropatterning, and sensor applications. Adv Mater 19: 521-524.
16. Chigome S, Torto N, 2011, A review of opportunities for electrospun nanofibers in analytical chemistry. Anal Chim Acta 706: 25-36.
17. Civit L et al., 2008, Amperometric Determination of Ascorbic Acid in Real Samples Using a Disposable Screen-Printed Electrode Modified with Electrografted o-Aminophenol Film. J Agric Food Chem 56: 10452-10455.
18. Cucchi I et al., 2007, Fluorescent Electrospun Nanofibers Embedding Dye-Loaded Zeolite Crystals. Small 3: 305-309.
19. Dai H et al., 2014, Carbon nanotubes functionalized electrospun nanofibers formed 3D electrode enables highly strong ECL of peroxydisulfate and its application in immunoassay. Biosens Bioelectron 61: 575-578.
20. Demirci Uzun S et al., 2014, Bioactive Surface Design Based on Functional Composite Electrospun Nanofibers for Biomolecule Immobilization and Biosensor Applications. ACS Appl Mater Inter 6: 5235-5243.
21. Devi R et al., 2011, Electrochemical detection of xanthine in fish meat by xanthine oxidase immobilized on carboxylated multiwalled carbon nanotubes/polyaniline composite film.

Biochem Eng J 58: 148-153.
22. Ding B et al., 2004, Titanium dioxide nanoribers prepared by using electrospinning method. Fiber Polym 5: 105-109.
23. Ding B et al., 2010. Electrospun nanomaterials for ultrasensitive sensors. Materials Today, 13: 16-27.
24. Ding Y et al., 2009, Electrospun hemoglobin microbelts based biosensor for sensitive detection of hydrogen peroxide and nitrite. Biosens Bioelectron 25: 2009-2015.
25. Drew C et al., 2004, Electrostatic layer-by-layer assembly of polyelectrolytes on surface functionalized electrospun nanofibers and metal oxide deposition. Abstr Pap Am Chem S 228: 513.
26. Duan A et al., 2011, Nanoparticles as stationary and pseudo-station+ ary phases in chromatographic and electrochromatographic separations. Trac-Trend Anal Chem 30: 484-491.
27. Duncan T, 2011, Applications of nanotechnology in food packaging and food safety: barrier materials, antimicrobials and sensors. J Colloid Interface Sci 363: 1-24
28. Dürüst et al., 1997, Ascorbic Acid and Element Contents of Foods of Trabzon (Turkey). J Agric Food Chem 45: 2085-2087.
29. Dutt V, Mottola H, 1974, Determination of uric acid at the microgram level by a kinetic procedure based on a pseudo-induction period. Anal Chem 46: 1777-1781.
30. Escarpa A, 2012, Food electroanalysis: sense and simplicity. Chem Rec 12: 72-91.
31. Falat L, Cheng H, 1983, Electrocatalysis of ascorbate and NASH at a surface modified graphite-epoxy electrode. J Electroanal Chem 157: 393-397.
32. Florou A et al., 2000, Flow electrochemical determination of ascorbic acid in real samples using a glassy carbon electrode modified with a cellulose acetate film bearing 2,6-dichlorophenolindophenol. Anal Chim Acta 409: 113-121.
33. Formo E et al., 2008, Functionalization of electrospun TiO2 nanofibers with Pt nanoparticles and nanowires for catalytic applications. Nano Lett 8: 668-672.
34. Fu J et al., 2014, Laccase Biosensor Based on Electrospun Copper/Carbon Composite Nanofibers for Catechol Detection. Sensors 14: 3543-3556.
35. Granato F et al., 2008, Disposable electrospun electrodes based on conducting nanofibers. Electroanal 20: 1374-1377.
36. Granato F et al., 2009, Composite polyamide 6/polypyrrole conductive nanofibers. Macromol Rapid Comm 30: 453-458.
37. Grieshaber D et al., 2008, Electrochemical biosensors-Sensor principles and architectures. Sensors 8: 1400-1458.
38. Guanghan L et al., 1994, Determination of ascorbic acid in fruits and vegetables by stripping voltammetry on a glassy carbon electrode. Food Chem 51: 237-239.
39. Guorong Z. et al., 2000, β-Cyclodextrin–ferrocene inclusion complex modified carbon paste electrode for amperometric determination of ascorbic acid. Talanta 51:1019-1025.
40. Hart J et al., 2005, Some recent designs and developments of screen-printed carbon electrochemical sensors/biosensors for biomedical, environmental, and industrial analyses. Anal Lett 37: 789-830.
41. Hart J, Wring S, 1997, Recent developments in the design and application of screen-printed electrochemical sensors for biomedical, environmental and industrial analyses. Trend Anal Chem 16: 89-103.
42. HerricksT et al., 2005, Direct fabrication of enzyme-carrying polymer nanofibers by electrospinning. J Mater Chem 15: 3241-3245.
43. Hou H, Reneker D, 2004, Carbon nanotubes on carbon nanofibers: a novel structure based on electrospun polymer nanofibers. Adv Mater 16: 69-73.
44. Hu et al., 2000, Biosensor for detection of hypoxanthine based on xanthine oxidase immobilized on chemically modified carbon paste electrode. Anal chim acta 412: 55-61.

45. Ijeri V et al., 2004, Electrocatalytic Determination of Vitamin C Using Calixarene Modified Carbon Paste Electrodes. Electroanal 16: 2082-2086.
46. Janshoff A, Steinem C, 2006, Transport across artificial membranes–an analytical perspective. Anal Bioanal Chem 385: 433-451.
47. Ji Y et al., 2006, Structure and nanomechanical characterization of electrospun PS/clay nanocomposite fibers. Langmuir 22: 1321-1328.
48. Jones N et al., 1964, Rapid estimations of hypoxanthine concentrations as indices of the freshness of chill-stored fish. J Sci Food Agr 15: 763-774.
49. Kalimuthu P et al., 2012, Low-Potential Amperometric Enzyme Biosensor for Xanthine and Hypoxanthine. Anal chem 84: 10359-10365.
50. Kilmartin P, 2001, Electrochemical detection of natural antioxidants: Principles and protocols. Antioxid Redox Sign 3: 941-955.
51. Kit-Anan W et al., 2012, Disposable paper-based electrochemical sensor utilizing inkjet-printed Polyaniline modified screen-printed carbon electrode for Ascorbic acid detection. J Electroanal Chem 685:72-78.
52. Kriegel C et al., 2008, Nanofibers as carrier systems for antimicrobial microemulsions. Part I: fabrication and characterization. Langmuir 25: 1154-1161.
53. Kreno L et al., 2011, Metal–organic framework materials as chemical sensors. Chem Rev 112: 1105-1125.
54. Kulys J, D'Costa E, 1991, Printed electrochemical sensor for ascorbic acid determination. Anal Chim Acta 243: 173-178.
55. Lau O et al., 1989, Simultaneous determination of ascorbic acid, caffeine and paracetamol in drug formulations by differential-pulse voltammetry using a glassy carbon electrode. Analyst 114: 1047-1051.
56. Lee J et al., 2011, Fabrication of ultrafine metal-oxide-decorated carbon nanofibers for DMMP sensor application. ACS Nano 5: 7992-8001.
57. Li F et al., 2011, Carbon Nanotube-Adsorbed Electrospun Nanofibrous Membranes as Coating for Electrochemical Sensors for Sulfhydryl Compounds. Electroanal 23: 1773-1775.
58. Liu L et al., 2006, A novel electrochemical sensing system for inosine and its application for inosine determination in pharmaceuticals and human serum. Electrochem Commun 8: 1521-1526.
59. Liu W et al., 2003, Aluminium nitride coated nanofiber. Polym Prepr 44: 132-133.
60. Liu Y et al., 2009, Nonenzymatic glucose sensor based on renewable electrospun Ni nanoparticle-loaded carbon nanofiber paste electrode. Biosens and Bioelectron 24: 3329-3334.
61. Lu X et al., 2005, Fabrication of PbS nanoparticles in polymer-fiber matrices by electrospinning. Adv Mater 17: 2485.
62. Lucena R et al., 2011, Potential of nanoparticles in sample preparation. J Chromatogr 1218: 620-637.
63. Luo H et al., 2001, Investigation of the electrochemical and electrocatalytic behavior of single-wall carbon nanotube film on a glassy carbon electrode.Anal Chem 73: 915-920.
64. Luoh R, Hahn T, 2006, Electrospun nanocomposite fiber mats as gas sensors. Compo Sci Technol 66: 2436-2441.
65. Manesh K et al., 2007, Electrospun poly (vinylidene fluoride)/poly (aminophenylboronic acid) composite nanofibrous membrane as a novel glucose sensor. Anal Biochem 360: 189-195.
66. Manjunatha R et al., 2010, Simultaneous determination of ascorbic acid, dopamine and uric acid using polystyrene sulfonate wrapped multiwalled carbon nanotubes bound to graphite electrode through layer-by-layer technique. Sens Actuat B-Chem 145: 643-650.
67. Mannino S, Cosio M, 1997, Determination of ascorbic acid in foodstuffs by microdialysis sampling and liquid chromatography with electrochemical detection. Analyst 122: 1153-1154.

68. Mao X et al., 2013, Electrospun carbon nanofiber webs with controlled density of states for sensor applications. Adv Mater 25: 1309-1314.
69. Marselli B et al., 2003, Electrogeneration of hydroxyl radicals on boron-doped diamond electrodes. J Electrochem Soc 150: D79-D83.
70. Mateos R, Bravo L, 2007, Chromatographic and electrophoretic methods for the analysis of biomarkers of oxidative damage to macromolecules (DNA, lipids, and proteins). J Sep Sci 30: 175-191.
71. Milakin K et al., 2013, Polyaniline-Based Sensor Material for Potentiometric Determination of Ascorbic Acid. Electroanal 25: 1323-1330.
72. Min Y et al., 2008, The role of interparticle and external forces in nanoparticle assembly. Nat Mater 7: 527-538.
73. Min Y et al., 2008, The role of interparticle and external forces in nanoparticle assembly. Nat Mater 7: 527-538.
74. Nassef H et al., 2007, Simultaneous detection of ascorbate and uric acid using a selectively catalytic surface. Anal Chim Acta 583: 182-189.
75. Nilsson C et al., 2007, Use of nanoparticles in capillary and microchip electrochromatography. J Chromatogr 1168: 212-224.
76. Nováková L et al., 2008, HPLC methods for simultaneous determination of ascorbic and dehydroascorbic acids. Trend Anal Chem 27: 942-958.
77. Numnuam A et al., 2014, An amperometric uric acid biosensor based on chitosan-carbon nanotubes electrospun nanofiber on silver nanoparticles. Anal Bioanal Chem 406: 3763-3772.
78. O'Connell, M, 2012, Carbon nanotubes: properties and applications. CRC press.
79. Ouyang Z et al., 2013, Fabrication, characterization and sensor application of electrospun polyurethane nanofibers filled with carbon nanotubes and silver nanoparticles. J Mater Chem B 1: 2415-2424.
80. P. Gibson, H. Schreuder-Gibson, D. Rivin, Colloid Surf. A, Physicochem. Eng. Asp. 2001, 187, 469.
81. Pakapongpan et al., IEEE International Conference on Electron Devices and Solid State Circuit (EDSSC). Bangkok 3-5 Dec. 2012, 1–3.
82. Patel A et al., 2006, In situ encapsulation of horseradish peroxidase in electrospun porous silica fibers for potential biosensor applications. Nano Lett 6: 1042-1046.
83. Pavan F et al., 2005, Congo Red Immobilized on a Silica/Aniline Xerogel: Preparation and Application as an Amperometric Sensor for Ascorbic Acid. Electroanal 17: 625-629.
84. Pham C et al., 2003, A novel electrochemically active and Fe (III)-reducing bacterium phylogenetically related to Aeromonas hydrophila, isolated from a microbial fuel cell. FEMS Microbiol Lett 223: 129-134.
85. Pinto N et al., 2003, Electroless deposition of thin metallic films on polymer fibers prepared via electrospinning. Abstr Pap Am Chem S 226: 308.
86. Pundir C, Devi R, 2014, Biosensing methods for xanthine determination: A review. Enzyme Microb Tech 57: 55-62.
87. Pumera M, 2007, Electrochemical nanobiosensors. Sens Actuators B, 123: 1195-1205.
88. Ramakrishna et Al. 2006, Science and engineering of polymer nanofibers. In Functional Nanomaterials, Rosenberg, K.E.G.a.E., Ed.
89. Ren G et al., 2006, Electrospun poly (vinyl alcohol)/glucose oxidase biocomposite membranes for biosensor applications. React Funct Polym 66: 1559-1564.
90. Renedo D et al., 2007, Recent developments in the field of screen-printed electrodes and their related applications. Talanta 73: 202-219.
91. Reneker D, Chun I, 1996, Nanometre diameter fibres of polymer, produced by electrospinning. Nanotechnology 7: 216.
92. Roy P et al., 2004, Electrooxidation and Amperometric Detection of Ascorbic Acid at GC Electrode Modified by Electropolymerization of N,N-Dimethylaniline. Electroanal 16: 289-

297.
93. Satheesh T et al., 2010, Gold Nanoparticles Modified Titania Nanotube Arrays for Amperometric Determination of Ascorbic Acid. Anal Lett 43: 2809-2822.
94. Sawicka Katarzyna et al., 2005, Electrospun biocomposite nanofibers for urea biosensing. Sensor Actuat B-Chem 108: 585-588.
95. Scampicchio M et al., 2008, Electrospun nanofibers as selective barrier to the electrochemical polyphenol oxidation. Electrochem Commun 10: 991-994.
96. Scampicchio M et al., 2009, Optical nanoprobes based on gold nanoparticles for sugar sensing. Nanotechnology 20: 135501.
97. Scampicchio M et al., 2010, Nylon nanofibrous biosensors for glucose determination. Electroanal 22: 1056-1060.
98. Scampicchio M et al., 2012, Electrospun nonwoven nanofibrous membranes for sensors and biosensors. Electroanalysis 24: 719-725.
99. Scida K et al., 2011, Recent applications of carbon-based nanomaterials in analytical chemistry. Critical review. Anal Chim Acta 691: 6-17.
100. Senecal A et al., 2008, Development of functional nanofibrous membrane assemblies towards biological sensing. React Funct Polym 68: 1429-1434.
101. Sha Y et al., 2013, A Simple and Rapid Electrochemical Method for Determination of Ascorbic Acid. Appl Mech Mater 341: 866-869.
102. Shen J et al., 2012, Graphene quantum dots: emergent nanolights for bioimaging, sensors, catalysis and photovoltaic devices. Chem Commun, 48, 3686-3699.
103. Shi J et al., 2004, Recent developments in nanomaterial optical sensors. Trac-Trend Anal Chem 23: 351-360.
104. Shi W et al., 2009, The fabrication of photosensitive self-assembly Au nanoparticles embedded in silica nanofibers by electrospinning. J Colloid Interf Sci 340: 291-297.
105. Smith J, Hong-Shum L, Antioxidants. In Food Additives Data Book Second Edition. Wiley-Blackwell, Oxford, UK. 2011, p 59.
106. Speek A et al., 1984, Fluorometric determination of total vitamin C and total isovitamin C in foodstuffs and beverages by high-performance liquid chromatography with precolumn derivatization. J Agric Food Chem 32: 352-355.
107. Sýkora D et al., 2010, Application of gold nanoparticles in separation sciences. J Sep Sci 33: 372-387.
108. Szeto Y et al., 2002, Total antioxidant and ascorbic acid content of fresh fruits and vegetables: implications for dietary planning and food preservation. J. Nutr. 2002, 87: 55-59.
109. Terry L et al., 2005, The Application of Biosensors to Fresh Produce and the Wider Food Industry. J Agric Food Chem 53: 1309-1316.
110. Thangamuthu R et al., 2007, Direct amperometric determination of l-ascorbic acid (Vitamin C) at octacyanomolybdate-doped-poly(4-vinylpyridine) modified electrode in fruit juice and pharmaceuticals. Sens Actuat B-Chem 120: 745-753.
111. Tian L et al., 2006, Electrochemical determination of ascorbic acid in fruits on a vanadium oxide polypropylene carbonate modified electrode. Sens Actuat B Chem 113: 150-155.
112. Toghill K, Compton R, 2010, Electrochemical non-enzymatic glucose sensors: a perspective and an evaluation. Int J Electrochem Sci 5: 1246-1301.
113. Vadgama P, Crump P, 1992, Biosensors: recent trends. A review. Analyst 117: 1657-1670.
114. Valcárcel M et al., 2008, Analytical nanoscience and nanotechnology today and tomorrow. Anal Bioanal Chem 391: 1881-1887.
115. Vanegas D et al., 2014, Xanthine oxidase biosensor for monitoring meat spoilage. Proc. SPIE 9107, Smart Biomedical and Physiological Sensor Technology XI, 91070V.
116. Vaseashta A, Dimova-Malinovska D, 2005, Nanostructured and nanoscale devices, sensors and detectors. Sci Technol Adv Mat 6: 312-318.
117. Vohra V et al., 2011, Electroluminescence from conjugated polymer electrospun nanofibers in

solution processable organic light-emitting diodes. ACS nano 5: 5572-5578.
118. Wang H et al., 2007, Polypyrrole-coated electrospun nanofibre recovery of Au(III) from aqueous membranes for solution. J Membrane Sci 303: 119-125.
119. Wang J, Lin, Y, 2008, Functionalized carbon nanotubes and nanofibers for biosensing applications. TrAC Trends Anal Chem 27:619-626.
120. Wang W et al., 2009a, Three-dimensional network films of electrospun copper oxide nanofibers for glucose determination. Biosens Bioelectron 25: 708-714.
121. Wang W et al., 2009d, Electrospun palladium (IV)-doped copper oxide composite nanofibers for non-enzymatic glucose sensors. Electrochem Commun 11: 1811-1814.
122. Wang X et al., 2002, Electrospun nanofibrous membranes for highly sensitive optical sensors. Nano Lett 2: 1273-1275.
123. Wang X et al., 2004, Electrostatic assembly of conjugated polymer thin layers on electrospun nanofibrous membranes for biosensors. Nano Lett 4: 331-334.
124. Wang Z et al., 2009b, Carbon nanotube-filled nanofibrous membranes electrospun from poly (acrylonitrile-co-acrylic acid) for glucose biosensor. J Phys Chem C 113: 2955-2960.
125. Wang Z et al., 2009c, Enzyme immobilization on electrospun polymer nanofibers: an overview. J Mol Catal B-Enzym 56: 189-195.
126. Wei Q et al., 2006, Surface functionalisation of polymer nanofibres by sputter coating of titanium dioxide. Appl Surf Sci 252: 7874-7877.
127. Wu H et al., 2010, Electrospun metal nanofiber webs as high-performance transparent electrode. Nano Lett 10: 4242-4248.
128. Yang T et al., 2009, Synergistically improved sensitivity for the detection of specific DNA sequences using polyaniline nanofibers and multi-walled carbon nanotubes composites. Biosens Bioelectron 24: 2165-2170.
129. Zampetti E et al., 2011, Biomimetic sensing layer based on electrospun conductive polymer webs. Biosens Bioelectron 26: 2460-2465.
130. Zare H, Nasirizadeh, 2010, Simultaneous determination of ascorbic acid, adrenaline and uric acid at a hematoxylin multi-wall carbon nanotube modified glassy carbon electrode. Sensor Actuat B-Chem, 143: 666-672.
131. Zhang X et al., 2013, A glassy carbon electrode modified with a polyaniline doped with silicotungstic acid and carbon nanotubes for the sensitive amperometric determination of ascorbic acid. Microchim Acta 180: 437-443.

2

NANOFIBERS AS SYSTEMS FOR ENCAPSULATION AND CONTROLLED RELEASE OF BIOACTIVES

2.1 INTRODUCTION

Encapsulation, in the context of the present study, consists in entrapping active ingredients (the cargo), for example food-related bioactive compounds like vitamins, antioxidants, fatty acids, etc., or biological systems such as probiotic cells, digestive enzymes, ect. within "protective"/"barrier" wall materials, e.g., polymers, lipids, gels, supramolecular assemblies, porous minerals, etc. (the carrier). Encapsulation is a thriving research field with many implications and applications in food science and technology, since it is related to key concepts in nutrition and food processing and conservation, in particular with stability, bioavailability and controlled release, but also with undesirable-flavours masking (de Vos *et al.*, 2010). With regard to controlled release, also referred to as extended release, continuous release and targeted release or delivery, it might be defined as the set of technological approaches by which one or more active compounds or ingredients become available in a desired site or time, under desired conditions, at a desired rate, this increasing their effectiveness (Pothakamury & Barbosa-Cánovas, 1995). It has been widely studied and applied in the pharma industry for drugs and active principles, since approximately the mid-XX century (Langer & Pepas, 1983; Brayden, 2003). More recently, in the field of food science and technology a lot of efforts have been focused on the application of such technologies to foodstuffs, in part as a manifestation of the growing trend towards the design of "healthy" food-products, nutraceuticals and the so-called functional foods, i.e., food products or ingredients that are able to provide specific health benefits, beyond the nutrient delivery. In this framework, controlled release primarily pursues two types of objectives: (i) the development of food or food ingredients that, when ingested, are able to fulfil specific functions such as transporting bioactives to precise locations of the digestive tract in which their presence would allow or potentiate the desired biological activity, minimizing any loss or damage (Wildman, 2001; Chen *et al.*, 2006); and (ii) the development of edible devices that, being a part of a food formulation, allow for modulating the release of flavour-related compounds over the shelf-life of the product and during its consumption (Mc Clements, 1998; Piazza and Benedetti, 2010). Controlled release of bioactives is also relevant in active food packaging materials, i.e. materials that offer additional protection against physicochemical and microbiological spoilage of food products during their shelf-life, other than the "inert" barrier features. This includes antimicrobial and oxygen scavenging agents (Rooney, 1995) that interacts directly with the food matrix or, more commonly, are released to the food headspace, helping to preserve the product.

There are several micro- and nanoencapsulation techniques with their particular advantages and drawbacks, and profuse literature has been devoted to this regard (Ezhilarasi *et al.*, 2013). These techniques include freezy-drying, coacervation, emulsification, nanoprecipitation, etc. Amongst these techniques both electrospraying and electrospinning have demonstrated to be very appealing since, besides their straightforwardness and cost-effectiveness, these techniques allow the simple, ultra-fast, single-step synthesis of micro and nanocapsules, either in the form of particles or fibers, in dried form. Besides, the electrohydrodynamic process is appropriate for thermic-labile compounds as it is worked at room conditions (Kriegel *et al.*, 2008; Vega-Lugo & Lim, 2009; Bhushani & Anandharamakrishnan, 2014).

Encapsulating bioactive compounds in nanofibers offer additional benefits with respect to other encapsulation systems. In a certain way, nanofibrous membranes allow for combining the advantages of having fabric-like encapsulating materials (e.g., cast films and sheet carriers), which are "continuous", and have management-versatility and good mechanical features compared to encapsulated powders, together with the advantages of powdery micro- or nanoparticle encapsulating materials, which in turn have larger loading capacities and, by virtue of the sub-micron scale and large surface areas, are more sensitive to changes in the surrounding environment compared to conventional fabric-like materials. Since virtually any release-triggering stimulus can be understood as a particular thermodynamic "state" or "state-alteration" in the surrounding environment, the sensitivity of the encapsulated system to such changes becomes critical for enabling a tuneable delivery of the entrapped compounds.

Therefore, nanofibers constitute outstanding structures for encapsulation and controlled release of molecules. As a consequence of this fact, in the pharmacology field, since the first study on the application of electrospun nanofibers for the sustained release of a model drug using poly (lactic acid) and poly(ethylene-co-vinyl acetate) (Kenawy *et al*., 2002), these materials have been profusely used to achieve many different controlled release profiles, such as immediate/fast, pulsatile, smooth, delayed and biphasic releases (Zhang *et al.*, 2005; Wang *et al.*, 2010a; Hu *et al.*, 2014) of many different drugs and therapeutic agents from antibiotics and anticancer agents to proteins, aptamer, DNA, and RNA (Zamani *et al.*, 2013). Because of their macroscopic morphology, nanofibrous membranes can be applied as a ready-to-use scaffold or tissue, as a continuous coating, or be reduced to smaller pieces, according to the specific needs. It must be noticed that despite of the enormous potential in food-based applications, the use of nanofibers in food processing and preservation has been much less-widely investigated (Kriegel et al., 2008; Bhushani & Anandharamakrishnan, 2014).

Current approaches in electrospun nanofibrous encapsulation systems

Nanofibers can be used mainly (but not only) under three approaches as encapsulation systems for bioactive compounds (Figure 2.1):

(i) By the homogeneous dispersion of the active components within the fibers matrix (Figure 2.1a). In this case the polymer of the fibers act as the only wall material and therefore the only diffusion barrier for the cargo. The properties of the system, like stability and release behaviour, depend mainly on the polymer/bioactive/surrounding environment interactions and on the way the cargo is distributed in the fibers. Usually this type of conformation is achieved by dissolving (or dispersing in the case of insolubility) either the polymer and the active component in the same solvent as a blend before the electrospinning; it is a simple approach and the most common encapsulation method that involves electrospinning (Luong-Van *et al.*, 2006; Yu *et al.*, 2009; Natu *et al.*, 2010; Wang *et al.*, 2010b; Wang *et al.*, 2012). During electrospinning the blend solidifies as the solvent quickly evaporates in the flight towards the collector. The active component remains entrapped inside the polymeric fibers in the dry state, usually in the form of well-separated nanoscopic aggregates comparable to nanoparticles (Neo *et al.*, 2013b). Even though the process generally allows for highly homogeneous dispersion of the active component –especially if the component was solubilized, not dispersed-, due to the flash evaporation of the solvent during the electrospinning and to the ionic strength of the active component, it tends to be located at a higher concentration on the nanofiber surface, favouring the burst release He *et al.*, 2006), causing this approach to be more attractive for fast-delivery applications. Nevertheless, the burst release can be alleviated by tuning the compatibility between the active component and the polymeric carrier at the molecular level (Buschle-Diller *et al.*, 2007; Martins *et al*., 2010; Natu *et al.*, 2010; Wang *et al.*, 2010a), which in some cases has allowed even zero-order-like kinetics (Zeng *et al.* 2005; Alhusein *et al.*, 2012).

(ii) By the homogeneous dispersion of primary cargo-carrier systems within the fibrous membrane matrix (Figure 2.1b), in the form of nanocomposites. The primary encapsulation systems can be basically of any kind as far as they are dispersable in the polymeric solutions: e.g., polymeric or metallic nanoparticles (Wang et al., 2010b), liposomes (Mickova et al., 2012), cyclodextrins (Uyar *et al*., 2009a, 2009b), and more recently mesoporous silica particles (Acosta et al., 2014), amongst others. These structures can be obtained by different variations of the electrospinning process or by post-electrospinning modifications, depending on the type of primary cargo-carrier system; these strategies include: electrospinning of emulsions (Qi *et al*., 2006) and dispersions (Sen, 2004; Stoiljkovic *et al.*, 2007), electrospinning using countercharged nozzles (Park & Lee, 2010), "sacrificial" electrospinning (Ionescu *et al.*, 2010) and surface loading after electrospinning.

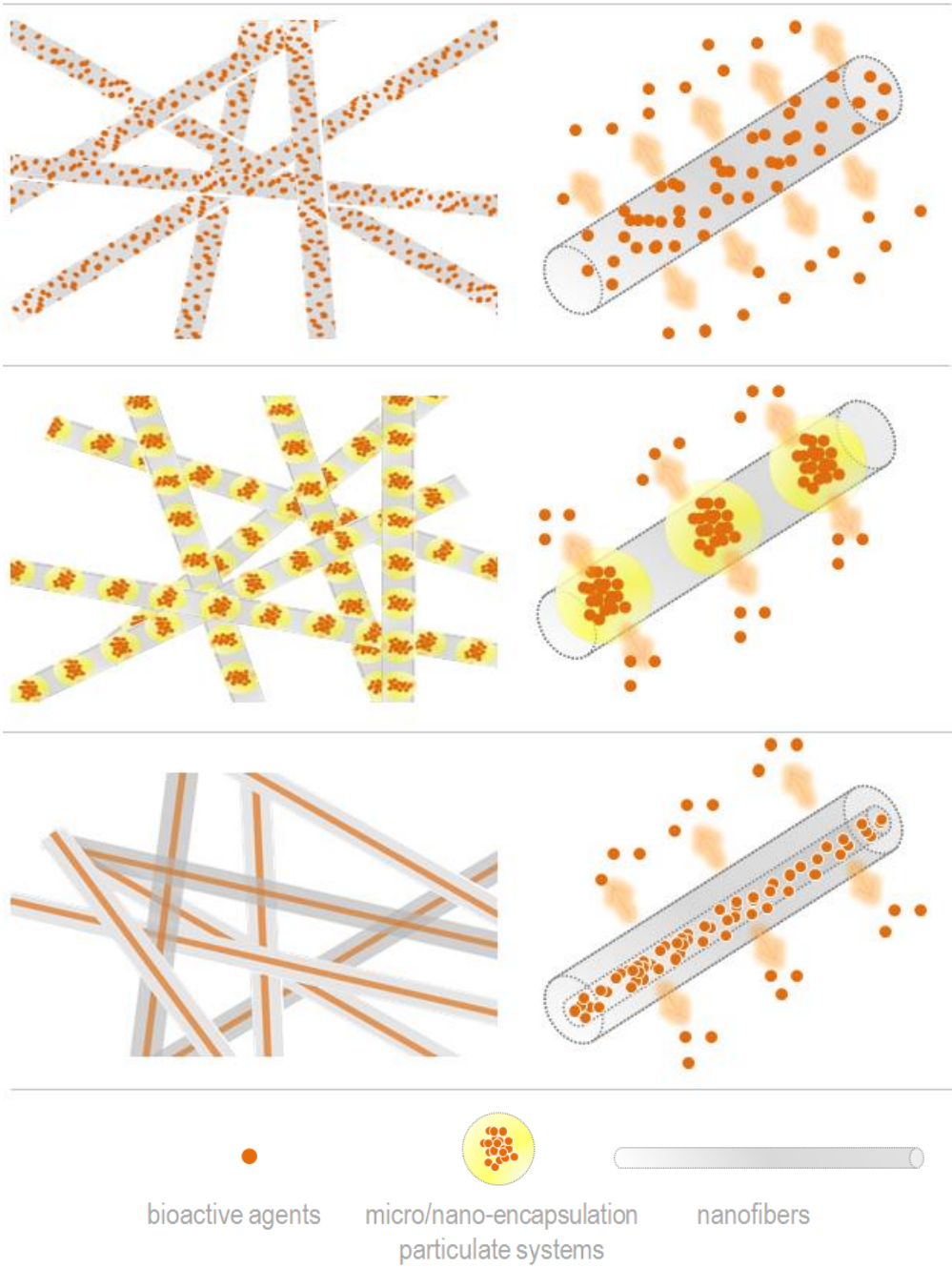

Figure 2.1. Schematic representation of different approaches on the use of nanofibers for encapsulation of bioactive compounds; (i) top: direct dispersion of the bioactive into the nanofiber matrix; (ii) middle: as composites by the incorporation of primary encapsulation systems, e.g., nano/micro-particles, liposomes, etc. in the nanofibrous network; (iii) bottom: as core-shell nanofibrous containers.

Besides the direct dispersion of encapsulation systems in the electrospinning solution, the *emulsion* electrospinning has attracted great attention. In this case, the active element is surrounded by emulsifiers or surfactants and impregnated into the polymeric carrier (Liao *et al.*, 2008; Arecchi *et al.*,

2010). In any case, electrospun matrices embedding particles or other encapsulation systems potentially enable for greater control of bioactives release. This is because both the particle encapsulating the active compound and the fiber material hosting the particle can be tailored for meeting a broader range of specific needs (Meinel *et al.*, 2012). Moreover, under this approach it would be possible to encapsulate active principles that are sensitive to the electrospinning process (Ionescu *et al.*, 2010). In this case, the stability and the release behaviour of the whole system will be defined either by the characteristics of the primary cargo-carrier system, for instance the nanoparticles, and by the nature and degree of molecular interaction between the latter and the polymeric fibrous matrix. The primary encapsulation system can be within the nanofiber or deposited onto it (Beck-Broichsitter *et al.*, 2010; Wang *et al.*, 2010b; Park *et al.*, 2010). This kind of conformation opens numerous opportunities because it enables the combination of the achievements two decades of research on micro- and nanoparticles functionalized for controlled release, with the potentiality of electrospun nanofibers; Meiner et al. (2012) indicates for example, the possibility of encapsulating different nanoparticle species into (or onto) the same matrix, that would offer new options for achieving temporarily staggered release of different active components.

(iii) With a core-shell nanofiber structure (Figure 2.1c). In this approach, an inner fiber or chamber acts as a reservoir for the bioactive element, whereas a an outer layer coats the inner fiber and controls (at least partially) the release of the cargo. These structures can be obtained by coaxial electrospinning or by layer-by-layer assembly. In coaxial electrospinning a concentric spinneret with two nozzle -each of which has a different diameter- is used. Two polymer solutions, dispersions or emulsions are added to the inside and outside spinneret, respectively. Just as normal single-nozzle electrospinning, coaxial electrospinning works electric forces acting on both polymeric solutions and results in significant stretching of polymer jets due to the direct pulling and growth of the electrically driven bending perturbation (Hu *et al*., 2014). By adjusting the flow rates of each liquid and the applied voltage – granted the Taylor's cone stability-, core-shell-structured nanofibers can be obtained. This methodology is particularly interesting since it allows for obtaining nanofibers out of polymers that are not electrospinnable, when they are spun from the inner spinneret. Since this technique was reported for the first time (Loscertales *et al.*, 2002) for obtaining monodisperse capsules containing water-soluble drugs, its application in bioactives encapsulation has been explored widely (Liao *et al*., 2006; Yarin *et al*., 2011). Coaxial electrospinning, compared to normal electrospinning allows for the fabrication of a much wider spectrum of fiber sizes and configurations (Chakraborty *et al*., 2009). On the other hand, layer-by-layer assembly is based on the progressive adsorption of polyelectrolytes or other electrostatically charged components onto the surface of previously prepared electrospun fibers, to form stable encapsulation complexes (Drew *et al.*, 2006). This methodology has been less widely used, although it is of great potential in encapsulation of active compounds for highly-specific delivery, for instance it has been demonstrated that hydrophobic interactions, hydrogen bonding, covalent bending and molecular recognition can be applied in multilayer building up, meaning a great potential for encapsulation purposes (Stockton & Rubner, 1997; Serizawa *et al.*, 2002; Such *et al.*, 2006). This technique has been used for encapsulating polyphenols (Shutava *et al.*, 2009), drugs, herbicides and dyes as "proof-of-concept molecules" (Chunder *et al.*, 2007; Sakai et al., 2009; Wang & Zhao, 2013). It has been suggested that electrospun polyelectrolyte fibers in association with stimuli-responsive polymers could be a promising encapsulation platform for sustained release of active components (Yoo *et al.*, 2009).

Other approaches regard after-electrospinning modifications to the fibers, and they include for instance the physical adsorption or chemical immobilization of compounds onto the nanofibers (Hsieh *et al*., 2005; Ma & Ramakrishna *et al*., 2008).

Polymeric materials

The selection of the polymer material is probably the most critical step in designing

electrospun nanofibrous materials intended for encapsulation of bioactive components, especially regarding food-related applications. Polymer selection is strictly related to the selection of the solvent that is more accurate for dissolution: for food-grade or food-contact materials, not only the electrohydrodinamic parameters related to the electrospinning process itself need to be considered, but also aspects such as toxicity, safety, biocompatibility, etc., must be taken into account.

If the encapsulation system is conceived to be used in a food formulation as a functional ingredient, or in any case, if the final application implies the ingestion/intake of the nanofibrous device, the polymer material (and preferably also the solvent used for the electrospinning solution), must be food-grade, i.e., substances generally recognized as safe (GRAS). This is why so much attention has been paid to the categories of edible polymers, food-grade polymers and biopolymers in this research field. A wide range of natural biopolymers, proteins and polysaccharides are already broadly used for encapsulation, thanks to their controlled release features Chen *et al.*, 2006; Jones & McClements, 2011; Kriegel *et al.* (2008), Schiffman & Schauer (2008), Stijnman *et al.* (2011), Meinel *et al.* (2012), Bhushani & Anandharamakrishnan (2014), Hu *et al.* (2014) have provided comprehensive insights to the issue of the use of food-grade biopolymers in electrospun nanomaterials, with a particular focus on active principles encapsulation.

Protein-based wall materials used in electrospinning include: whey protein isolate, whey protein concentrate (WPC), soy protein isolate, egg albumen, collagen, gelatin, zein, casein, protein isolated from cereals (e.g., amaranth), hordein, gliadin and gluten (López-Rubio & Lagaron, 2012; Neo *et al*., 2012; Aceituno-Medina *et al.*, 2013; Bhushani & Anandharamakrishnan, 2014; Okutan *et al*., 2014). Saccharide- and polysaccharide-based encapsulating materials used in electrospinning include: different types of chitosan, chitin, alginates, cellulose, cellulose derivatives, dextrans, guar gum, pectin, starch and pullulan (Homayoni *et al*., 2009; Fukui *et al.*, 2010; Stijnman *et al*., 2011; Barber *et al.*, 2013; Ghayempour & Mortazavi, 2013; Kong & Ziegler, 2013).

Blends of biopolymers with biocompatible synthetic polymers used in pharmacological applications have been also explored for the fabrication of nanofibrous encapsulation systems, in part with the aim of enhancing the mechanical features of the resulting material or in order to improve the fiber forming ability of the biopolymer (Kriegel *et al.*, 2009). Poly(ethylene oxide) (PEO) and polyvinyl alcohol (PVA), for instance, combined with biopolymers such as egg albumen and cellulose acetate have made feasible the fiber formation by capturing protein within an entangled network (Wongsasulak *et al.*, 2007; Wongsasulak *et al.*, 2010). Whey protein isolate/β-lactoglobulin/PEO (Sullivan *et al.*, 2014), PVA together with the soluble fraction of cereal wastes (Kuan *et al*., 2011), PVA/alginates (Safi *et al.*, 2007; Islam & Karim, 2010), Pectin/chitosan/PVA (Lin *et al*., 2012, PVA/gelatin (Yang D *et al*., 2007), PVA/casein (Xie & Hsieh, 2003), PEO/chitosan (Wongsasulak *et al.*, 2014), PEO/alginates (Bhattarai *et al*., 2006; Lu J *et al*., 2006; Safi *et al*., 2007; Bonino *et al.*, 2011), PEO/casein (Xie & Hsieh, 2003), are examples of electrospun bio/synthetic blends that have been used in the production of nanofibers.

Other bio-materials that have been successfully used in nanofibrous encapsulation systems include cyclodextrins (CD) (α-CD, β-CD, γ-CD), CD-derivatives (e.g., hydroxypropyl-β-CD, hydroxypropyl-γ-CD, methyl-β-CD) (Uyar *et al.*, 2009; Celebioglu & Uyar, 2012; Manasco *et al.*, 2012; Kayaci *et al.*, 2013; Sun *et al*., 2013;) and edible resins (Thammachat *et al.*, 2011).

If the encapsulation system is conceived as a food-contact material (e.g., food packaging or food coatings), ideally the polymeric material need to be natural or environmentally sustainable, efficient, resistant, non-toxic and off-flavour-free in order to be acceptable by consumers (Neo *et al.*, 2013); in the case of food-coatings, the material needs also to be edible. Along with the use of bioactive plant extracts or natural compounds with antimicrobial or antioxidant capacities to be encapsulated and used as active agents for prolonging the shef-life, there is also a fertile research field devoted to polymer and polymer blends that are able to perform well regarding the release of this kind bioactive compounds in a controlled way while meeting the above-mentioned characteristics. Polymers such as zein, cellulose acetate, soy protein isolate (SPI), gelatin, chitosan, PLA, PEO, PVA, polyvinylpyrrolidone (PVP), polycaprolactone (PCL), PCL/PLA, PCL/poly(trimethylene carbonate

(PTMC), SPI/PLA/β-CD, zein/PLA/PEO, have been used for electrospinning of nanofibrous carrier materials for encapsulating plant or fruit extracts and essential oils (Sikareepaisan *et al.*, 2008; Han *et al*., 2009; Opanasopit *et al*., 2009; Vega-Lugo & Lim, 2009; Gomez-Estaca *et al*., 2012; Charernsriwilaiwat *et al*., 2013; Karami *et al.*, 2013; Pérez Masiá *et al*., 2013; Wang *et al.*, 2013).

In this chapter, the use of nanofibrous membranes as systems for encapsulation and controlled release of bioactive materials, with potential uses as functional ingredients or food active packaging devices, is explored. The first case-study (section 2.2) regards the use of blend electrospinning to produce edible nanofibers and nanofibrous composites –either fast disintegrating and not- for the encapsulation and fast release of antioxidants, namely hydrophobic and hydrophilic phenolic compounds. The second case-study (section 2.3) consist in the production by electrospinning of nanofiber/mesoporous silica microparticles (NF-MSP) composites for the encapsulation of hydrophobic antioxidants (naringenin); in this case, the MSP functionalization with pH-responsive molecular gates (i.e. a polyamine) allows for a highly specific release at neutral pH (7) whereas entrapping the cargo in acid media (pH 2). In the third case-study (section 2.4) the potential of electrospinning in the encapsulation of aroma volatile compounds is explored; model aroma compounds (perillaldehyde, limonene, eugenol) are encapsulated in β-CD inclusion complexes and homogeneously dispersed in polysaccharide nanofibrous membranes in a single electrospinning step and the release of the volatile compound occurs beyond a threshold of water activity ($a_w \geq 0.9$) of the environment.

2.2 DIRECT INCLUSION OF ANTIOXIDANT PHENOLIC COMPOUNDS IN EDIBLE NANOFIBROUS MEMBRANES

Phenolic compounds are more than eight thousand naturally occurring substances such as flavonoids, phenolic acids and tannins, with different bioactive functionalities, usually found in plant and plant products (Harborne *et al*., 1999). Flavonoids are the largest group of plant phenolics and the variations in their structure result in the major flavonoid classes: flavonols, flavones, flavanones, flavanols, isoflavones and anthocyanidins. Similarly, phenolic acids constitute another important class of phenolic compounds that can be classified as hydroxybenzoic and hydroxycinnamic acids, according to their structure.

In particular, phenolics are considered among the largest contributors to the antioxidant potential of plant-origin food products (Larson, 1998). Probably the most largely described feature of almost all the groups of phenolic compounds is their antioxidant capacity. This is due to their redox properties, which play an important role in scavenging free radicals and oxygen species or decomposing peroxides (Nijveldt *et al.*, 2001); such properties varies from one specific polyphenol to the other, and are closely related to their chemical structure, especially to the number of hydroxyl groups on the aromatic ring and conjugated double bonds, but also to their degree of O-methylation, the 2-3 double bond and 4-oxo function and their degree of polymerization, amongst others (Foti *et al*., 1996; Natella *et al*., 1999; Silva *et al*., 2000; Heim, *et al*., 2002).

Furthermore, phenolics are one of the major classes of antimicrobial plant products (Cowan, 1999). The mechanisms thought to be responsible for phenolic toxicity to microorganisms include enzyme inhibition by the oxidized compounds, substrate deprivation, membrane disruption, binding to adhesins, complexing with cell walls, interaction with eukaryotic DNA, amongst others (Mason & Wasserman, 1987; Brinkworth *et al*., 1992; Toda *et al*., 1992; Perrett *et al*., 1995; Fernandez *et al.*, 1996; Keating & O'Kennedy, 1997). Also in this case, the bioactivity can be very molecule-specific and they are determined by the chemical structure, for instance to the degree of hydroxylation of the phenol group (Geissman, 1963).

In the food industry, phenolic compounds have gained great attention either as possible functional ingredients in food formulations and as functional materials in food packaging. In the first case because they have been claimed to have abilities to promote human health, e.g., reduction in the incidence of some degenerative diseases including cancer and diabetes (Conforti *et al.*, 2009 and Kim *et al*., 2009), reduction in risk factors of cardiovascular diseases (Jiménez *et al.*, 2008), anti-mutagenic and anti-inflammatory effects, etc. (Parvathy *et al*., 2009). In the second case, for their antimicrobial effects and because they represent an alternative to synthetic antioxidants added to polymeric packagings for avoiding the packaging material degradation while reducing lipid oxidation by their release from the package into the food matrix during commercialization (Gómez-Estaca *et al.*, 2014). In sum, polyphenols are currently the major group of interest amongst plant-origin bioactive compounds (Cowan, 1999; Aridogan *et al.*, 2002; Belščak-Cvitanović *et al.*, 2011; Gou *et al*., 2011).

The presence and distribution of functional groups in their molecules (e.g., hydroxyl, carbonyl, amide, aromatic rings, carbon-hydrogen skeleton of sugars, etc.) define the hydrophobicity of phenolic compounds, which is a determinant factor in their ability to complex with proteins and polysaccharides, which in turn is critical for many of the typical biological roles of polyphenols (including antimicrobial activity and oxidation-inhibitor capacity) (Haslam, 1996). Consequently they also define their solubility in aqueous media. There are a wide range of water-solubility values for each class of phenolic compounds and, although in the natural state polyphenol-polyphenol interactions usually ensure some minimal solubility in aqueous media, some plant polyphenols may be difficulty soluble in water (Haslam, 1996) and, regretfully, a low water and poor bioavailability are limiting factors for their use as bioactive agents (Shulman *et al.*, 2011). Moreover, most of the phenolic compounds with proven bioactivities are quite reactive, and therefore labile at some extent towards a number of environmental factors. The relevance of phenolic compounds as bioactive agents can therefore be limited by their low solubility and stability. In order to preserve the structural integrity,

phenolics need to be sheltered by a finishing formulation able to protect them and deliver them to the physiological targets without losing any bioactivity (Fang & Bhandari, 2010; Munin & Edwards-Lévy, 2011).

A valid way for stabilization and encapsulation of phenolic compounds is electrospinning (Fernández *et al.*, 2009; Li *et al.*, 2009; Neo *et al.*, 2013b). Shen *et al.* (2011) suggested that incorporating such materials in ultrathin fibers by this technique allows the improvement and enhancement of their functionalities thanks to the nano-scale effects. In the particular case of hydrophobic polyphenols, another interesting approach consists in their encapsulation in cyclodextrins inclusion complexes (IC) which can serve as vehicles for the protection of polyphenols, enhancing the solubility of the lipophilic "guest" while stabilizing it against derivatizing agents such as oxygen, light and heat (Buschmann & Schollmeyer, 2002; Szejtli, 2003; Del Valle, 2004; Duan *et al*., 2005; Jug *et al.*, 2008; Manakker *et al*., 2009; Pinho *et al.*, 2014).

In this work, two types of highly antioxidant phenolic compounds of very different hydrophobicity, namely **gallic acid (GA)** (phenolic acid, water-solubility: ~1.4 x 10^4 mg kg^{-1} at 23°C) and **naringenin (NAR)** (flavanone, poorly water-solubility: ~1.6 x 10^1 mg kg^{-1} at 23°C) (Figure 2.2), are encapsulated by blend electrospinning in ultrafine fibers made of two different edible biopolymers, namely **zein** (a hydrophobic protein extracted from corn maize) and **pullulan** (a water-soluble linear polysaccharide industrially produced by fermentation or starch syrup with a selected strain of *Aureobasidium pullulans*). Aditionally, the single-step electrospinning formation of **pullulan/β-CD** inclusion complex composites, were explored as an alternative for improving the naringenin water-solubility. The stability and morphology of the systems is studied along with the type of possible interactions cargo-carrier; the release of the antioxidants in aqueous media is studied at different pH conditions.

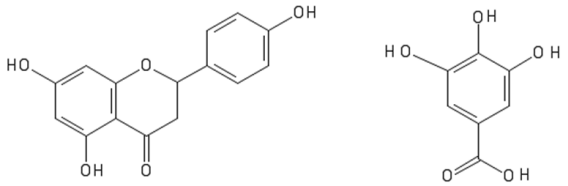

Figure 2.2. Molecular structures of (left) naringenin [(±)-2,3-dihydro-5,7-dihydroxy-2-(4-hydroxyphenyl)-4H-1-benzopyran-4-one, 4′,5,7-trihydroxyflavanone] and (right) gallic acid [3,4,5-trihydroxybenzoic acid].

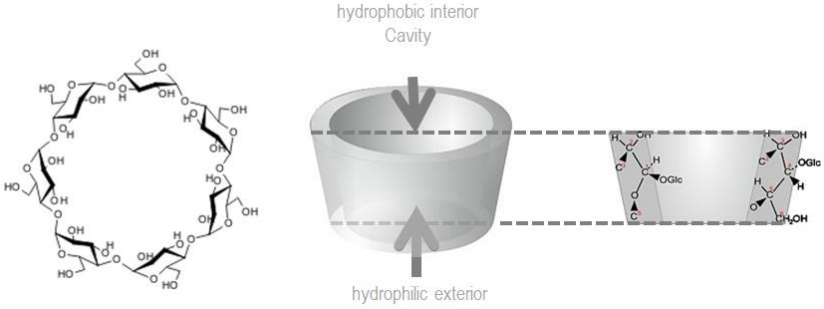

Figure 2.3. Molecular structure of β-cyclodextrin, representation of the hydrophobic conical cavity/hydrophilic exterior and cross-section of a molecule showing the arrangement of a glucose unit.

2.2.1 Materials and methods

2.2.1.1 Chemicals

Gallic acid, naringenin, β-cyclodextrine, zein (from maize, Z3625 CAS 9010-66-6) were purchased from Sigma Aldrich (Milan, Italy). With regard to zein, currently, there are four classes of zein recognized: α, β, γ, and δ. These classes are expressed sequentially in maize and are found to interact with each other for stability. Zein from corn was reported to be approximately 35% α-zein, which includes 2 prominent bands of 22 and 24 kDa. β-zein fails to enter an SDS-PAGE gel without reduction. Reducing SDS-PAGE analysis shows that β-zein has 3 major bands of 24, 22, and 14 kDa (Esen, 1986). The amino acid sequences of this zein have been published (Phillips & McClure, 1985). Pullulan, was a food grade preparation (PF-20 Grade, 200kD) of Hayashibara Biochemical Laboratories Inc. (Okayama, Japan) and was kindly supplied by Giusto Faravelli (Milan, Italy). It is a natural, water-soluble linear polysaccharide industrially produced by fermentation of starch syrup with a selected strain of *Aureobasidium pullulans*. It consists of maltotriose units (α-1,4 linked glucose molecules) polymerized by α-1,6- glucosidic bonds forming a stair-step-type structure. Ethanol (absolute), citric acid monohydrate, sodium citrate, sodium chloride, potassium biphosphate, potassium phosphate, was purchased from Sigma-Aldrich (Milan, Italy) or Fluka analytical (Spain). For release experiments, naringenin solubility studies and analytical determinations of the antioxidants concentration, citrate buffer (0.1 M; pH 2.0, 0.1M adjusted with HCl and 0.1 M pH 4.5) and phosphate buffer (0.1 M; pH 7.0 and pH 8.0) were used. In every case double distilled water was used; chemicals and solvents were used without any further purification protocol.

2.2.1.2 Preparation of the phenolic-loaded zein nanofibers by electrospinning

Gallic acid-zein and naringenin-zein ethanolic solutions for production by electrospinning of **zein-GA** and **zein-NAR**, were prepared as described by Neo et al. (2013b) with some modifications. The polymer solutions were prepared by dissolving zein (25% w/w) in a hydroalcoholic solution (ethanol:water 4:1) containing the previously dissolved desired amount of gallic or naringenin (in such a way for obtaining 5% w/w of the phenolic with respect to electrospun material, i.e. of dry matter), under constant stirring at room temperature. Solutions were placed in a 10 mL syringe with a metallic needle and put in a KDS 100 (KD-Scientific, USA) syringe pump. The needle was connected to a high voltage generator (Spellman SL150) by an alligator clip. Applied voltage was 16 kV and flow rate of electrospinning solution was 0.5 mL h^{-1} and the collection time was 1 h. A foil-covered copper tray located at 12 cm from the needle tip was used as a collector for the electrospun fibers. After electrospinning, the fibers (still attached to the foil) were taken off and then left to dry at room conditions, before storing them in plastic envelopes.

2.2.1.3 Solubility studies of naringenin and β-CD complexes

For the completion of this work, the solubility of naringenin and naringenin- β-CD complexes in aqueos media at different pH and different temperatures had to be experimentally determined. These studies were done using UV-Vis spectrophotometry (UV-VIS Carry 100 BIO). For the quantification, as described by Shullman *et al.* (2011), concentratred stock solutions of naringenin in ethanol (10^4 mg L^{-1}) were used for the preparation of naringenin solutions (0-100 mg L^{-1}) in buffers at pH 2.0, 4.5, 7.0, 8.0 and pure water. The absorbance spectra for these solutions were recorded from 800 nm to 200 nm wavelength. The peak absorbances of naringenin in each solution (288.7 nm for pH 2.0; 287.8 nm for pH 4.5 and pure water, 321.6 nm for pH 7.0 and 322.05 nm for pH 8.0) were correlated with its concentration allowing for the build-up of the corresponding pH-specific calibration curves. For the determination of naringeninn solubility at room temperature, excess amount of the compound were added to the different aqueous media, stirred for 6 hours, sonicated for 10 min and then centrifuged (8000 rpm for 30 min), the resulting supernatant was readily dissolved 20-fold (for avoiding possible temperature-induced re-precipitation) and its naringenin content was determined. For the solubility at

37.5°C, a similar procedure was followed but as a difference, the solutions were stirred under incubation at that temperature for 6 hours and then solutions were left to decant overnight, before up-taking the supernatant.

Naringenin-β-CD complexes were prepared as follows: excess amounts of naringenin and β-CD were added to water and incubated under constant stirring at 37.5 °C for 5 hours; the supernatant was taken then and filtered (0.45 µm) and readily dissolved 20- to 50-fold for solubility at 37.5°C. For solubility at room temperature, the previously incubated mixtures were left under stirring at room temperature until temperature arrived to 23°C. Since β-CD-complexation exerts no effect on the absorbance spectra of naringenin, naringenin concentrations could be determined also by UV-Vis.

All these experiments were done at least by triplicate.

2.2.1.4 Preparation of the phenolic-loaded pullulan and pullulan-β-CD nanofibers by electrospinning

Pullulan-GA electrospinning solutions were prepared by dissolving the pullulan (20% w/w) in gallic acid solutions in water at 10^4 mg L^{-1} at room temperature under stirring for 4 h. **Pullulan-NAR** electrospinning solutions were similarly prepared by dissolving the pullulan (20% w/w) in naringenin solutions in water at 10 mg L^{-1} or for **pullulan-NAR-excess** in naringenin oversaturated mixtures (5 x 10^3 mg L^{-1}) that were additionally homogenised with UltraTurrax (17 krpm, 2 min). For **pullulan-β-CD-NAR** the electrospinning solutions were prepared dissolving the pullulan (20% w/w) at room temperature under stirring for 4 h in a previously prepared saturated solution of the complex (see above). Electrospinning of these mixtures was the same to that followed for the zein-phenolic materials (see above), but with the difference that process was followed by 20 min since after that time, less stable Taylor's cone conditions were observed.

2.2.1.5 Morphology of the fibers

The fiber morphology of the electrospun materials was studied by Field-Emission Scanning Electron Microscopy (FE-SEM). FE-SEM microphotographies were acquired by a FE-SEM ULTRA 55-44-22, evaluated by secondary (SE2) and backscattered electrons (AsB) detectors. Samples were coated with platinum and examined at 5 kV.

2.2.1.6 Loading efficiency

For evaluating loading efficiency of the electrospinning processes, a portion of the membrane was weighed (typically from 10 to 30 mg), dissolved in 10 mL ethanol (for phenolic-zein fibers) or in water (for phenolic-pullulan fibers), stirred for 3 h and sonicated for 10 min,. The concentration was then determined. For gallic acid: An amount of the dissolution was diluted properly in a pH 7 buffer and its concentration was determined by means of cyclic voltammetry. In this case, measurements were done from 0 to 1 V with screen-printed electrodes DS 410 (DropSens, Spain) and correlated with previously built calibration curves at the corresponding buffer conditions. For naringenin, the same spectrophotometric assays described above were followed. The corresponding value of phenolic amount in the membrane was then reported to the corresponding membrane weigth for obtaining the loading value (e.g., mg of compound/g of electrospun material, or mg of compound/g of polymer). The percentage loading efficiency is defined as: [*experimentally determided loading value / theoretical loading value] x 100*. Results were obtained with at least 4 replicates.

2.2.1.7 Release studies at different pH

For naringenin: a proper amount of membrane (ranging typically 1 to 3 mg for zein-NAR, pullulan-NAR-excess and pullullan-β-CD-NAR, or from 15 mg to 30 mg for pullulan-NAR) was weighed and placed in a glass containing 50 mL the corresponding buffer (releasing medium), at pH 2.0, 4.5, 7.0 for zein-NAR, or in water for pullulan materials, with very gentle stirring. After times of 1, 3, 5, 7, 25, 45, 52 s, 1 mL sample of the reselasing was taken , its UV abs- spectra was recorded from 800 to 200 nm and finally it was carefully re-added to the releasing medium for minimizing

losses or dilution/concentration-effects. Note: since solubility in water for this compound is very low, it is worth to say that attention was paid in order to guarantee that a maximum theoretical concentration well below the naringen solubility could be released to the medium, thus ensuring bulk release conditions.

For gallic-acic: a proper amount of membrane (typically from 10 to 17 mg), was weighed and placed in a glass containing 40 mL of the corresponding buffer (releasing medium), at pH 2.0, 4.5, 7.0 for zein-GA, or in water for pullulan-GA, with very gentle stirring. A screen-printed sensor allowed to record cyclic voltammograms (0 – 1 V) (as explained above) directly in the releasing media, which was then correlated to the gallic acid concentrations.

The cumulative release is defined as *the amount of phenolic released per mass unit of encapsulation system at a certain time* (e.g., mg g^{-1} electrospun mat) and the percentage cumulative release is defined as the *[cumulative release/experimentally determined loading value] x 100.*

All the releasing experiments were done at least by duplicate.

2.2.2 Results and discussion

2.2.2.1 Production and morphology of nanofibrous encapsulating systems

Zein-GA and zein-NAR nanofibers

At the electrospinning working conditions it was possible to obtain pure zein electrospun mats that macroscopically looked smooth of a slight pale-yellow colour, but appeared whiter than zein powder. SEM pictures showed that these mats are conformed by randomly-oriented bead-free ribbon-like fibers in the sub-micron scale (Figure 2.4a) with the typical morphology of zein electrospun fibers at the selected working conditions i.e., 25% (w/w) of zein in 80% hydroalcoholic mixtures (w/w) (Yao *et al.,* 2007). The pure zein fibers displayed smooth surfaces and typical diameters ranging between 230 to 396 nm, although some thicker fibers were observed (even above 0.8 µm).

Under similar electrospinning conditions, it was possible to obtain fibers loaded at 5% (g per 100 g of electrospun mat) with gallic acid and naringenin. The phenolic-loaded electrospun mats showed no difference with respect to the pure zein fibers neither macroscopically nor microscopically (Figure 2.4b-c). The fact that no physical separation or particles from these fibers was observed and that the fibers surface appeared smooth just as the pure polymeric electrospun material, suggests that the incorporation of the phenolic compound occurs homogeneously within the fibrous matrix. Neo *et al.* (2012; 2013) obtained similar results when electrospinning zein-gallic acid blends at these working conditions. Thanks to their observations, it is possible to know that the phenolic compound is distributed within the fibers likely in the form of well-separated aggregates rather similar to amorphous nanoparticles (not as crystals). Albeit for the scope of this work the zein fibers were loaded with 5% of the cargo, it was possible to obtain by this methodology bead-free zein fibers carrying up to 20% a phenolic compound, probably entailing a significant increase of the fiber diameters. Such high loadings are possible because of the high solubility of these type of phenolic compounds in the zein electrospinning solvent, namely ethanol-water mixtures.

Phenolics interact at the molecular level with the zein in the phenolic-zein electrospun fibers (as suggested by changes in the infra-red absorbance spectra in particular for the N-H, methyl and amide bands, in the case of gallic acid-zein systems reported by Neo *et al*., 2013, probably forming a complexated form of the phenolic, which is apparently reversible to the non-complexated form.

Pullulan-GA and pullulan-NAR nanofibers

Pure pullulan nanofibers were obtained by the electrospinning of 20% (w/w) polymer solutions in water. Macroscopically, the membranes appeared homogeneous, white and smooth. SEM images revealed randomly-oriented uniform pullulan fibers, with diameters varying in the 250 ± 50 nm range (Figure 2.4d).

The main approach in blend electrospinning consists in using solutions containing both the

fiber-forming polymer and the cargo in a perfectly-dissolved state. This facilitates a more homogeneous distribution of the cargo in the polymeric matrix during the ultra-fast fiber formation in the electrospinning process.

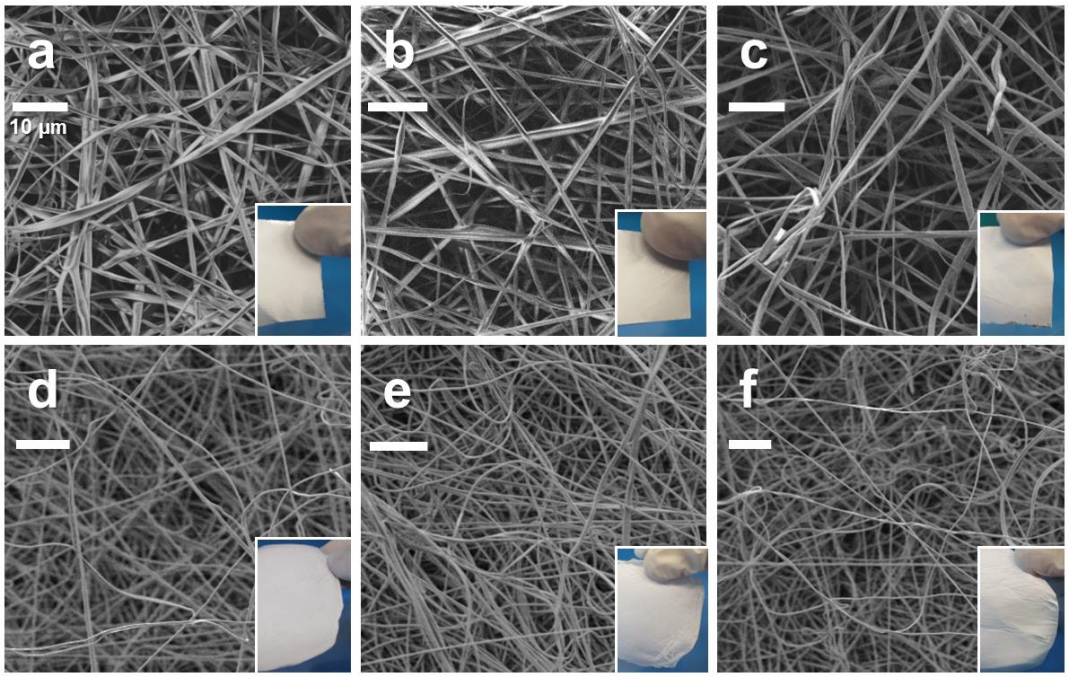

Figure 2.4. SEM micrographs of (a) zein, (b) zein-NAR, (c) zein-GA, (d) pullulan, (e) pullulan-NAR and (f) pullulan-GA electrospun fibers (all the white bars correspond to 10 µm); in the inserts, a photography with a detail of their macroscopic appearance.

Therefore, the amount of cargo loadable by this approach will be perforce limited by the bioactive solubility in the electrospinning solvent. In the particular case of pullulan-phenolic blends, working with perfectly-dissolved electrospinning solutions means that the loading amount is limited by the water-solubility of the respective phenolic compound. Water solubility of gallic acid is about 1.4 x 10^4 mg kg^{-1} at room temperature (Daneshfar *et al*., 2008). Thus, for the **pullulan-GA** blend, the electrospinning solution was prepared by dissolving the pullulan in gallic acid acqueos solution at a concentration of 1.0 x 10^4 mg kg^{-1} –well below the saturation-, which should yield a 0.04 gallic acid/pullulan mass fraction or 3.9% of gallic acid (g per 100 g of electrospun mat). On the other hand, the water solubility of naringenin determined experimentally (as it will be discussed further below) was 16 mg kg^{-1} at room temperature. In this case, for the **pullulan-NAR** blend, the electrospinning solution was prepared by dissolving the pullulan in naringenin aqueous solution at a concentration of 10 mg kg^{-1} –again, well below the saturation-. This should yield a theoretical 0.05 mg naringenin/g pullulan.

The electrospinning of perfectly dissolved solutions allowed for obtaining nanofibrous mats with the same morphology as the pure pullulan electrospun material (Figure 2.4e-f), suggesting, also in this case, that the incorporation of the phenolic compounds occurs homogeneously within the fibrous matrix.

Pullulan-NAR-excess and pullulan-β-CD-NAR nanofibers

Two approaches were followed to cope with the low loadings issue of the naringenin/pullulan system. The first one consisted in producing electrospun mats out of oversaturated solutions of naringenin (**pullulan-NAR-excess**), namely dissolving the pullulan in 5 x 10^3 mg kg^{-1} naringenin

aqueous solution – several orders of magnitude above the solubility-, and subsequently homogenising with an Ultraturrax. This mixture should yield a theoretical 0.02 naringenin/pullulan mass fraction or 2.0% electrospun mat. The electrospinning of this material was possible at similar working conditions, although the process was much less stable, likely due to the presence of precipitated naringenin aggregates that continuously disrupted the Taylor's cone equilibrium. Macroscopically, the electrospun mats obtained by this approach appeared less regular and smooth compared with their pullulan-NAR counterparts (Figure 2.5), and in some areas of the mats it was possible to perceive by touch the formation of glassy patches, suggesting large crystal aggregations. This was confirmed by the SEM pictures, which showed that the characteristic nanofibrous morphology was achieved even though with large spots of dissolved polymer and frequent bulky solid accumulations (Figure 2.5), in concomitance with the observed Taylor's cone instability.

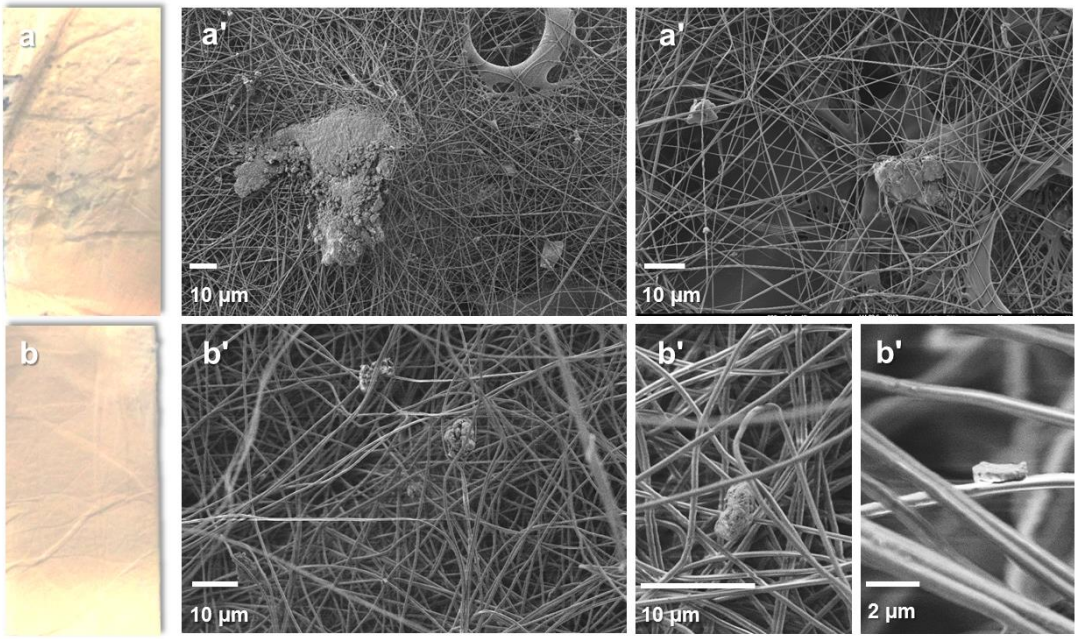

Figure 2.5. A detail of the acroscoscopic appereance of (a) pullulan-NAR-excess and (b) pullulan-β-CD-NAR; SEM micrographs of (a') pullulan-NAR-excess and (b') pullulan-β-CD-NAR.

The second approach consisted in preparing β-cyclodextrin-naringenin inclusion complexes (IC) with their subsequent incorporation in pullulan nanofibers by electrospinning (**pullulan-β-CD-NAR**). Tommasini *et al.* (2004) and Shulman *et al.* (2011) have demonstrated that the solubility of naringenin in water is enhanced by its complexation with β-CD, a compound that is approved either as excipient or as food additive. According to Tommasini *et al.* (2004), the complexes exist in a molar ratio of 1:1. In this study, following a simple methodology (Shulman *et al.*, 2011), the IC were prepared by mixing and incubating excesses of both β-CD and naringenin with the subsequent supernatant separation by centrifugation. The pullulan was dissolved in this supernatant containing the IC and then electrospun. The concentration of naringenin in this solution will be discussed in the following section. The membranes obtained by this approach appeared smooth, white and homogeneous (Figure 2.5) and SEM images showed a comparable morphology to those of pure pullulan or pullulan-NAR with the difference that there was the presence of IC irregular microcrystals of variable dimensions (around 0.7 to 5 µm) along the nanofibers (Figure 2.5). The fact that this type of composite mats can be prepared by directly dissolving the polymer in the IC supernatant represents

a strategic advantage since it does not require neither separation (for instance by filtration, lyophilisation or other drying techniques) nor reconstitution of the complexed antioxidant.

2.2.2.2 Loading and loading efficiency

Zein-GA and zein-NAR nanofibers

The theoretical loading values of these encapsulation systems was 5% (w/w) of electrospun mat. Results showed that the loading of fresh membranes was 4.93 ± 0.15 % (w/w) for **zein-GA** and 5.12 ± 0.60 % (w/w) for **zein-NAR**, meaning that no bioactive is lost during electrospinning process (100% loading efficiency). There was no significant variation after more than two months of storage at room temperature (RH < 60%) (p < 0.05), showing that the cargo was stable in the encapsulation system. It is worth to notice that the hydroalcoholic gallic acid solutions used for zein-GA were be prepared freshly (ideally the same day of electrospinning) since the solutions of this phenolic acid can lead to losses, whereas naringenin solutions showed a greater stability at the same conditions.

Pullulan-GA and pullulan-NAR nanofibers

The amount of bioactive quantified in the fresh pullulan-phenolic nanofibers prepared by perfectly-dissolved solutions were 3.43 ± 0.48 % (w/w) for **pullulan-GA** and 0.0540 ± 0.006 mg/g pullulan for **pullulan-NAR.** Considering that the theoretical loadings were 3.9% (w/w) and 0.05 mg/g pullulan for pullulan-GA and pullulan-NAR respectively, the electrospinning process entailed around 12% of loss of gallic acid and no loss for naringenin. There were no significant variation of these values after more than two months of storage at room temperature (RH < 60%) (p < 0.05) suggesting that the cargo/carrier system was stable at these conditions.

Pullulan-NAR-excess and pullulan-β-CD-NAR nanofibers

Fresh mats prepared by electrospinning of oversaturated solutions of naringenin, **pullulan-NAR-excess** had loading values of 0.0214 ± 0.0088 in mass fraction (naringenin/pullulan). Since the expected loading was 0.02 showing that there were not losses caused by electrospinning but also indicating a large variability in the bioactive loading across the material (RSD = 40%). This agrees with the observation of the heterogeneous appearance and the irregular aggregates formation of this material.

The loading value determined for **pullulan-β-CD-NAR** was 4.71 ± 0.09 mg g^{-1} pullulan. This value was superior to the loading value of **pullulan-NAR** system by 87-fold, demonstrating that this approach is successful for alleviating the low loading issue of poorly water soluble phenolics.

For determining the loading efficiency of these composite membranes, the theoretical loading is needed. This theoretical loading is given by the amount of compound contained in the β-CD-naringenin inclusion complexes (prior to the mixture with pullulan and electrospinning). The experiments that were followed for this determination are presented below.

First, the solubility of pure naringenin was studied in water and buffers at different pH (2.0, 4.5, 7.0 and 8.0) and different temperatures (23°C and 37.5°C). Results are shown in Figure 2.6. and summarized in Table 2.1.

Naringenin solubility is pH- and temperature-dependent. Solubility decreases substantially for pH lower than 7 and increases with the increase of temperature, in agreement with previous observations (Recourt *et al*., 1989; Zang *et al*., 2013). The solubility increase due to the increase in temperature was much more dramatic for pH > 7 i.e., at these pH conditions naringenin was 3 times more soluble at room temperature, whereas it was 15 times more soluble at body temperature. Naringenin, as other flavanones, presents successive dissociations which occur in the following sequence 7-OH, 4'-OH and 5-OH (Agrawal & Schneider, 1983). The pH-related increase in solubility is explained by the first deprotonation of the 7-hydroxy group occurring between pH 6 and 7; in fact, according to Martin *et al*., (2003) the first pK is 6.80 ± 0.01 (Figure 2.5). Therefore, at pH 5.5-6.0

(distilled water) or lower, the undissociated form of naringenin predominates, whereas at pH > 7 its first oxoanion is the major species. Since the solubility depends on temperature at a higher extent for ionized species, this dissociation also explains how at pH > 7 the temperature-induced increase of solubility was that much drastic.

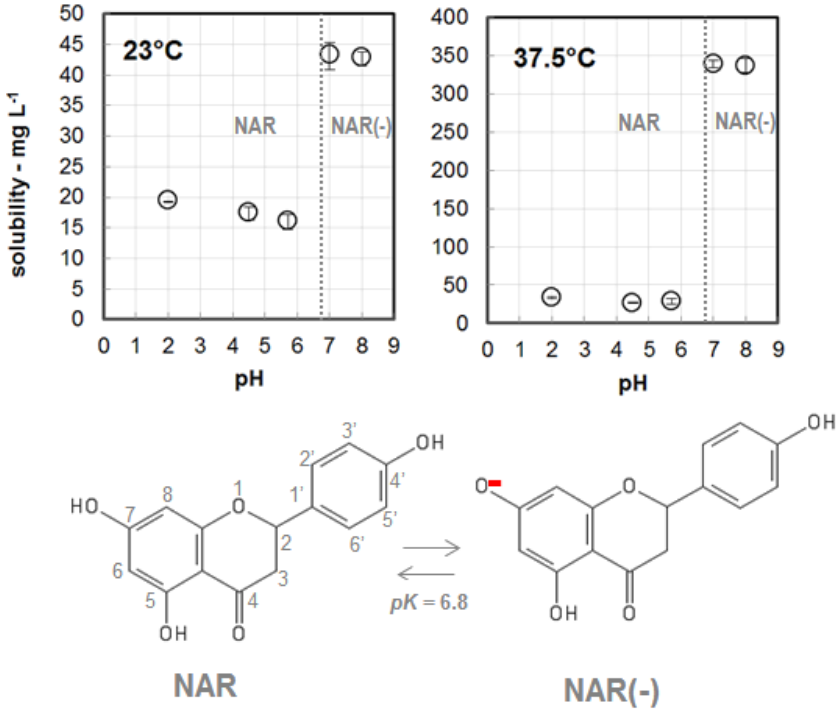

Figure 2.6. Top: naringenin solubility as as function of pH at 23°C and 37.5°C, dashed line indicates pH 6.8; bottom: dissociation of naringenin of 7-hydroxy group to form the first oxoanion, *pK* = 6.8.

Table 2.1 Solubility of naringenin at different pH and temperatures (n = 3)

Medium	Temp.	Naringenin Solubility (mg L^{-1})
water (pH ~ 5.7)	23°C	16.0 ± 1.3
	37.5°C	29.0 ± 3.6
pH 2.0	23°C	19.3 ± 0.1
	37.5°C	33.6 ± 1.2
pH 4.5	23°C	17.3 ± 1.1
	37.5°C	26.3 ± 0.6
pH 7.0	23°C	43.1 ± 2.2
	37.5°C	338.1 ± 4.8
pH 8.0	23°C	42.7 ± 1.2
	37.5°C	336.4 ± 9.1

Secondly, the solubility increase rate thanks to the β-CD complexation was determined. This was done for distilled water and at pH 7 and 8, and at two different temperatures (23°C and 37.5°C).

Results are shown in Table 2.2. The highest solubility (~ 1940 mg L^{-1}) was obtained at body temperature at pH > 7. The largest fold increase in naringenin solubility after β-CD IC formation was 71, obtained at room temperature in distilled water. This result is in partial disagreement with the observations of Shulman *et al.* (2011) who obtained nearly a double increase rate for the β-CD-naringenin IC.

Table 2.2 Solubility of β-CD-complexed naringenin at different pH and temperatures and fold increase due to complexation.

Medium	Temp.	Naringenin Solubility (mg L^{-1})	Fold increase in solubility due to complexation
water (pH ~ 5.7)	23°C	1136.6 ± 43.4	71
	37.5°C	1138.1	39
pH 7.0	23°C	1878.9 ± 13.4	44
	37.5°C	1938.4 ± 1.7	6
pH 8.0	23°C	1747.7 ± 16.6	41
	37.5°C	1937.2 ± 2.2	6

Although increasing the pH from 5.7 to 7.0 entailed an increase in solubility, a further pH increase did not cause remarkable changes, suggesting that rather than pH of the medium itself, the complexation process is affected by the naringenin dissociation. From Table 2.2 it results evident that increasing temperature did not exert the same extent of influence on solubility of complexed naringenin as it did for free naringenin. At the pH range evaluated, increasing temperature from 23°C to 37.5°C occasions only up to 10% of solubility increase of complexed naringenin, and consequently in all cases the fold-increase due to complexation was inferior at 37.5°C. This is not surprising considering that the solubility enhancement due to higher temperatures is counteracted by a negative contribution to the affinity of cyclodextrin, to the substance and therefore to the complex stability and final degree of solubility (Tommasini *et al.*, 2004).

Considering the above results and the methodology followed for the preparation of pullulan-β-CD-NAR nanofibers, an accurate theoretical value of loading corresponds to 4.55 mg g^{-1} pullulan, which leads to 104% of loading efficiency. Table 2.3 summarizes the loadings and loadings efficiencies for all the encapsulation systems developed.

Table 2.3 Loading values of the electrospun encapsulation systems (n = 4)

Phenolic compound	Electrospun encapsulation system	Loading	Units
Gallic acid	zein-GA	4.93 ± 0.15	% (g 100 g^{-1} mat)
	pullulan-GA	3.43 ± 0.48	% (g 100 g^{-1} mat)
Naringenin	zein-NAR	5.12 ± 0.60	% (g 100 g^{-1} mat)
	pullulan-NAR	0.054 ± 0.006	mg g^{-1} pullulan
	pullulan-NAR-excess	21.4 ± 8.8	mg g^{-1} pullulan
	pullulan-β-CD-NAR	4.71 ± 0.09	mg g^{-1} pullulan

2.2.2.3 Phenolics release in aqueous media

Zein-GA and zein-NAR nanofibers

In vitro release studies of the phenolic compounds encapsulated in the zein fibers were carried out in aqueous media, to test the influence of environmental pH; release was studied at three different values of pH: 2.0, 4.5 and 7.0. The results of the percentage of cumulative release for the first hour of experiment are presented in Figure 2.7 as percentage cumulative release agains time. The percentage cumulative release is calculated using as the maximum (100%) the value of phenolic concentration given by the actual loading values (Table 2.3).

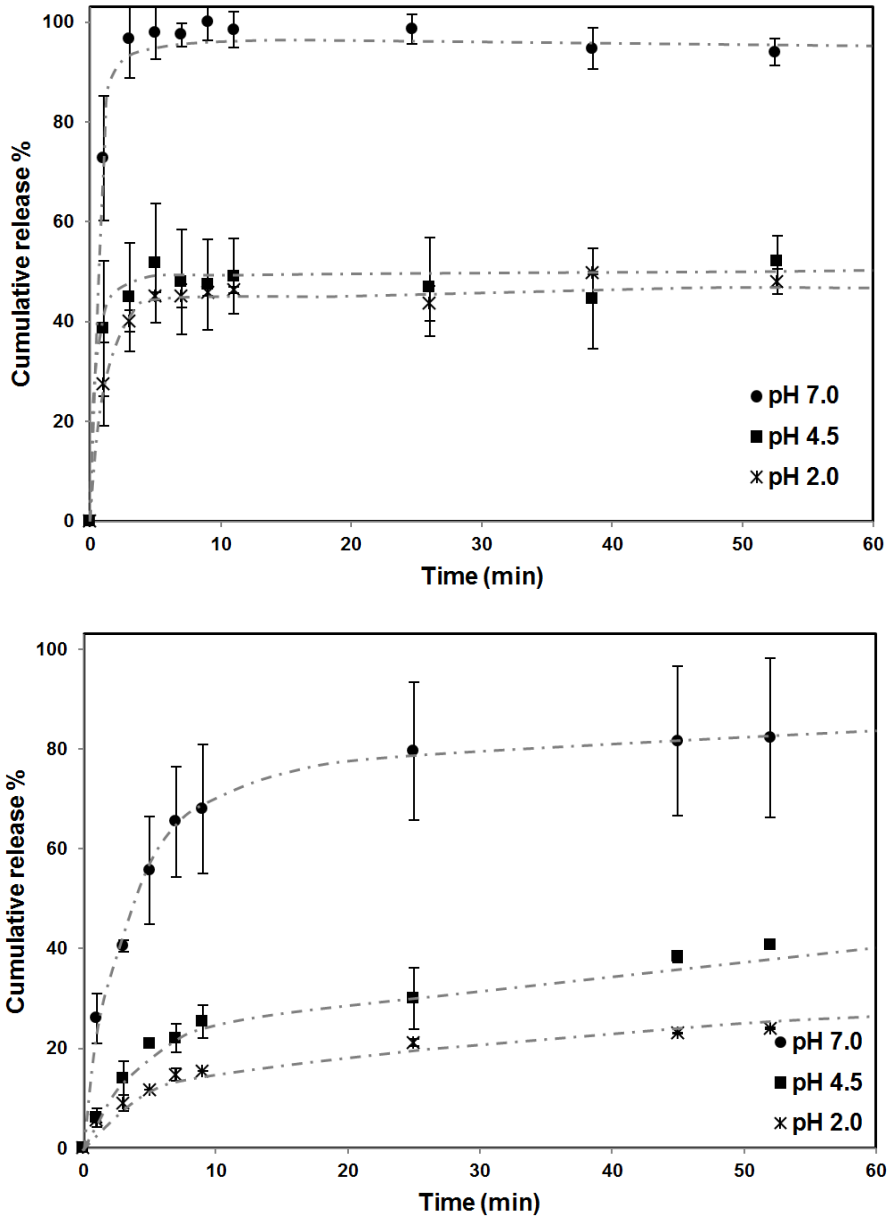

Figure 2.7 Release profiles of (top) gallic acid and (bottom) naringenin from zein-GA and zein-NAR respectively, at pH 2.0, 4.5 and 7.0, until 60 min.

At a first instance it appears that all the curves behave diffusively, with a long time plateau value ($Cw_{|\infty}$, i.e., the concentration of the phenolic in the aqueous phase, in the equilibrium) observed for $t > 25$ min in the case of naringenin and for $t > 3$min in the case of gallic acid. Increasing the pH results in an increase of $Cw_{|\infty}$, suggesting that specific interactions of the drug with the matrix (i.e. hydrogen bonds and electrostatic interactions between naringenin or gallic acid and zein) cannot be assumed negligible with respect to the osmotic pressure controlling the diffusion and release of drugs. The values of the cumulative amount of bioactive released is presented in Figure 2.8 (in % over the actual loading values), as a function of pH.

For both the tested bioactives these interactions appear more important when the pH is low (i.e., a lower value of $Cw_{|\infty}$,is observed), indicating that the overall phenolic release can be modulated by the environmental acidity. The release of gallic acid is much more rapid and is nearly completed after 5 min at pH 7; at this time, zein membranes at pH 2 have released only half of the initially loaded bioactive. The same behavior is observed for the release of naringenin, albeit in this case a complete release of the drug is apparently never reached. If we consider that at 1 h the system is in equilibrium, the partition coefficient, $Kc = Cp/Cw_{|\infty}$, where Cp and Cw are the concentration in the polymeric matrix and the aqueous phase respectively, are pH 2 > pH 4.5 > pH 7.0, for naringenin and pH 2, pH 4.5 > pH 7.0 for gallic acid ($p < 0.05$).

To better understand the diffusion velocity across the matrix, the quantity expressing the percentage of phenolic released, Cw has been normalized for its long time plateau value ($Cw_{|\infty}$) and plotted against the square root of time ($t^{0.5}$). This approach allows for direct comparison between the different release rates of the same bioactive from membranes at different pH. In Figure 2.9, the profiles of naringenin release are plotted against the square root of time. The linear behavior confirms a Fickian diffusion release (Kost & Langer, 2001; Luykx *et al*., 2008). Quite interestingly, we found no significant differences on the release rate (given by the slopes in Figure 2.8) for samples maintained at pH 2, 4 or 7. We conclude that pH only affect the quantity of naringenin released once the plateau is reached (barrier effect), whereas acidity does not have *any* effect on the apparent velocity in the diffusion driven stage of release. A similar conclusion can be hypothesized for the release of gallic acid. Unfortunately, in this case the few experimental data we collected before the plateau is reached do not support a direct evidence of this process. It seems clear though, that its release at all the conditions tested follows the trend of a burst release phenomenon (Huang & Brazel, 2001).

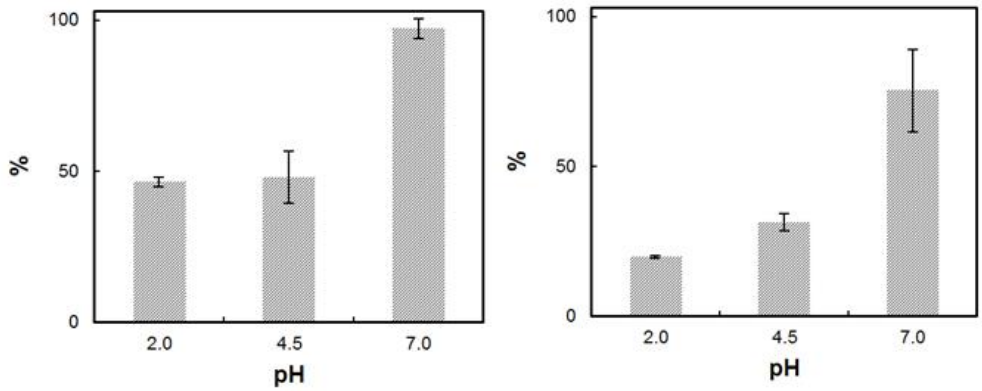

Figure 2.8. Cumulative amount of bioactive (left: gallic acid, right: naringenin) released to the medium at pH 2.0, 4.5 and 7.0 after 1 h ($n = 3$), expressed as % over the actual loading value.

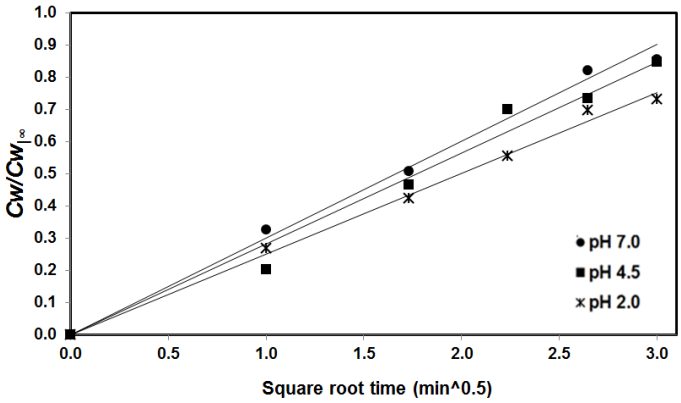

Figure 29. Cumulative amount of bioactive (naringenin) released to the medium, normalized by the long time plateau value ($Cw/ Cw_{|\infty}$,) as a function of square root time, at pH 2.0, 4.5 and 7.0 after 1 h.

For both of the phenolics the more drastic differences in the bioactive release occur in the pass from pH 4.5 to pH 7.0. These results indicate a strong effect of the cargo-carrier chemical affinity on the release behaviour, which results greatly affected by the acidity of the aqueous environment. Our proposal for elucidating this behaviour is that the release phenomenon is influenced by the pH-dependent surface charging of zein, and also by pH-dependent ionisation of the cargo compounds, which suffer important changes within this pH range, as explained below:

With respect to the pH-dependent surface charging of zein, according to de Folter *et al.*, (2012) who investigated the stability and electrostatic repulsions of colloidal zein at different pH, the isoelectric point of corn zein (same commercial reference as used in this work) is ca. pI 6.5. The ζ-potential of acqueous zein particles is maximum at pH 4 (+60 mV), close to zero between 6.2 and 6.5, and -20 mV at pH 7. Therefore, in aqueous media the neat charge of zein at pH 2.0 and 4.5 is very positive whereas it tends to be negative at pH 7.0.

On the other hand either naringenin or gallic acid suffer ionisation changes within this same range of pH that help to further explain changes in the cargo-carrier affinities. In the first place, naringenin undergoes a first dissociation around pH 6.8 as described above (Figure 2.6). With regard to gallic acid, this molecule has 4 potential acidic protons, the first one corresponding to $pKa \approx 4.5$ (carboxylic acid) and the rest to 8.7, 11.4 and 13.1 (Slabbert, 1977; Ji *et al*., 2006). Moreover, the dissociation of a gallic acid-derived free radical (Figure 2.10) has been determined (Eslami *et al.*, 2010) with a $pKa = 5$. In sum, at pH 7.0 the major species of both phenolics will be anionic, whereas at pH 4.5 and 2.0 they will be mainly in the undissociated form (although for gallic acid more precisely a mixture could be expected at pH 4.5).

At the acidic conditions (pH 2.0 - 4.5), the undissociated forms are more affine to the positively charged polymeric fibers, even complexing with the protein (Neo et al., 2013), and thus present a higher tendency to remain encapsulated, compared to the situation at pH 7.0. At the latter conditions the oxoanions have an increased solubility and are probably further repelled by the negative charges of the protein, thus favouring a larger release rate to the aqueous environment, as schematized in Figure 2.11.

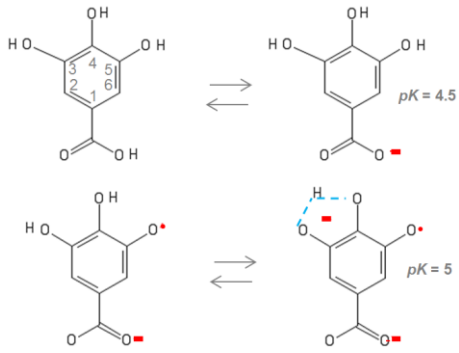

Figure 2.10. Top: dissociation of gallic acid (carboxylic acid), $pK \approx 4.5$; bottom; dissociation of phenolic hydrogen (3- or 4-hydroxy group) of the gallate radical of gallic acid, $pK = 5$.

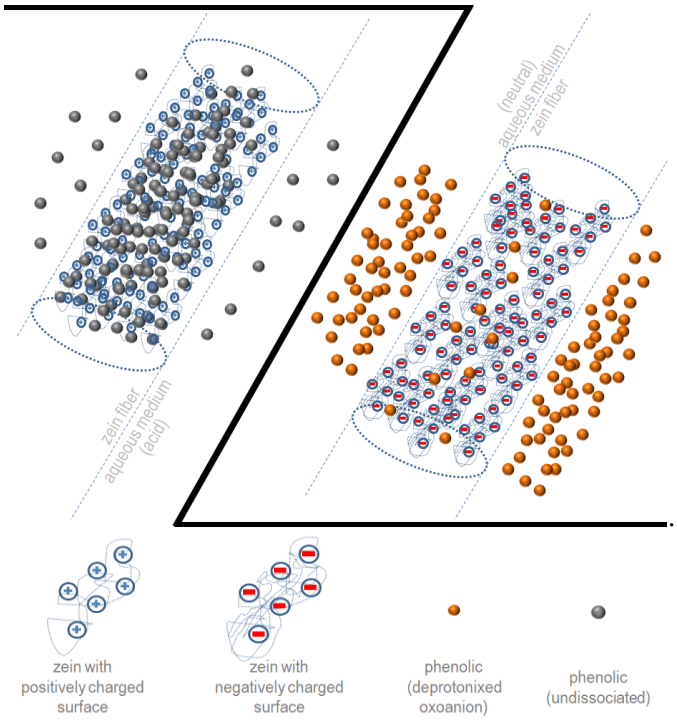

Figure 2.11. Proposed scheme of the pH-dependent total release of phenolics from the zein-phenolic fibers phenomenon. At lower pH (left) phenolics are in a more stable interaction state with zein and partially complexated. At neutral pH (right), an increased cargo affinity to the medium and electrostatic repulsion with the proteins weakens the cargo-carrier interactions, favoring the release.

Therefore, zein-GA and zein-NAR act as a pH-responsive, fully-edible carrier with great potential to be used as an active antioxidant ingredient or packaging/coating material, especially in applications in which the pH increases "downstream". For example, for delivery in the digestive system, this materials could be used for fast release of antioxidants in a first stage at the stomach environment (pH < 2) while "keeping a reserve" of antioxidants to be delivered in a second stage at the gastrointestinal tract (pH 7).

Pullulan-GA and pullulan-NAR nanofibers

Release behaviour of the phenolic compounds encapsulated in the pullulan nanofibers was examined in water. Results of the percentage of cumulative release for the first 30 min of experiment is presented in Figure 2.12. The percentual cumulative release is calculated using as the maximum (100%) the value of phenolic concentration given by the actual loading values (Table 2.3).

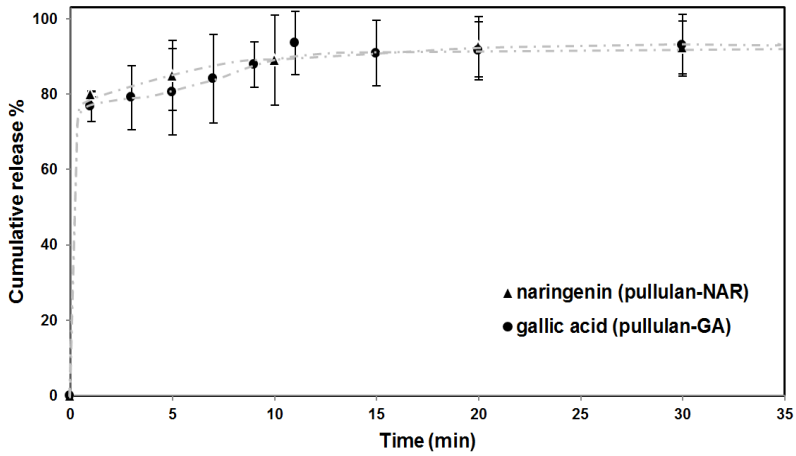

Figure 2.12. Fast release behavior of antioxidants in water from pullulan-gallic acid and pullulan-naringenin "perfectly-dissolved" blends.

In both cases, the antioxidant was rapidly released in the early stage of the experiments (before the first 5 min), after which the bioactive concentration in the medium remained constant, indicating that a plateau in the release trend was reached, following, also in this case, a characteristic burst release phenomenon (Huang & Brazel, 2001). Albeit the loading amount (Table 2.3) and the hydrophobicity of the cargo is very different for each material, there were no differences in the release behaviours. The relevance of this results relies on the fact that it demonstrates that the "nano" effect, in other words, the highly homogeneous distribution of the compound across a nanostructured polymer matrix comparable to a solid "dissolved" state, allows a hydrophobic compound to be released in water following the same trend as a hydrophilic compound.

Since pullulan is water soluble, these systems act as a "self-disintegrating"-fast release device in aqueous media. The principal advantage of the system with respect to the pure substance regards the easiness of handling and -for the applications in which a fast release is wanted-, the fact that they guarantee the dissolution to take place spontaneously within a very short period (e.g., before 1 minute around 80% of the compound is detectable in the aqueous phase) without any kind of mechanical or thermic aid. This latter can be beneficial especially for poorly soluble phenolics, such as naringenin, whose dissolution in water is a rather slow process (see Figure 2.14, discussed further below).

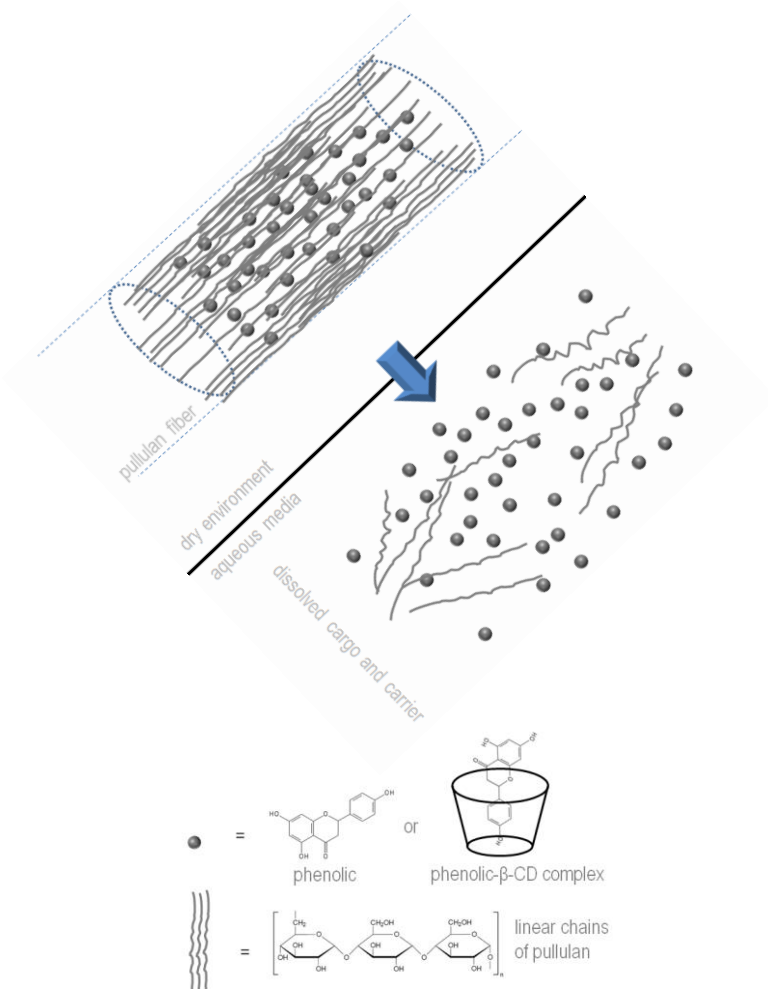

Figure 2.13. Schematic representation of the fast release of phenolics from pullulan-phenolics "perfectly-dissolved" blends.

Pullulan-NAR-excess and pullulan-β-CD-NAR nanofibers

Finally, the release behaviour of naringenin, provided by the two alternative encapsulation approaches for enhanced loading, was studied. Figure 2.14 shows the naringenin percentage cumulative release in water from pullulan-NAR-excess and the composite pullulan-β-CD-NAR. For comparison,the figure includes the release behaviour from pullulan-NAR and the dissolution profile of the pure antioxidant.

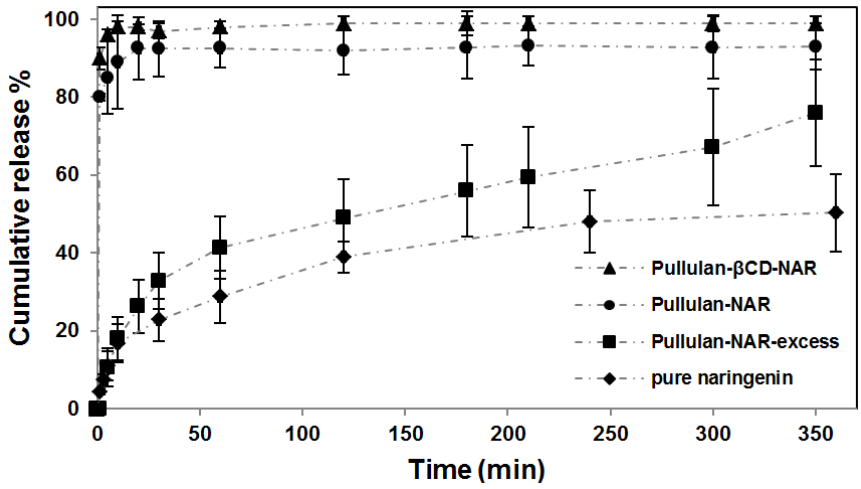

Figure 2.14. Release behaviors in water of naringenin encapsulated in the different pullulan-naringenin nanofibrous configurations, compared to that of pure naringenin.

The figure shows that β-CD-complexed naringenin was released to the medium following the same trend as from the perfectly dissolved (pullulan-NAR) electrospun material, showing that the "nano" effect is maintained. This is a further evidence that naringenin is incorporated in a very homogeneous distribution also by the IC-composite approach. Shulman *et al.* (2011) demonstrated that naringenin complexed in cyclodextrins (in that case hydroxypropoyl-β-cyclodextrin was used) increased its transport across a CaCo-2 model of the gut epithelium by 11-fold, the plasma concentrations when fed to rats and additionally, when the complex was administered prior to meals it decreased low density lipoproteins (VLDL) levels by 42% and increased the glucose clearance rate by more than 60% compared to naringenin alone. According to their results, it was not associated with damage to the intestine, kidney, or liver, suggesting that the complexation of naringenin is a viable option for its oral delivery as a therapeutic entity with applications in the treatment of dyslipidemia, diabetes, and HCV infection.

On the other hand, when electrospinning was done employing oversaturated solutions (pullulan-NAR-excess), the release behaviour drastically changed into a much slower Fickian-like diffusion, which is similar to the dissolution behaviour of the pure substance in the non-encapsulated powder form. This is a consequence of the crystal-forming tendency of the phenolic molecule, which promotes its uneven distribution during the fiber formation as bigger aggregates or crystals. When the pullulan nanofibers come into contact with water, once they are quickly disintegrated (or more properly, the pullulan is readily dissolved), the bulky naringenin particles are released into the medium, causing the overall release phenomenon to be governed by its solubility and the morphology of their aggregates. Being naringenin highly hydrophobic, and thus not prompt to be quickly dissolved in this form, its release into the medium entails the crystals shrinkage by erosion (just like a dissolution), which is usually a highly variable and much slower process.

In conclusion, each one of the systems developed, offered different release behaviours depending both on the cargo and on the carrier, meaning a broad range of potential tailored applications. In the next section, the production by electrospinning of pullulan nanofiborus composites including mesoporous silica microparticles (NF/MSP) functionalized for the pH-triggered release throughout the anchorage of molecular gates, as an additional approach for the pH-differentiated release composites for the encapsulation of the hydrophobic antioxidant (naringenin).

2.3 POLYSACCHARIDE NANOFIBERS/MESOPOROUS SILICA PARTICLES COMPOSITES FOR pH-CONTROLLED RELEASE OF ANTIOXIDANT PHENOLIC COMPOUNDS[1]

In the previous chapter, different approaches were presented for the encapsulation of naringenin as a model hydrophobic antioxidant in ultrafine fibers of edible polymers, through electrospinning. Its homogeneous incorporation in zein allowed for its pH-dependent release, i.e., for higher partition coefficients at acidic pH (2-4.5) and lower partition coefficients in neutral pH (7), meaning that a higher portion of the bioactive is released to aqueous medium in this latter conditions. Moreover, naringenin encapsulated in pullulan (polysaccharide) electrospun fibers allowed for a fast release, whereas its previous complexation with β-CD permitted to increase the naringenin loading, solubility and probably bioavailability.

In all the above case-studies release takes place in a very fast fashion (mostly burst release). In this chapter a new approach is explored for naringenin targeted delivery at neutral pH along with slower release trends.

This new approach consists in the incorporation of particles of an inorganic primary encapsulation system with gated supports, within the nanofibrous matrix. The primary encapsulation system is composed by (i) a suitable inorganic support that acts as the carrier (for loading the naringenin) and (ii) a switchable molecular "gate-like" ensemble that is able to be "opened" or "closed" upon the deliberate use or presence of a predefined stimulus (Coll *et al*., 2013), in this case, a neutral pH. The combination of these two components, depending on the material, determines the controlled release performance of the whole encapsulation system, whereas its inclusion in the nanofibers is aimed as an "auto-dispersing" aid and should not hinder or interfere with the release behaviour provided by the gated particles. A scheme of such systems is depicted in Figure 2.15.

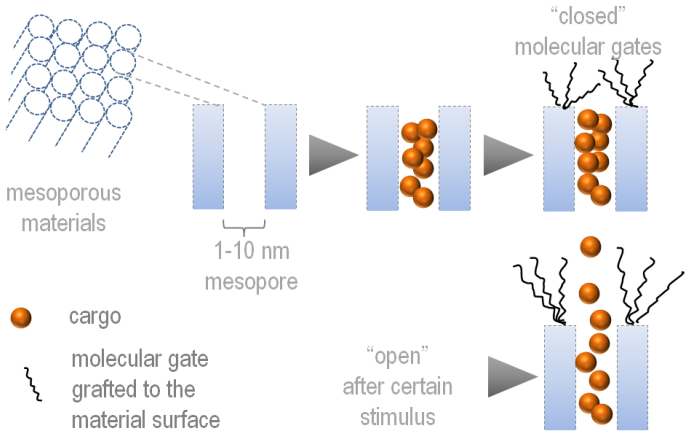

Figure 2.15. Schematic representation of the conceptual functioning of mesoporous materials functionalized with molecular gates for the on-command deliver of bioactive elements.

For this work, the selected inorganic support consisted in mesoporous silica particles functionalized troughout the anchorage of linear polyamines and the polymeric material for the

[1] This work was done in collaboration with Universidad Politécnica de Valencia, Spain (Center for Molecular Recognition – IDM and Food Research and Innovation Group): Profs. José Barat, María D. Marcos, Ramón Martínez-Máñez, and Drs. Carolina Acosta, Édgar Pérez-Esteve, Félix Sancenón and the Institute of Agricultural Chemistry and Food Technology - CSIC, Paterna, Spain (Food Packaging Research Group): Drs. Rafael Gavara and Pilar Hernández-Muñoz.

entangled nanofibrous structure was pullulan.

Anchoring organic or biological molecules on inorganic porous supports has recently attracted broad attention since the resulting hybrid materials show cooperative features, and in particular highly specific functional release behaviors (Descalzo *et al.*, 2006; Hoffmann *et al*., 2006; Aznar et al., 2009; Coti et al., 2009). Mesoporous silica of diverse morphologies and sizes have been extensively used (Carino *et al*., 2007; Heikkila *et al*., 2007; Tang *et al.*, 2012) and can be prepared in different conformations from nanometric to micrometric, with taylor-made pores in the 2-10 nm range. These materials are ideal candidates for delivery applications since they exhibit homogeneous pore sizes, very high specific surfaces (up to 1200 m^2 g^{-1}), large loading capacity, a comfortably high inertness and they are easily functionalized by covalent anchorage with a myriad of organic and biomolecules (Kresge *et al.*, 1992). Up to date, several molecular, supramolecular and nanoparticulated systems have been used for the gate ensemble to deliver entrapped cargos using external stimuli, e.g. redox potential variations, light, temperature, pH, presence of ions, molecules or biological systems (Mal *et al*., 2003; Park *et al*., 2009). With respect to traditional delivery systems based on diffusion-controlled processes, the gated mesoporous silica particles offer a very sophisticated alternative.

To the best of our knowledge there are very few previous works done dealing with the incorporation of silica mesoporous materials (Madhugiri *et al*., 2003) in electrospun fibers, and just until very recently this approach was explored for the masking and on-command release of garlic compounds, by the same research team (Universidad Politécnica Valencia – University of Milan) that took part in the realization of this part of the thesis (Acosta *et al*., 2014).

In this study, two types of mesoporous silica particles were synthesized and used (MCM-41 and SBA-15) for entrapping naringenin, and a pH-responsive linear polyamine (N3) was anchored covalently to the pore outlets of the loaded silica particles. Finally the resulting solids (MSP) were re-dispersed and electrospun with pullulan to produce the nanofibrous NF-MSP composites. The effective loading and release behaviour were studied at pH 7.5 and 2.0. The resulting composite material here developed provides a homogeneous, ready-to-use system with pH-triggered controlled release features with potential applications not only on the food field, but also on biomedicine and engineering.

The physical properties of the materials are not discussed in this document and will be available in a yet-to-be-published paper.

2.3.1 Materials and methods

2.3.1.1 Chemicals

All chemicals were purchased at the highest grade available and used directly without any further purification. Pullulan and naringenin used was the same as for the previous chapter (section 2.2.1.1). All solutions were prepared with acetonitrile (HPLC Gradient grade, Fisher Scientific) and deionized water of resistivity not less than 18.2 MU/cm-1 at 298 K (Millipore UHQ, Vivendi, U.K.). The chemicals tetraethylorthosilicate (TEOS), *N*-cetyltrimethylammonium bromide (CTAB), sodium hydroxide, triethanolamine (TEAH3), pluronic P123 (P123) and 3-aminopropyltriethoxysilane, 3-[2-(2-aminoethylamino) ethylamino]-propyl-trimethoxysilane (N3) were provided by Sigma-Aldrich Química S.L. (Madrid, Spain).

2.3.1.2 Synthesis of the mesoporous silica microparticles

MCM-41: these particles were first synthesized by "atrane route" (Cabrera *et al*., 2000) in which 4.68 g of CTAB were added at 118 °C to a solution of TEAH3 (25.79 g) containing 0.045 mol of a silatrane derivative (TEOS, 11 mL). Next, 80 mL of water were slowly added with vigorous stirring at 70 °C. After few minutes, a white suspension was formed. This mixture was aged at room temperature overnight. The resulting powder was collected by filtration and washed. Solid was dried at 70 °C and, finally, to remove the template phase, was calcined at 550 °C for 5 h using an oxidant atmosphere.

SBA-15: these particles were synthesized following the method reported by Zhao *et al*.(1998),

P123 was used as the structure-directing agent. The molar ratio of the reagents was fixed at 0.017 P123:1.0 TEOS:6 HCl:196 H_2O. The preparation was performed by mixing an aqueous solution of P123 with HCl solution and stirring for 2 h, after which the silica source, TEOS, was added. This final mixture was stirred for another 20 h.

The characteristics of these materials have been studied and discussed recently by Pérez-Esteve *et al*. (2014) and Acosta *et al*. (2014).

2.3.1.3 Loading of the bioactive (naringenin)

For the naringenin-loading of the mesoporous silica materials two different procedures were followed, that were determined as optimal for each one of them. *MCM-41*: a 5 $x10^3$ mg L^{-1} solution of naringenin in a 50% (v/v) hydroalcoholic solution were directly tear-added to MCM-41 particles in a ratio 0.15 mg naringenin/mg of silica solids, divided in three addition-steps; between each addition of naringenin solution, the ethanol was evaporated at 37°C. *SBA-15*: SBA-15 particles were suspended in 5 $x10^3$ mg L^{-1} solution of naringenin in a 50% (v/v) hydroalcoholic solutions in a ratio 0.5 mg naringenin/mg of silica solids, the mixture was stirred for 24 h at room temperature, then the mixture was filtered and dried at room temperature for 24 h.

2.3.1.4 Functionalization of naringenin-loaded with molecular gates

An excess of N3 (0.43 mL) was added to 100 mg of the solids in acetonitrile. The final mixtures were stirred for 5.5 h at room temperature under nitrogen inert atmosphere. Solids were filtered and washed with acid solutions at pH 2.0 (acidified with sulphuric acid). The solids obtained after this procedure are called MSP-41 (those obtained with MCM-41) and MSP-15 (those obtained with SBA-15).

2.3.1.5 Electrospinning of composites

Pullulan solutions in acidified water (acetic acid, 10% v/v) were mixed with an amount of the MSP (typically 5% with respect to dry mass in the electrospun material) and subjected to electrospinning. The different conditions evaluated as an optimization of this process will be discussed further below. The experimental set-up used to carry out the electrospinning corresponded to the YFLOW Ltd (Málaga, Spain) configuration. It consists of a stainless steel needle charged by a high voltage power supply with a range of 0–30 kV. The collector plate was fixed at a working distance of 12 cm below the needle tip and connected to the grounded counter electrode of the power supply (this electrospinning apparatus is set to be operated vertically). A 5 mL plastic syringe was filled with the solution and a syringe pump was used to control the flow rate at which the solution was dispensed. The syringe outlet was connected to the needle through a Teflon® pipe. A video camera connected to a monitor was used to monitor the cone-jet mode. A brass covered with aluminum foil was used as a collector. The systems allows for monitoring the relative humidity and temperature inside the electrospinning chamber, which varied between 45% and 55%, and 22°C and 25°C respectively.

2.3.1.6 Morphology of mesoporous materials and nanofibrous composites

Field emission scanning electron microscope images of the nanofibrous composites were acquired by FE-SEM ULTRA 55-44-22, evaluated by secondary (SE2) and backscattered electrons (AsB) detectors. Samples were coated with platinum and examined at 5 kV. An X-ray EDS detector was used for qualitative elements analysis. Dynamic Light Scattering (DLS) studies. For transmission electron microscopy (TEM) analysis, the mesopotrous particles obtained were dispersed in dichloromethane and sonicated for 2 min to preclude aggregates, these suspensions were deposited onto copper grids coated with a carbon film (Aname SL, Madrid, Spain). Imaging of the samples were performed using a JEOL JEM-1010 (JEOL Europe SAS, France) operating at an acceleration voltage of 80 kV. The single-particle size was estimated by averaging the measured size values of 50 particles.

2.3.1.7 Release studies and effective loading efficiency

For the release studies using MSP, an amount of MSP (around 2 mg) were weighed and suspended in 1.5 mL of buffers at pH 2.0 (0.1M; acetate) and pH 7.5 (0.1 M; phosphate) in Eppendorf tubes. The mixtures were constantly stirred at room temperature. After certain times (typically 15, 30, 60, 120, 210, 310, 420 min), the mixtures were centrigued (8500 rpm x 5 min) and their absorbance spectra were recorded (at pH 2.0 peak wavelength for naringenin was 288 nm and at pH 7.5 it was 323 nm). The absorbance was then correlated to the naringenin concentration by means of pH-specific calibration curves and the cumulative release was defined as *amount of naringenin released at a certain time / mass unit of MSP* (e.g., in µg of naringenin/mg of MSP). The loading efficiency in this work will be defined as the *amount release (cumulative) after 5 hours*.

2.3.2 Results and discussion

2.3.2.1 Gated particles

In this work, MCM-41 and SBA-15 were used as the inorganic supports. A TEM image of typical particles of these two solids is shown in Figure 2.16. The synthesized MCM-41 are irregularly-shaped particles and display mesopores in the 2-3 nm ranges, whereas SBA-15 are elongated particles with a rather-defined hexagonal mesoporous distribution with mesopores in the range 7-9 nm, in agreement with previous observations (Pérez-Esteve *et al.*, 2014). The particle sizes in the dry state varied between approximatly 1 to 1.5 µm for MCM-41 and SBA-15.

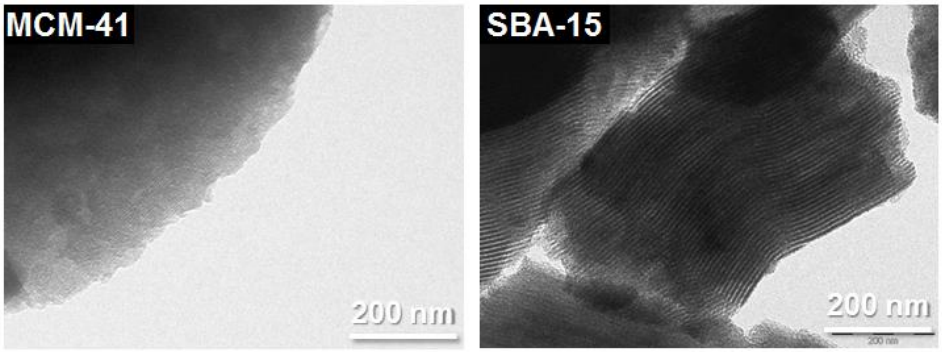

Figure 2.16. TEM images of the mesoporous materials (left) MCM-41 and (right) SBA-15).

For the synthesis of the pH-responsive particles, a pH-responsive open-chain polyamine, namely the derivative 3-[2-(2 aminoethylamino)-ethylamino]propyltrimethoxysilane (N3), was selected on the basis that it is simple, and suitable to be stably anchored though covalent bonds on the pore outlets of the silica solids (Acosta *et al*., 2014).

The first step after the solid supports are obtained is the bioactive loading inside the porous channels of the MCM-41 and SBA-15. The loading procedures were done using concentrated ethanol solutions of naringenin. Then solids are functionalized, i.e., polyamine is anchored (grafted) to the surface of the solids, enclosing the bioactive compound inside the pores, using acetonitrile as the reaction medium. Finally the excess of polyamine, along with the non-encapsulated bioactive and the reaction medium, are washed from the solids, which are then accurately dried. The gated particles obtained by this methodology will be called **MSP-41** (corresponding to gated MCM-41) and **MSP-15** (corresponding to SBA-15).

In order to determine that the loading and gating procedures were successful, suitable amount of the solid were dispersed in constantly stirred aqueous media at two different pH (7.5 and 2.0) and the bioactive concentration was measured after 5 h. It must be noticed that the experiments were done well below the solubility value (which is 17 mg L^{-1} at pH 2 or higher at pH 7.5), to guarantee the bulk

release conditions. The results showed that after this period, naringenin concentration at pH 2 was 16% of that at pH 7.5 for MSP-41, and 14% for MSP-15. Conversely, the difference in the release at these two pH given by the corresponding non-functionalized solids was in all cases less than 15%. This indicates that pH changes control the release of the bioactive into the medium, indicating the successful functioning of the "open/closed" switch-mechanism of the molecular gates.

2.3.2.2 Release of naringenin from the gated particles

First, the dissolution behaviour of naringenin was characterized at low and high pH (Figure 2.17). This experiment was done by adding the amount of naringenin necessary for obtaining a 5 mg L^{-1} to constantly stirred aqueous media at the respective pH. Even though the hydrophobicity of naringenin varies greatly for this pH range (as discussed in the previous section), well below the saturation concentration pH does not seem to affect greatly the dissolution behaviour of naringenin and after nearly 4 h a plateau value was reached with about 90% of the compound dissolved. It must be noticed that this behaviour differs from that of pure naringenin being dissolved in pure water without mechanical energy input, in which case nearly half of naringenin has been dissolved after that time (as discussed in the previous chapter).

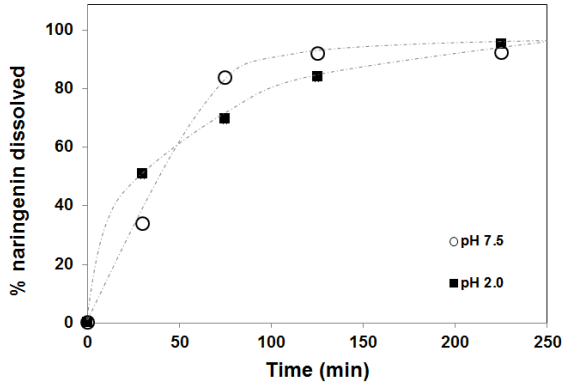

Figure 2.17. Dissolution profiles of naringenin at pH 7.5 and pH 2.0, expressed as the percentage of the total naringenin.

The release behaviour of naringenin encapsulated in MSP-41 and MSP-15 for the first 7 h is presented in Figure 2.18 Cumulative release here is presented as the amount of cargo released to the medium per mass of the carrier particle (μg mg^{-1}). The particles allowed for a remarkably enhanced release at the higher pH compared to the more acidic condition.

According to these results and to previous evidence for this kind of systems, the switch mechanism of the molecular gate consists in open-closed cycles due to protonation/deprotonation processes of the grafted polyamines. At low pH, the nitrogen atoms of the polyamines are fully protonated causing strong electrostatic repulsions between the anchored polyamines. Such strong repulsions push away the protonated polyamines blocking the pores of the inorganic support which in turn inhibits the cargo release. At neutral pH the polyamines are only partly deprotonated and the electrostatic repulsions are highly diminished. This allows for pore opening because of the more flexible conformation of polyamines compared to polyammonium, with the consequent cargo release.

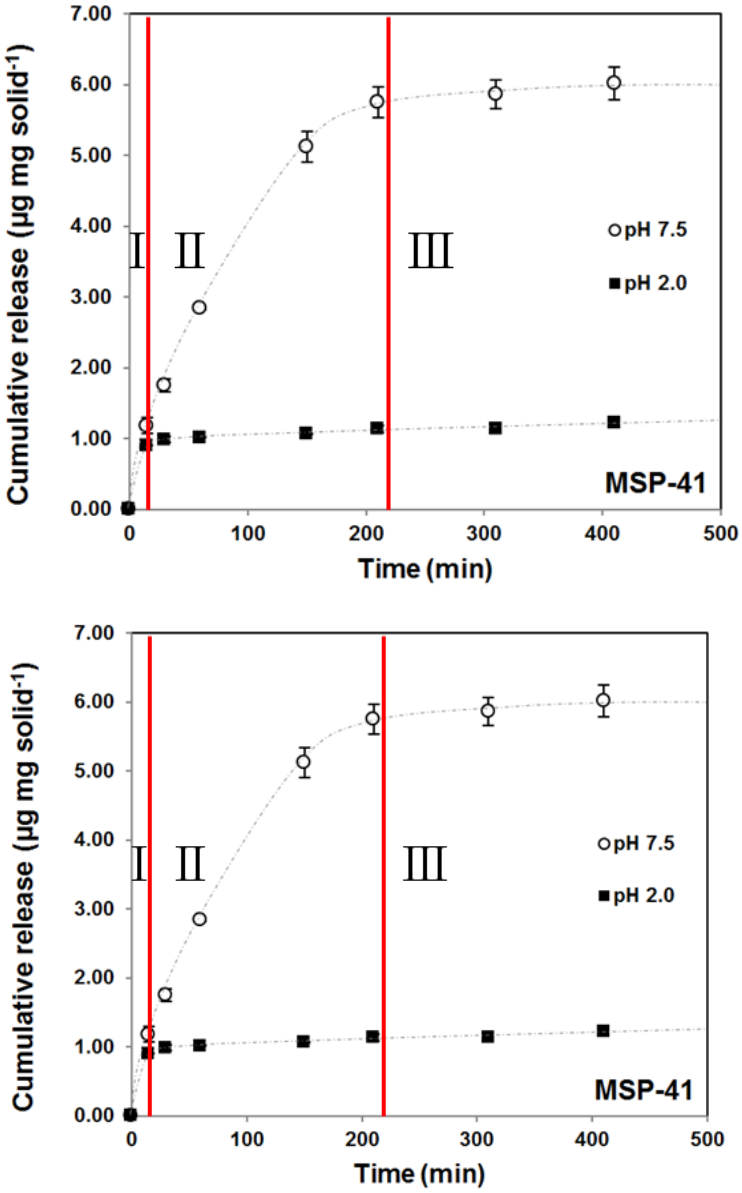

Figure 2.18. Naringenin release from the molecular gate-functionalized mesoporous materials (right) MSP-41and (left) MSP-15 in aqueous media at pH 2.0 ("closed gate") and pH 7.5 ("open gate").

In the approach that considers these materials as possible functional food ingredient, an actual value of loading efficiency is given by the amount released after 5 h, taking into account an approximate time for ingested food to arrive to the gastrointestinal level, where bioactivity of polyphenols in terms of their antioxidant activity is more significant (Holst & Williamson, 2008). In that approach, the bioactive loading efficiency of the system MSP-41 is 6.02 µg mg^{-1} and whereas that of the system MSP-15 is 0.73 µg mg^{-1}.

In both cases the release profiles could be clearly divided in three different phases, as depicted

in the plots (red lines indicating the limits). Phase I corresponds to a fast release (<15 min), probably due to the presence of remaining excess of non-encapsulated naringenin outside the pores, and to a slight delay for the typical conformation of the molecular gates to be established. During phase II, at pH 7.5 the bioactive compound is released to the medium in at a nearly constant release rate, until a plateu is reached. In phase III a much slower release takes place. The duration of phase II was about 200 min for MSP-41 and 300 min for MSP-15, meaning that the latter permits a longer sustained release of the antioxidant.

Considering after the end of phase II that the system is in equilibrium, if we define that the naringenin partition coefficient is $K_c = C_{s,\infty}/C_{w,\infty}$, where C_s and C_w are the concentration of naringenin in the solid particles and the aqueous phase respectively, are K_c at pH 2 >> K_c at pH 7.0, for both of the solid systems.

For better understanding the release process, one can consider only phases I and II and plot the amount of naringenin per mass unit (μg mg^{-1}) against the square root of time (min^{-1}). The linear trend observed for the release profiles at pH 7.5 in Figure 2.19 shows that within these phases, at the higher pH ("open gates") the solids release naringenin in a Fickian diffusion-driven fashion. The marginal release taking place at the acidic conditions ("closed gates") did not follow such a trend.

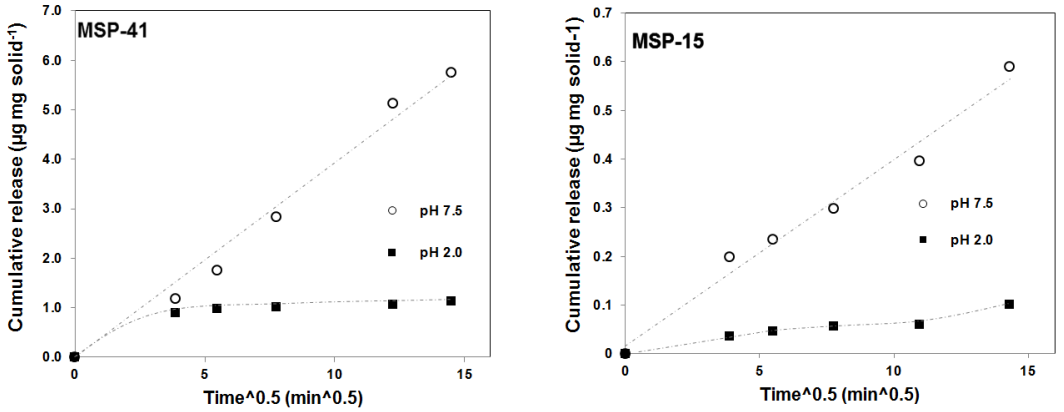

Figure 2.19. Amount of naringenin released from (left) MSP-41 and (right) MSP-15 in aqueous media at pH 2.0 and pH 7.5 as a function of the square root of time.

2.3.2.3 Synthesis of the NF-MSP composites through electrospinning

In order to incorporate the previously prepared solids into the meshes of nanofibrous polymers, the solids need to be re-suspended in aqueous solutions containing the pullulan, prior to the electrospinning. Since the release mechanism is pH-controlled, this re-suspension medium needs to avoid the "open" gate situation (which occurs at neutral pH) for preventing the cargo to be released. Aditionally, to ensure the best regular distribution of the particles in the final nanofibrous composite, the solids must be accurately dispersed in the polymeric solution. The electrospinning in different acidic media and with different homogenisation strategies were explored to address this issues.

A series of experiments to evaluate the electrospinability of the mixture at the acidic and solid-rich conditions. Pullulan solutions (20%wt) were prepared in acidified water using diluted sulphuric acid (leading to pH 2.0), acetic acid at 10% (v/v) (leading to pH 2.3) and acetic acid at 5%(v/v) (leading to pH 2.5). Also, three homogenisation strategies consisting in mixing the suspended solids at different MSP concentrations (2, 5 and 10%wt with respect to pullulan) with both ultra-turrax or soft stirring, before or after the dissolution of the polymer. These experiments were done using the bare MSP (MCM-41 and SBA-15), not functionalized. The main results are summarized in Table 2.4. In Figure 2.20 the electrospinning set-up and examples of stable Taylor's cone for different

experiments are presented.

In the first place, it was observed that pure pullulan does not lose its electrospinnability in 5% and 10% acetic acid whereas it is not electrospinnable with sulphuric acid. SEM pictures of the pullulan membrane obtained at pH 2.3 (Figure 2.21) (experiment #3 in Table 2.4) shows that there are no apparent morphological effects with respect to pullulan obtained using pure water. For the consecutive experiments, this acidic solution was used as the electrospinning solvent.

The X-ray EDS-SEM analysis allowed for the verification of the particles presence, through the elementary detection of silica. Membranes loaded with 5% of solids presented a homogeneous macroscopic appearance and SEM pictures revealed fairly good distributions of the particles across the nanofibrous matrix (Figure 2.22 and 2.23). It was possible to obtain nanofibrous membranes loaded with up to 10% of solids (experiment #7), however, these materials had a rough macroscopic appearance and SEM pictures revealed bulky aggregations (data not shown). For the successive production of the pullulan-functionalized MSP composites, loading values of 5% of solid were considered suitable.

Table 2.4. Electrospinning parameters and dispersion strategies for obtaining pullulan-MCM-41 and pullulan-SBA-15 nanofibrous composites

Exp#	Electrospinning solvent	pH	Type of solid	% Loading (solid/pullulan)	Dispersion strategy*	Electro-spinnability**	Flow rate (mL h^{-1})
1	water	5.7	-	-	-	Yes (13 kV)	0.50
2	acetic acid 5%	2.5	-	-	-	Yes (14 kV)	0.50
3	acetic acid 10%	2.3	-	-	-	Yes (13 kV)	0.50
4	sulphuric acid (dil.)	2.0	-	-	-	No	-
5	acetic acid 10%	2.3	SBA-15	2	Hard	Yes (15 kV)	0.40
6	acetic acid 10%	2.3	SBA-15	5	Hard	Yes (15.5 kV)	0.44
7	acetic acid 10%	2.3	SBA-15	10	Hard	Yes (16 kV)	0.40
8	acetic acid 10%	2.3	MCM-41	2	Hard	Yes (15 kV)	0.38
9	acetic acid 10%	2.3	MCM-41	5	Hard	Yes (15 kV)	0.38
10	acetic acid 10%	2.3	SBA-15	5	Medium	Yes (16 kV)	0.40
11	acetic acid 10%	2.3	MCM-41	5	Medium	Yes (15 kV)	0.38
12	acetic acid 10%	2.3	MCM-41	5	Soft	Yes (15 kV)	0.38

* Hard: 10 min ultrasonication + 2 min UltraTurrax (13 k rpm) + ultrasonication; Medium: 10 min ultrasonication + stirring 350 rpm; Soft: stirring 350 rpm)

** Taylor's cone stability

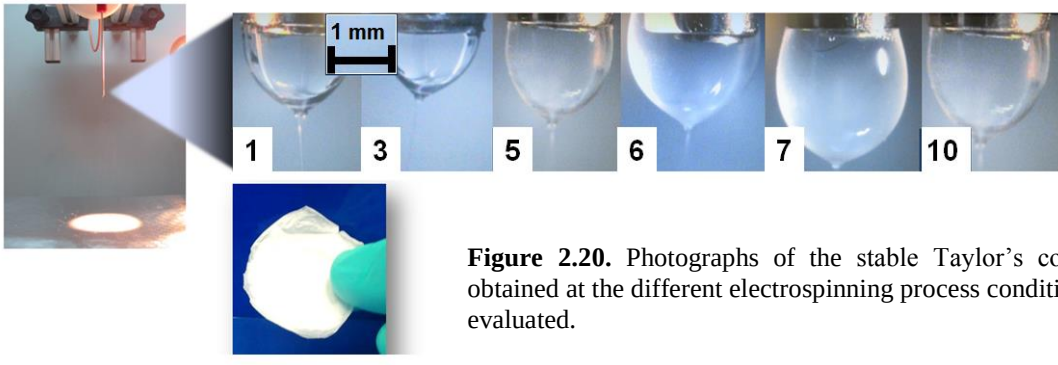

Figure 2.20. Photographs of the stable Taylor's cones obtained at the different electrospinning process conditions evaluated.

With regard to the homogenisation procedure, even though the "hard" and "medium" dispersion strategies seemed to provide better particle distributions across the fibrous nets, there was the risk that high energy inputs "damage" the particle structures which is especially undesirable when functionalized materials are used, because this situation could lead to the breakage of the encapsulation system with the consequent loss of the controlled release features. Moreover, as it will be discussed further, the loading and gating procedures are expected to help in the particle dispersivity by increasing their ζ-potential values (Pérez-Esteve *et al.*, 2014). For that reason a "soft" homogenisation strategy was considered more suitable for the production of the pullulan composites with naringenin-loaded functionalized solid materials (NF-MSP composites).

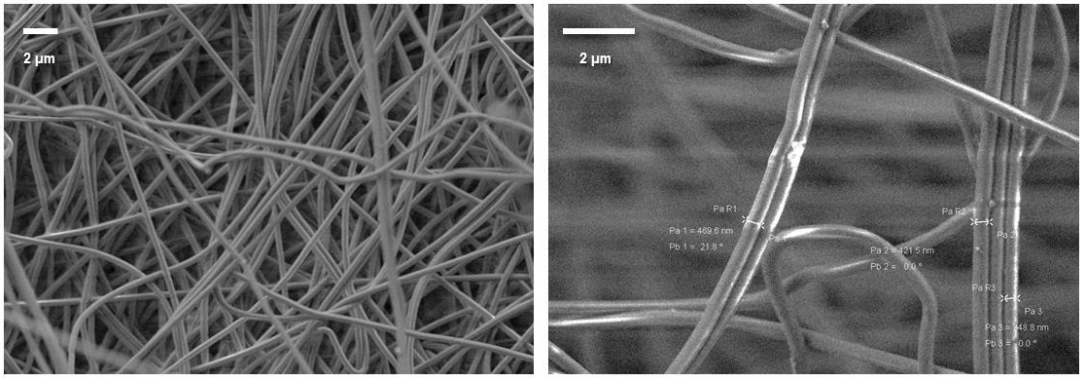

Figure 2.21. SEM micrographs of nanofibers obtained by electrospinning of acidic solutions of pullulan (20% (w/w) in 10% (v/v) of acetic acid).

Finally, with the selected electrospinning parameters, the naringenin-loaded and N3-gated, pH-responsive solids MSP-41 and MSP-15 were incorporated in pullulan nanofibrous networks. Macroscopically, the membranes had the characteristic appearance Figure 2.24 shows the SEM image of these NF-MSP composites. EDX spectra allowed to reveal the presence of nitrogen on the MSP particles, which is a further evidence of the N3 molecular gate functionalization (Figure 2.25).

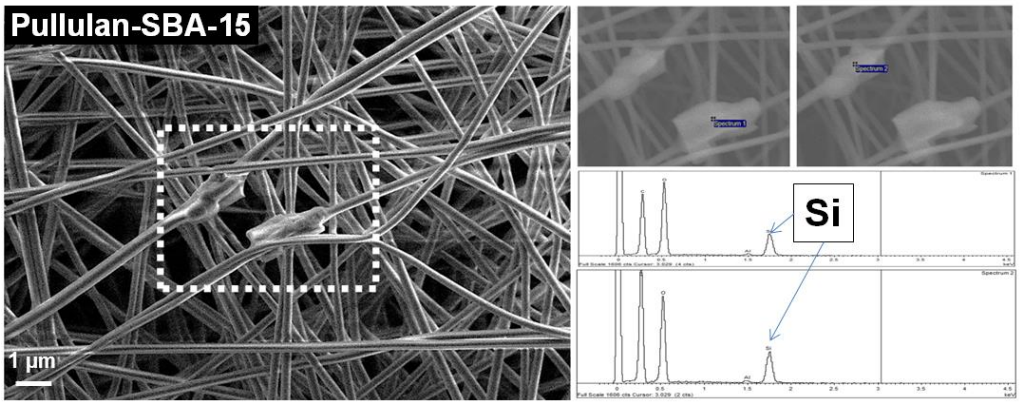

Figure 2.22. SEM micrographs (left) of composite nanofibers pullulan-SBA-15 and X-Ray EDS spectra of the composite materials.

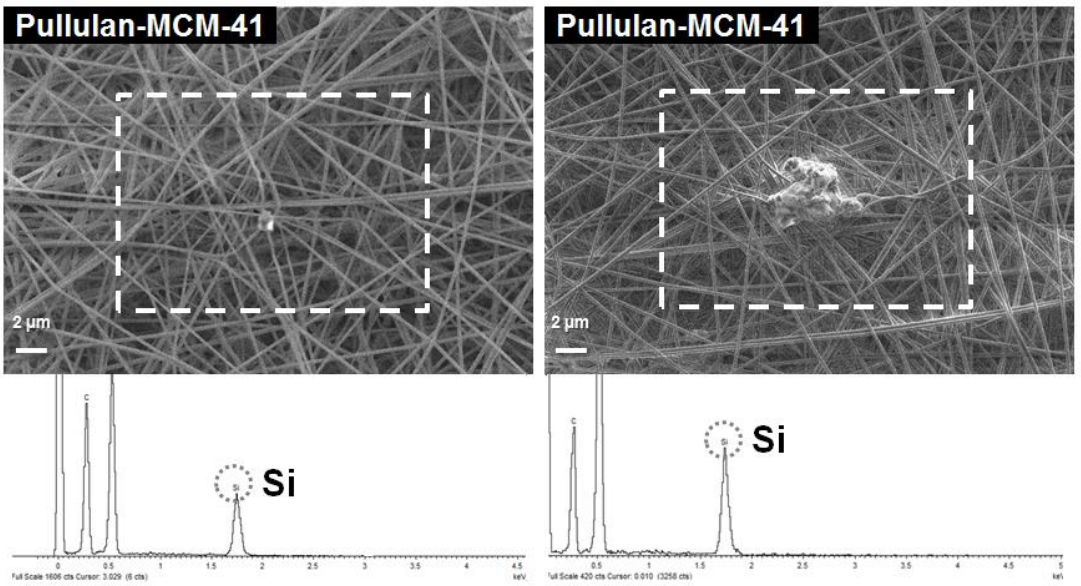

Figure 2.23. SEM micrographs (left) of composite nanofibers pullulan-MCM-41 and X-Ray EDS spectra of the composite materials.

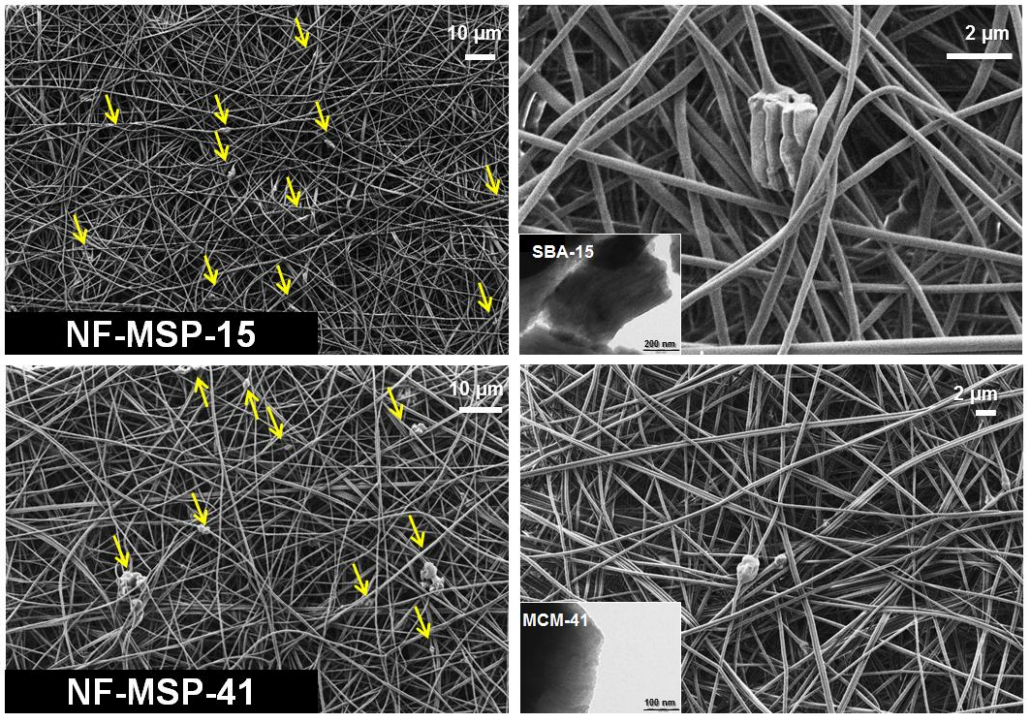

Figure 2.24. SEM micrographs of composite nanofibers (top) NF-MSP-15 and (bottom) NF-MSP-41. In the inserts, TEM images of the corresponding silica mesoporous solids.

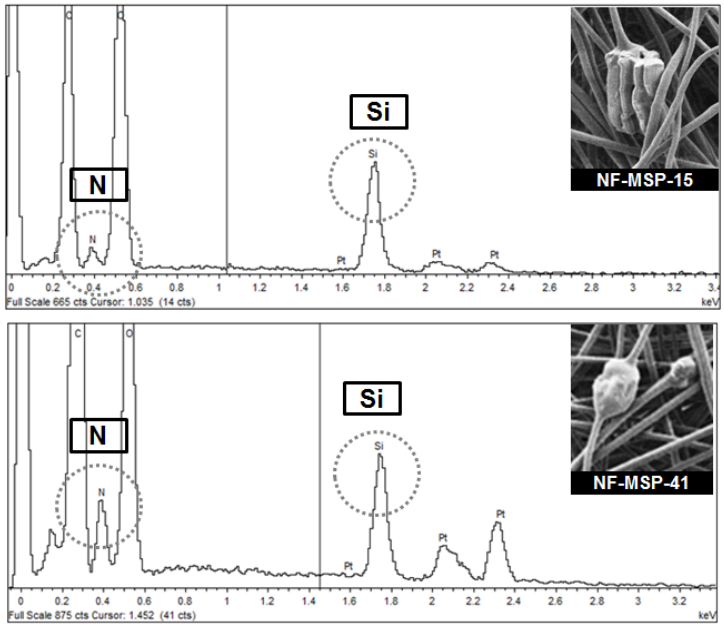

Figure 2.25. X-Ray EDS spectra of the detected mesoporous materials

2.3.2.4 Release of naringenin from the NF-MSP composites

Figure 2.26. shows the release behaviour for NF-MSP-15 and NF-MSP-41 composite materials in the aqueous media at neutral (pH 7.5) and acidic conditions (pH 2.0). The cumulative release corresponds to the amount released of naringenin per mass unit of composite material (95% pullulan - 5% MSP) at a certain time.

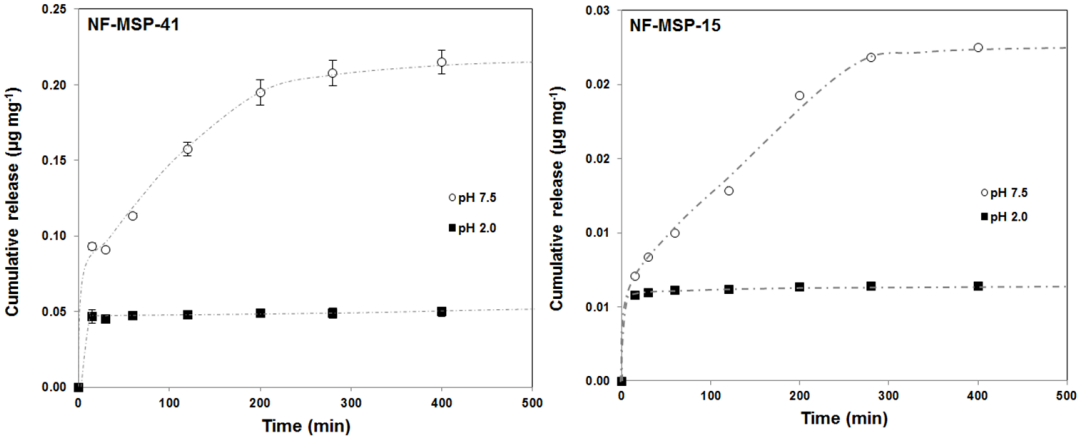

Figure 2.26. Naringenin release from the molecular nanofibrous composites with gate-functionalized mesoporous materials (right) NF-MSP-41and (left) NF-MSP-15 in aqueous media at pH 2.0 ("closed gate") and pH 7.5 ("open gate").

The water-soluble polysaccharide membranes disintegrate (dissolve) themselves in the releasing medium as soon as they enter in contact. While this happens, the functionalized naringenin-loaded silica particles (MSP) are immediately dispersed in the medium and start to deliver the cargo.

No delay in the release process was observed, with respect to the MSP. In fact, globally, the obtained release trends did not differ from the corresponding MSP at both the pH values except for two aspects: (i) an increased portion of bioactive is released in the first phase of the process following a burst release trend, being more noticeable for NF-MSP-15; (ii) the bioactive release at pH 2 follows exclusively a burst release trend, which means that after a very short time the plateau release was reached. As it was discussed above, albeit the functioning of the "open-closed" gate-like behaviour of the solids, at pH 2 still a marginal amount of bioactive compound is delivered. This means that first mentioned difference is probably due to this marginal release, which occurs while the solids are dispersed in the electrospinning solutions (pH 2.3). Most likely, the pre-released naringenin remains entrapped within the nanofibers (as in the case of pullulan-NAR materials whose development anc characteristics were presented in the previous section of the document) and is then readily released as soon as the composite membranes are put to release.

Therefore these systems can be claimed to be "self-dispersing"- pH controlled release devices in aqueous media. An schematic representation of their mechanism of functioning is presented in Figure 2.27.

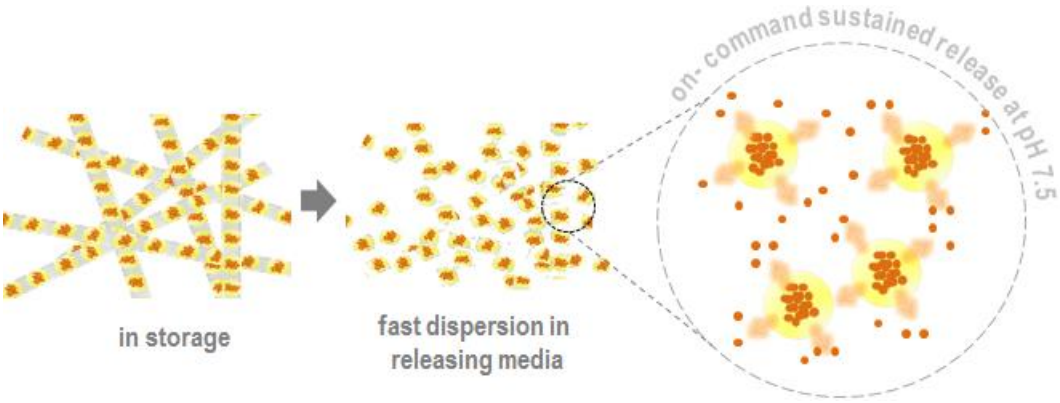

Figure 2.27. Schematic representation of the "self-dispersive", pH-triggered, sustanained release, NF-MSP composite system.

2.4 BIOPOLYMER COMPOSITE NANOFIBERS FOR HUMIDITY-TRIGGERED RELEASE OF VOLATILE BIOACTIVE COMPOUNDS

Volatile substances with antimicrobial features, such as natural essential oils, absolutes, essences, extracts, resins, infusions, etc. are of great interest for the active packaging industry and their efficient encapsulation and release represent a major challenge, considering their high fugacity and the fact that they are very sensitive to heat, oxygen and light. Most of the active packaging studies reported in the literature concern the dispersion of the active agent in carriers with limited surface areas, such as polymer films and layers, sometimes with not negligible losses of volatile compounds during production and storage (Appendini & Hotchkiss, 2000; Guillard *et al*., 2009). The controlled release of active substances from these structures is mainly governed by concentration-dependent passive diffusion (Vega-Lugo & Lim, 2009).

Because of their submicron to nano-scale diameter and very large surface area, electrospun fibers may offer additional advantages compared to film and sheet carriers, as they are more responsive to changes in the surrounding atmosphere, which enables a tunable release of the entrapped compounds (Vega-Lugo & Lim, 2009). Moreover, since the electrospinning process takes place at ambient conditions, the produced fibers are more suitable to encapsulate thermally-labile substances than fibers prepared by conventional processes, or other encapsulation methods, such as spray drying and fluid bed coating (Qi et al., 2006; Xu et al., 2006; Lesmes & McClements, 2009) . Furthermore, electrospinning seems suitable to trap aroma compound inclusion complexes (AC-IC) within the meshes of the membrane. This is the case of cyclodextrins inclusion complexes with hydrophobic substances. In this kind of 'reservoir type' encapsulation, a shell is present around the active agents, whereas in the 'matrix type' the active agent is much more dispersed throughout the carrier material (Zuidam & Shimoni, 2007). The former is more effective for the stabilization/protection of hydrophobic volatile aroma compounds (Koontz *et al*., 2009).

To the best of our knowledge, only few works reported in the literature are focused on electrospinning of edible polysaccharides biopolymers used for a controlled release of bioactive substances, in particular of volatile substances. Edible polysaccharides are commonly used in food applications as coating agents, thickening agents, or additives for technological aims; they are not allergenic and do not need toxic solvents to be electrospun (Stijnman *et al*., 2011; Karim *et al*., 2009).

In this part of the thesis, we develop a system that is produced by a single-step electrospinning process in which β-cyclodextrin crystals encapsulate aroma compounds (limonene and perillaldehyde are used as model volatile bioactives) as they are simultaneously fixed to the meshes of edible pullulan nanofibers. The retentive capacity of the edible nanofibrous system was evaluated, and the release of aroma compounds was investigated under storage conditions and at various relative humidity (RH) and described phenomenologically.

2.4.1 Materials and methods

2.4.1.1 Chemicals

Pullulan was a food grade preparation (PF-20 Grade, 200kD) of Hayashibara Biochemical Laboratories Inc. (Okayama, Japan) and was kindly supplied by Giusto Faravelli (Milan, Italy). β-Cyclodextrin was purchased from Sigma Aldrich (Milan, Italy). Aroma compound (AC), i.e. R-(+)-limonene (Sigma Aldrich, Milan, Italy) and perillaldehyde, were used as models of bioactive aroma compound. With regard to perillaldehyde, for a series of preliminary experiments the samples were provided by Pr. Angela Bassoli and co-workers who extracted the compound according to their standardized procedures (Bassoli *et al*., 2013; Cattaneo *et al.*, 2014) whereas for the experiments whose data are presented herein a commercial reference of the compound (Sigma Aldrich) was used. It must be noticed that no differences were observed in the results obtained by both materials. and . Doubly distilled water was used as solvent to prepare the emulsions. Sodium chloride, potassium chloride and potassium nitrate were purchased from Sigma Aldrich (USA). Methanol and ethanol were

supplied by Fluka analytical (Spain).

2.4.1.2 Electrospinning

Polymer solutions were prepared by dissolving pullulan dry powder in water (20 wt %) at room temperature under 4 hour stirring. After dissolution, two different methods were used:
(i) The pullulan solution was mixed with a preformed AC-IC in a ratio of 25% of AC-IC with respect to the dry pullulan. The mixture was homogenised in 10 mL glass vials using an Ultra Turrax T25 IKA blender (IKA Works, Guangzhou, China) running at 10.000 rpm for 5 min. The AC-IC preparation was performed with the precipitation method at 16:84 wt % (AC:β-cyclodextrin)25 in water solution. The product was then filtrated and dried.
(ii) The pullulan solution was mixed with an amount of dry free β-cyclodextrins (25 wt % with respect to dry pullulan) and with 10% wt % (AC/ β CD), containing more than 90 wt % of the active compound perillaldehyde. The solution was emulsified using the UltraTurrax in the same conditions of (i) (10.000 rpm x 5 min). It must be noticed that on adding cyclodextrins the system turns to a water-in-water emulsion because of the thermodynamic uncompatibility of the two polymers (Grinberg & Tolstoguzov, 1997): cyclodextrin rich aqueous droplets (few micron size) are dispersed within an aqueous pullulan rich phase.

Plastic syringes (10 mL) fitted with a metallic needle (Hamilton) were filled with the polymeric emulsions and placed in a KDS100 syringe pump (KD-Scientific, New Hope, PA) at flow rates of 0.5 mL h^{-1}. The needle of the syringe was linked to a Spellman SL150 high voltage power supply by an alligator clip, while a foil-covered copper tray, positioned at 12 cm in front of the needle, was used as collector and grounded. For the electrospinning of the emulsions, the electrical potential was set at values of 15 kV. The production time of a single membrane was stopped at 15 min, the membrane were removed from the collector and dried.

2.4.1.3 FE-SEM

Field-Emission Scanning Electron Microscopy (FE-SEM). Scanning electron microscopy images were obtained from a Sigma Field Emission microscope (Carl Zeiss Microscopy, LLC) at accelerating 5KV voltage and 6 mm working distance, with a 30 micron width slit. The samples were first gold sputtered (Sputtering Polaron E 5100) for 30 s (rate 1 nm s-1) with argon and 18 mA current intensity.

2.4.1.4 Thermogravimetric analyses (TGA)

TGA were performed under nitrogen atmosphere with a Perkin Elmer TGA 4000 instrument. Scans at a constant 20 °C/min heating rate (30 °C- 450 °C). Raw data were converted into time derivative trace, DTG, and expressed in mg/K. This part of the work was done with collaboration of Pr. Giuseppe Di Silvestro, Dr. Marco Ortenzi and Pr. Alberto Schiraldi.

2.4.1.5 Bioactive loading efficiency

Volatiles were extracted by immersing the membrane in 5 mL of methanol and stirring by 24 h / 500 rpm followed by an ultrasonic for 10 min. Alcoholic phase containing the aroma was analysed via total vaporization by head space gas chromatography (HSGC) (Mod HS 40, Perkin Elmer) equipped with a TRB-WAX column (30 m x 0.53 mm, film thickness of 1μm) and a flame ionization detector (FID). Helium was used as carrier gas (2 mL/min). Injector and detector were set at 230 and 260 °C. The residual quantity was quantified with an external standard. The extraction efficiency was >90%. For quantifying losses during storage, membranes were stored at 55% RH and 23 °C for 45 days, and then analysed with HSGC.

2.4.1.6 Release from membranes during storage and at variable humidity

In order to quantify the losses during storage, membranes were stored at 55% RH and 23 °C for 45 days, and then analysed with HSGC and electronic nose. Electronic nose analyses were

performed with a Portable Electronic Nose (PEN2) (Win Muster Airsense (WMA) Analytics Inc. (Schwerin, Germany)) operating with the Enrichment and Desorbtion Unit (EDU). A 35 mg membrane sample was placed in a 22.5 mL airtight Pyrex® glass vial with a Silicon/Teflon disk in the cap for 1 h equilibration at 35 ± 2 °C. The disk was eventually pierced before the analysis with the electronic nose and EDU. The relevant operating procedure was reported in a previous work25. All samples were analysed three times and the average of the sensor responses was used for the statistical analysis. Principal Component Analysis (PCA)27 was applied, as an exploratory tool, to study the changes of the aroma compounds in the head-space of the vial containing the membrane at the various RH conditions tested. Calculations were performed with MATLAB v. 6.5 program (Mathworks). The same glass vials were analysed also with HSGC to identify and quantify the aroma compound released from the membranes immediately after production and at 1, 2, 6 days after electrospun process. In this case the sample was let rest at 35 °C for 1 hour as equilibration time, while the GC conditions were the same as above (paragraph 2.6). Both electronic nose and HSGC data were compared using PCA analysis (MATLAB software v. 6.5). Single membranes were weighed and put in different chambers at 23 ± 2 °C and constant relative humidity (RH) of 55 %, 75 %, 85 % and 92 %. Membranes were removed from the chambers at given time intervals; the amount of volatile was immediately determined with the extraction method described above. This part of the work was done in collaboration with Dr. Erika Mascheroni, Pr. Luciano Piergiovanni and the PackLab team of the DeFENS.

2.4.2 Results and discussion

2.4.2.1 Production and morphology of the membranes

As it has been demonstrated above, carbohydrate can be electrospun to prepare nonwoven membranes that can be referred to as edible polymeric matrix able to incorporate β-CD AC-IC. Pure pullulan nanofibers were obtained by electrospinning of aqueous solutions by using the following optimal process parameters. SEM images showed in these conditions thin (250 ± 50 nm diameter) and uniform pullulan fibers and a morphology characterized by randomly oriented fibers, creating a pseudo-porous structure (Figures 2.28 and 2.29). Macroscopically, the membranes appeared white, homogeneous and smooth (Figures 2.28a and 2.29a). The same process conditions were found suitable also for the electrospinning of solutions containing pullulan, β-cyclodextrin (25wt% with respect to pullulan) and the aroma compound (10 wt % and 20% with respect to β-cyclodextrin for perillaldehyde and limonene respectively), which allowed the formation of AC-IC complexes. Membranes containing the β-cyclodextrin AC-IC and membranes prepared with pullulan alone showed comparable morphologies: the only difference was the presence of AC-IC crystals along the entangled fibers of the formers (Figure 2.28c,d,f and 2.29b,c).

These results show that it is possible to encapsulate aroma compounds directly in a single step electrospinning treatment applied to a dispersed aqueous system containing β-CD, aroma compound and pullulan, without the need of preforming the AC-IC crystals. No differences were evidenced in the morphology of the membranes produced by electrospinning with or without the AC-IC preformation step (Figure 2.28d-c). This is probably due to the fact that electrospinning implies the instantaneous evaporation of the solvent, transforming the starting emulsion in a dry nanofibrous matrix embedding crystalline structures

One of the advantages of the formation of the AC-IC within the nanofibrous membrane in a single step is that these membranes can directly be used as active macroscopically homogeneous devices to be glued as labels onto a packaging wrap without use of adhesives. Moreover, the encapsulation achieved with the precipitation method implies first a decrease of temperature for precipitation and then a temperature rise that is required to slowly evaporate the solvent: the final result is a mixture of amorphous and polycrystalline material where crystal growth can progress (Figure 2.28e).

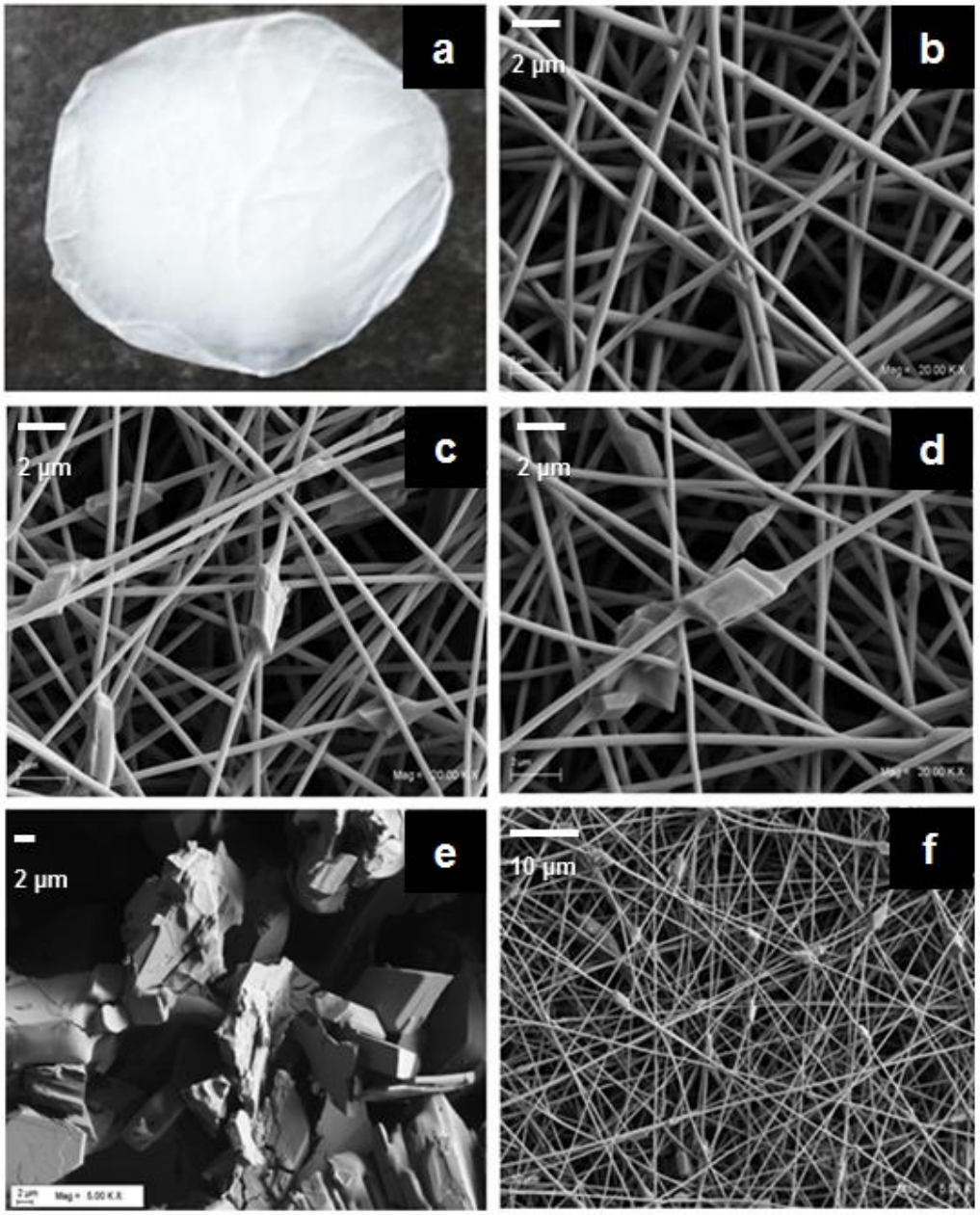

Figure 2.28. Images of macroscopical appeareance electrospun pullulan membrane (a); scanning electron micrograph of nanofibers prepared by using: pullulan solution (b), pullulan, β-cyclodextrin and perillaldehyde solution (c) and pullulan solution with preformed AC-IC. Morphological structures of AC-IC (e) and AC-IC in the nanofibrous membranes (f)

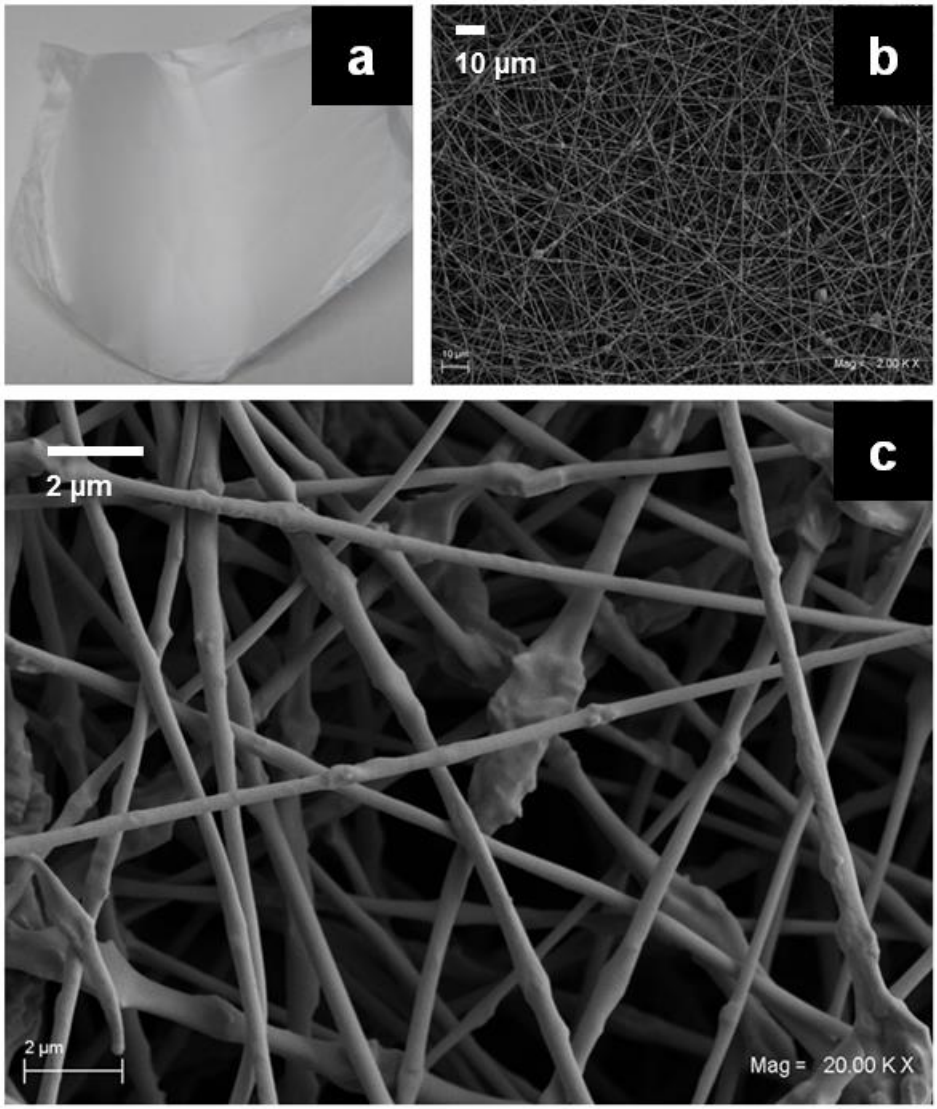

Figure 2.29. Macroscopical appearance of the membranes (a); scanning electron micrographs of nanofibrous membranes with the β-CD-limonene inclusion complex.

.

In the case of encapsulation within a nanofibrous pullulan matrix, the situation is totally different: the crystals formed are smaller and regularly dispersed within the pullulan nanofibrous matrix (Figure 2.28f and 2.28b), probably as a consequence of the rapid solvent evaporation. Apparently, the crystals "envelope" the fibers. This can be explained reminding that, in spite of the chemical similarity (saccharide nature), β-CD and pullulan are thermodynamically uncompatible, which means that they tend to form separate aqueous phases in the presence of excess solvent, because of different exclusion volumes (Beebe *et al*., 1998). These phases form a dispersed system, namely droplets of aqueous β-CD are dispersed in the aqueous pullulan rich solution. The thermodynamic incompatibility that takes the β-CD droplets apart from the surrounding pullulan-rich dispersion medium is equivalent to a surface tension effect between the β-CD aqueous droplets and solvated

bunches of pullulan molecules (Schiraldi *et al.*, 2012). Once the solvent is quickly sucked out in the electrospinning process, the β-CD rich droplets generate small crystals (with a 50-100 nm size) around the pullulan fibers that come from the starting solvated polymer.

2.4.2.2 Loading capacity and losses during storage

The amount of volatile encapsulated immediately after the preparation via electrospinning as quantified by HS-GC, was, 1.85 ± 0.1 wt% perillaldehyde/dry membrane, which corresponded to 8.2 ± 0.5 wt% perillaldehyde/β-CD and 3.10 ± 0.3 wt% limonene/dry membrane, which corresponded to 16.1 ± 0.6 wt% limonene/β-CD. The conical cavity of the β-CD is hydrophobic and able to bind non-polar molecules in water solutions. Considering that the molecule of β-CD (1134.98 gmol) can bind one molecule of perillaldehyde (150.22 gmol) or limonene (136.24), the maximum amount of aroma that can be encapsulated by β-CD is less than 9% of its weight for perilladehyde and around 12% for limonene. The experiments with different mass ratios confirmed that these values actually correspond to the maximum retention capacity of the system and that any excess of free perillaldehyde or limonene is lost during either the electrospinning process or the earlier stage of storage, as discussed below. The retention capacity of pure pullulan nanofibrous membranes (i.e., in absence of β-CD) resulted almost negligible (<0.1 wt% over total dry matter in the membranes). The two ways of fixing the AC-IC complexes to the pulluan membranes (namely, by mixing preformed complexes and by a one-step electrospinning) did not show significant differences as for the amount of encapsulated according to the results (in this case the experiments were done using only perillaldehyde).

Accordingly, the maximum retention capacity of the system is determined by the amount of β-CD. This was confirmed by the study of the storage effect (Figure 2.30). After 3 days, the encapsulated limonene was 13.4 wt% limonene/β-CD, and after 7 to 45 days this remains stable around 12.7 wt% limonene/β-CD. An analogue situation was observed with perillaldehyde, which remained stable after losing 15% of the initial amount in the first week arriving to nearly 7.0 wt% perillaldehyde/ β-CD. Thus, the evidences show that release of aroma during the early stage of storage is due to the excess of volatile that cannot be effectively encapsulated inside the β-CD. Once this excess is quickly lost, the system remains stable without losses during months if kept at a relatively low humidity. The nanofibrous device is suitable to preserve the volatile compound and masking its odour until use at high relative humidity.

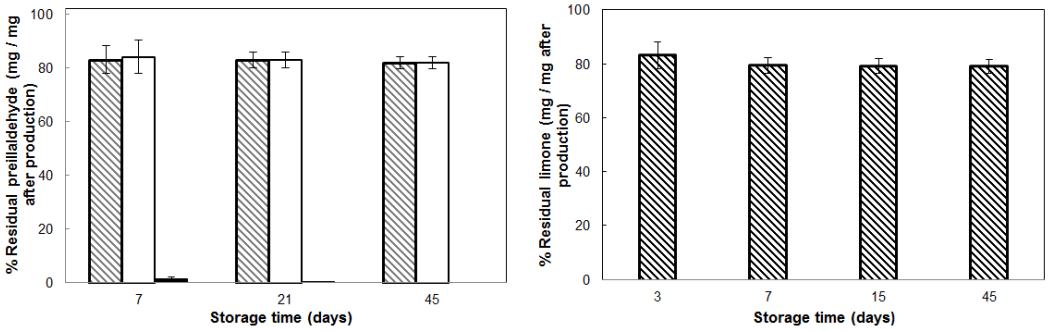

Figure 2.30. Left: Residual aroma compound (perillaldehyde) in nanofibrous membranes after electrospinning process: with single-step-formed AC-IC (gray), with preformed AC-IC (white) and with free AC (black); right: limonene encapsulated in the nanofibrous membranes after different storage times. (% referred to the to the amount of perillaldehye or limonene as quantified right after membrane production)

2.4.2.3 Thermal characteristics

Thermo-gravimetric Analysis (TGA) was used to assess the thermal stability of: pure aroma compound (AC) with dry β-cyclodextrins, AC-IC complexes, and AC-IC complexes fixed within the pullulan membrane. The record of a TGA run encompasses a wide temperature range (see insert in Figure 2.31a) where mass loss occurs because of various events such as release of water, release of the aroma compound, degradation of perillaldehyde and pullulan, which take place in different temperature spans with partial overlaps. It is expedient to use the corresponding time derivative (DTG) trace where the different contributions to the overall mass loss appear as peaks or shouldered peaks. In the present case, the DTG data were referred to the fraction, α, of the overall mass released at the end of the run namely, dα/dt, and, since the experiments were carried out at a given and constant heating rate, were expressed in K^{-1} units (Figure 2.31).

The relevant DTG traces were, if necessary, de-convoluted in a sum of Gaussian components to split the shouldered peaks of the original record. Figure 2.31b indicates that the release of perillaldehyde started at 129 °C and reached a maximum rate at 180 °C. Figure 2.31a (dotted line) shows the DTG trace collected from a AC-IC humid sample: the mass lost in the 30-to-150 °C and 210-315 °C temperature ranges was related to the release of moisture and perillaldehyde, respectively, while the mass loss at higher temperature was related to the volatiles formed in the thermal degradation of β-CD. Figure 2.31c reports the DTG trace of the AC-IC complex embedded in a pullulan matrix: the comparison with the trace in Figure 2.31a (dotted line) indicates an enhanced stability of the complex. The deconvolution in Gaussian components of the trace allowed the split of the water release in a couple of contributions and suggests that water can be present in at least two different environments (e.g., imbibing water and water bound to CD and/or pullulan). The signal related to the perillaldehyde starts at 230 °C (i.e. at higher temperature with respect to the behavior of the AC-IC powder) and is weaker and spanned in a smaller temperature range.

TGA was also used to assess the thermal stability of pure limonene and limonene – β-CD complexes fixed within the pullulan membranes. Figure 2.31d indicates that therelease of limonene started at ambient temperature and reached a maximum rate at 170°C (dashed line). The same figure (continuous line) shows the DTG trace collected from limonene β-CD complexes fixed within the pullulan membrane. The mass lost in the 30-to-150°C was related to the release of moisture and the mass lost in 260-300 °C temperature range was related to limonene encapsulated in β-CD pullulan matrix. It is clear the great increase of stability of limonene when encapsulated in the nanofibrous matrix, confirming that the increased thermal stability of volatiles is a consequence of the morphological characteristics described above.

.

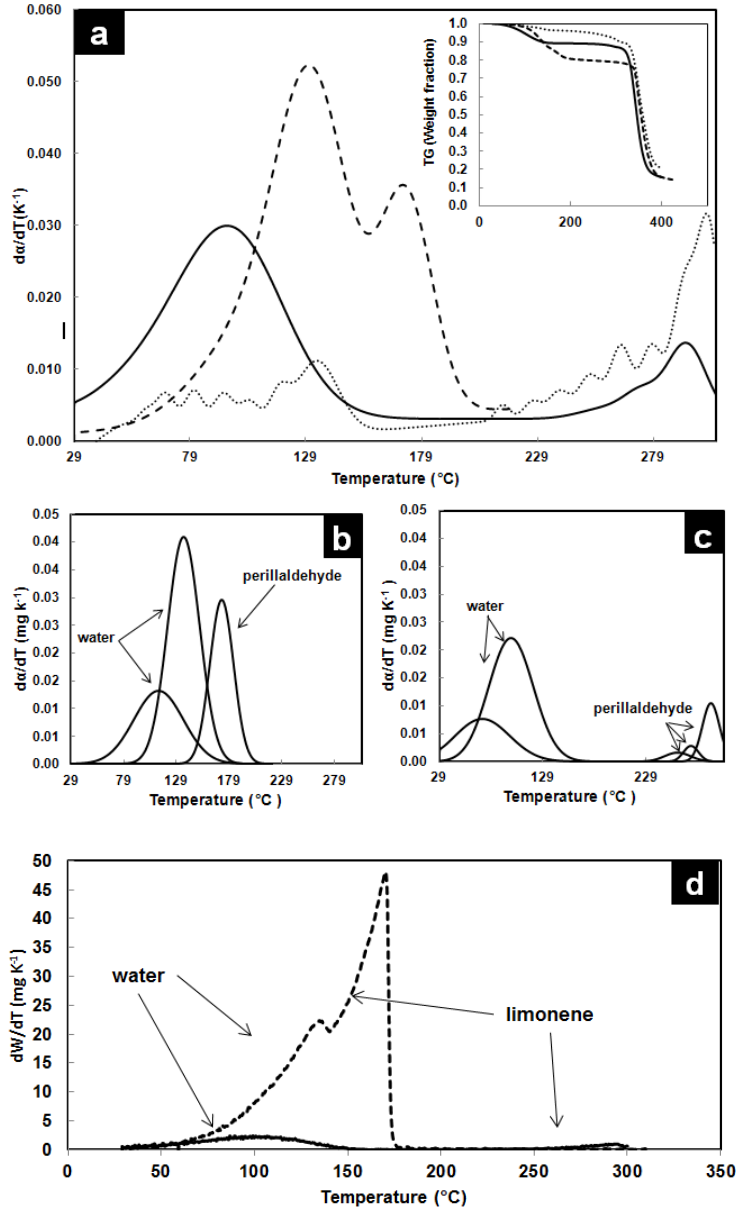

Figure 2.31. (a) Raw TGA traces referred to the mass fraction (in the box) and the respective DTG traces of a mixture of perillaldehyde and β-cyclodextrin (dashed line), aroma compound inclusion complex (AC-IC) (dotted line), and nanofibrous membranes with AC-IC (continuous line); (b) deconvolution of DTG trace of a mixture of perillaldehyde and β-cyclodextrins; (c) deconvolution of DTG trace of nanofibrous membranes with AC-IC; (d) DTG traces of pure limonene (dashed line) and of nanofibrous pullulan matrix with limonene –β- CD IC.

2.4.2.4 Relative humidity-triggered release of aroma

Various mathematical models are present in literature to describe controlled delivery processes that can be of interest for food and pharmaceutical applications (Pothakamury & Barbosa-Canovas, 1995; Siepmann & Siepmann, 2008). These models mainly differ for the role the carrier

plays in controlling core release (Ayala *et al*., 2008). The discussion on this subject should start from the fundamental assumption that, no matter the kinetic model chosen, the behavior of the system is mainly governed by the "distance" from the thermodynamic equilibrium relevant to encapsulated and released species. The state of the system considered in the present work can be described with a couple of co-existing thermodynamic equilibrium, each governed by equilibrium constant:

$$CD + n_1(H_2O) \leftrightarrow CD(aq)$$

$$K_h = \frac{c(CD,aq)}{c(CD) \times a_w^{n_1}} \qquad (1)$$

$$c(CD,aq) + AC \leftrightarrow CD - AC(aq) + n_2 H_2O$$

$$K = \frac{c(CD-AC,aq) \times a_w^{n_2}}{c(CD,aq) \times c(AC)} \qquad (2)$$

where *CD*, *AC* and *CD-AC* stand for β-cyclodextrin, free aroma compound (wheter it is limonene or perillaldehyde) and inclusion complex, respectively, *c* is the symbol for any suitable kind of concentration, and a_w is the activity of water ($a_w = RH/100$).

Both equations explicitly indicate the major role played by the relative humidity, *RH* on the release of process. Taking into account that the overall mass of perillaldehyde is split in the free and bound species, namely, *M*(*AC*) = [*m*(*AC*) + *m*(*AC* in *CD-AC*)], the relevant concentration ratio, *c(AC)/c(CD-AC)*, in eq 2 can be replaced by the corresponding mass fractions of *AC*, namely *φ/(1-φ)* Combining eq 1 and eq 2, the following expression for *φ* can be obtained:

$$\varphi = \frac{a_W^{\ n}}{a_W^{\ n} + K_{app}} \qquad (3)$$

where $n = (n_2 - n_1)$ and $K_{app} = K \times K_h \times c(CD)$. Eq. 3 was used to fit the trend of the experimental data that are reported in Figure 2.32. The figure shows that the release of the volatile may take place for $a_W \geq 0.9$, while it is much smaller for lower a_W. This suggests that the hydrophobicity of the volatiles may play a key role in the releasing process. The excess water molecules could weaken the interaction between host and guest of the complexes *CD-AC*, e.g., because of conformational changes, thus favouring the expulsion the hydrophobic compound towards the external environment. The macroscopic effect of this change is the color variation of the membranes that turn from white to translucent (Figure 2.33) on increasing *RH*.

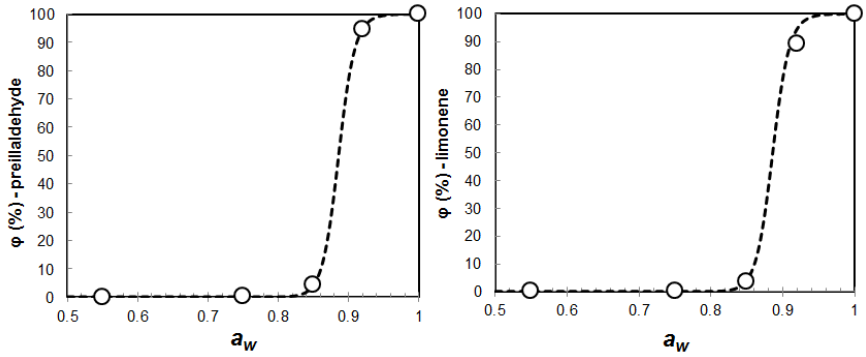

Figure 2.32. Fraction of the aroma compound release at equilibrium (φ) as a function of activity of water at 23 °C: experimental data (circles) and related fit (dotted line) according to eq 3.Left: perillaldehyde; right: limonene.

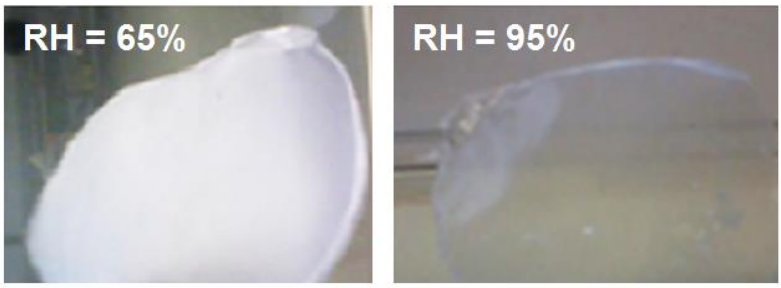

Figure 2.33. Macroscopic aspect of membranes during storage at 65% RH and 92% RH.

At *RH* > 92%, the release of the perillaldehyde is practically complete and can be described (at room temperature) with a classical kinetic expression:

$$\frac{d\phi}{dt} = k(1-\phi)^{v} \quad (4)$$

Figure 2.34 shows the fit of the experimental data for the perillaldehyde system with v = 2.64 and k = 6.63 h^{-1}. Although eq 4 has a phenomenological meaning, the large value of the kinetic order, v, suggests a multi-step mechanism that may not be assessed on the basis of the evidence collected for the present work.

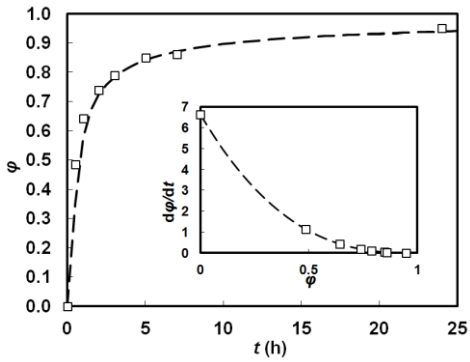

Figure 2.34. Kinetic parameterization and fitting of the perillaldehyde release at 92% RH at room temperature. φ is the mass fraction of released aroma.

A novel single-step methodology for encapsulation of bioactive/antimicrobial hydrophobic volatile compounds (e.g., limonene and perillaldehyde) was developed. The process consists in electrospinning of a dispersed aqueous solution containing pullulan, β-CD and the volatile, resulting in nanofibrous non-woven membranes that are ready-to-use. The system is stable during months without significant loss when kept. in relatively dry conditions, even at high temperatures (up to 260 °C). The release of the volatile from the membranes is triggered by relative humidity changes, taking place at $a_w \geq 0.9$. This system can be potentially used in active packaging, in particular of fresh foods, for which the risk of microbial degradation increases at high a_w conditions, and therefore demand special protection. A scheme of the functioning mechanism of the novel humidity-triggered release material is depicted in Figure 2.35.

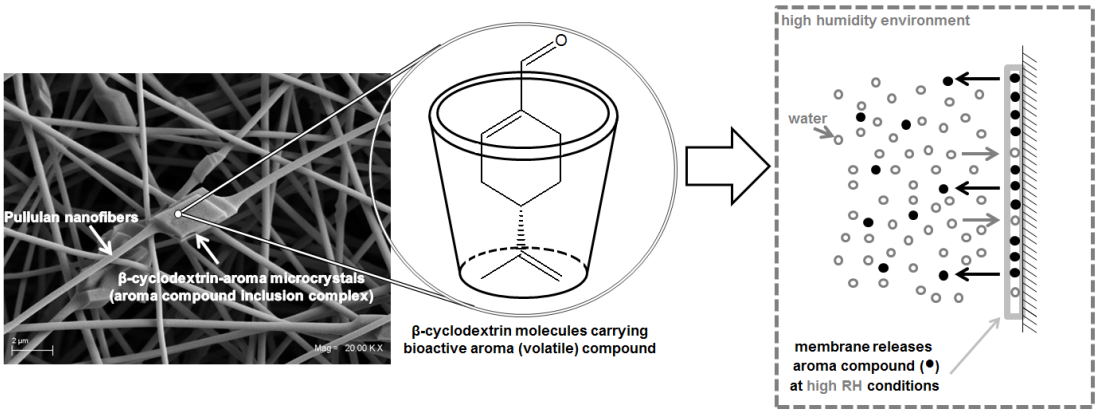

Figure 2.35. Schematic representation of the functioning of the volatile bioactive compound humidity-triggered , release system.

2.5 REFERENCES

1. Aceituno-Medina M et al., 2013, Development of novel ultrathin structures based in amaranth (Amaranthus hypochondriacus) protein isolate through electrospinning. Food Hydrocolloid 31: 289-298.
2. Acosta C et al., 2014, Polymer composites containing gated mesoporous materials for on-command controlled release. ACS Appl Mat Interf 6: 6453-6460.
3. Agrawal P & Schneider H, 1983, Deprotonation induced 13 C NMR shifts in phenols and flavonoids. Tetrahedron Letters, 24: 177-180.
4. Alhusein N et al., 2012, Electrospun matrices for localised controlled drug delivery: release of tetracycline hydrochloride from layers of polycaprolactone and poly(ethylene-co-vinyl acetate). Drug Deliv Trans Res 2: 477-488.
5. Appendini P, Hotchkiss JH, 2002, Review of antimicrobial food packaging. Inn Food Sci Emerg Tech 3: 113–126.
6. Arecchi A, 2010, Electrospinning of poly(vinyl alcohol) nanofibers loaded with hexadecane nanodroplets. J Food Sci, 75: N80-N88.
7. Aridogan B et al., 2002, Antimicrobial activity and chemical composition of some essential oils. Arch Pharmacal Res 25: 860–864.
8. Ayala-Zavala JF et al., 2008, High Relative Humidity In Package of fresh cut fruits and vegetable: Advantage or Disadvantage Considering Microbiological Problems and Antimicrobial Delivering Systems? J Food Sci 73: 41-47.
9. Aznar E et al., 2009, Controlled Release Using Mesoporous Materials Containing Gate-Like Scaffoldings. Expert Opin. Drug Deliv 6: 643−655.
10. Barber PS et al., 2013, Electrospinning of chitin nanofibers directly from an ionic liquid extract of shrimp shells. Green Chem 15: 601-607.
11. Bassoli A et al., 2013, Analogues of perillaketone as highly potent agonists of TRPA1 channel. Food Chem 141: 2044-2051.
12. Beebe KR et al. Chemometrics, a Pratical Guide. Wiley, New York, USA. 1998
13. Belščak-Cvitanović R et al., 2011, Encapsulation of polyphenolic antioxidants from medicinal plant extracts in alginate–chitosan system enhanced with ascorbic acid by electrostatic extrusion. Food Res Int 44: 1094–1101.

14. Bhattarai N et al., 2006, Alginate-based nanofibrous scaffolds: structural, mechanical, and biological properties. Adv Mater 18: 1463-1467.
15. Beck-Broichsitter M et al., 2010, Novel 'nano in nano' composites for sustained drug delivery: biodegradable nanoparticles encapsulated into nanofiber nonwovens. Macromol Biosci 10: 1527–1535.
16. Bonino CA et al., 2011, Electrospinning alginate-based nanofibers: From blends to crosslinked low molecular weight alginate-only systems. Carbohyd Polym 85: 111-119.
17. Bhushani JA, Anandharamakrishnan C, 2014, Electrospinning and electrospraying techniques: Potential food based applications. Trends Food Sci Tech 38: 21-33.
18. Brayden, DJ, 2003, Controlled release technologies for drug delivery. Drug Discovery Today, 8: 976-978.
19. Brinkworth RI et al., 1992, Flavones are inhibitors of HIV-1 proteinase. Biochem. Biophys. Res. Commun. 188:631–637.
20. Buschle-Diller G et al., 2007, Release of antibiotics from electrospun bicomponent fibers. Cellulose 14: 553-562.
21. Buschmann HJ, Schollmeyer E, 2002, Applications of cyclodextrins in cosmetic products: A review. J Cosmet Sci 53: 185-191.
22. Cabrera S et al., 2000, Generalised Syntheses of Ordered Mesoporous Oxides: The Atrane Route. Solid State Sci 2: 405−420.
23. Carino IS et al., 2007, Silica-Based Mesoporous Materials as Drug Delivery System for Methotrexate Release. Drug Deliv 14: 491−495.
24. Cattaneo AM et al., 2014, Response of the European grapevine moth Lobesia botrana to somatosensory-active volatiles emitted by the non-host plant Perilla frutescens. Physiological entomology 39: 229-236.
25. Celebioglu A, Uyar T, 2012, Electrospinning of nanofibers from non-polymeric systems: polymer-free nanofibers from cyclodextrin derivatives. Nanoscale 4: 621-631.
26. Chakraborty S et al., 2009, Electrohydrodynamics: a facile technique to fabricate drug delivery systems. Adv Drug Deliv Rev 61: 1043–1054.
27. Charernsriwilaiwat N et al., 2013, Electrospun chitosan-based nanofiber mats loaded with Garcinia mangostana extracts. Int J Pharm 452: 333-343.
28. Chen L et al., 2006, Food proteinbased materials as nutraceutical delivery systems. Trends Food Sci Tech 17: 272-283.
29. Chunder A et al., 2007, Fabrication of ultrathin polyelectrolyte fibers and their controlled release properties. Colloid Surface B 58: 172-179.
30. Coll C et al., 2013, Gated Silica Mesoporous Supports for Controlled Release and Signaling Applications. Acc Chem Res 46: 339−349.
31. Conforti F et al. 2009, Comparative chemical composition, free radical-scavenging and cytotoxic properties of essential oils of six Stachys species from different regions of the Mediterranean Area. Food Chem, 116: 898–905
32. Coti KK et al., 2009, Mechanised Nanoparticles for Drug Delivery. Nanoscale 1: 16−39.
33. Cowan MM , 1999, Plant Products as Antimicrobial Agents. Clin Microbiol Rev 12: 564-582
34. Daneshfar A et al., 2008, Solubility of gallic acid in methanol, ethanol, water, and ethyl acetate. J Chem Eng Data 53: 776-778.
35. de Folter et al., 2012, Oil-in-water Pickering emulsions stabilized by colloidal particles from the water-insoluble protein zein. Soft Matter 8: 6807-6815.
36. Del Valle E, 2004, Cyclodextrins and their uses: A review. Process Biochem 39: 1033–1046.
37. Descalzo AB et al., 2006, The Supramolecular Chemistry of Organic−Inorganic Hybrid Materials. Angew Chem Int Ed Engl 45: 5924−5948.
38. De Vos P et al., 2010, Encapsulation for preservation of functionality and targeted delivery of bioactive food components. Int Dairy J 20: 292-302.
39. Drew C et al. Electrostatic assembly of polyelectrolytes on electrospun fibers. In Polymeric

Nanofibers. ACS symposium series, Washington DC, 2006, pp.137-148.
40. Duan MS et al., 2005, Cyclodextrin solubilization of the antibacterial agents triclosan and triclocarban: Formation of aggregates and higher-ordercomplexes. Int J Pharm, 297: 213–222.
41. Esen A, 1986, Separation of alcohol-soluble proteins (zeins) from maize into three fractions by differential solubility. Plant Physiol 80: 623-627.
42. Eslami A et al., 2010, Free radicals produced by the oxidation of gallic acid: An electron paramagnetic resonance study. Chem Cent J, 4: 1-4.
43. Ezhilarasi PN et al., 2013, Nanoencapsulation techniques for food bioactive components: a review. Food Bioprocess Tech 6: 628-647.
44. Fang Z, Bhandari B, 2010, Encapsulation of polyphenols – A review. Trends Food Sci Tech 21: 510–523.
45. Fernandez A et al., 2009, Novel route to stabilization of bioactive antioxidants by encapsulation in electrospun fibers of zein prolamine. Food Hydrocolloid 23: 1427-1432.
46. Fernandez MA et al., 1996, Antibacterial activity of the phenolic acids fraction of Scrophularia frutescens and Scrophularia sambucifolia. J Ethnopharmacol 53:11–14.
47. Foti M et al., 1996, Flavonoids, coumarins, and cinnamic acids as antioxidants in micellar system. Structure-activity relationship. J Agr Food Chem 44:497–501.
48. Fukui Y et al., 2010, Preparation of monodispersed polyelectrolyte microcapsules with high encapsulation efficiency by an electrospray technique. Colloid Surface A 370: 28-34.
49. Geissman TA. Flavonoid compounds, tannins, lignins and related compounds, p. 265. In M. Florkin and E. H. Stotz (ed.), Pyrrole pigments, isoprenoid compounds and phenolic plant constituents, vol. 9. Elsevier, New York, N.Y. 1963
50. Ghayempour S, Mortazavi SM, 2013, Fabrication of microenanocapsules by a new electrospraying method using coaxial jets and examination of effective parameters on their production. J Electrostat 71: 717-727.
51. Gomez-Estaca J et al., 2012, Formation of zein nanoparticles by electrohydrodynamic atomization: effect of the main processing variables and suitability for encapsulating the food coloring and active ingredient curcumin. Food Hydrocolloid 28: 82-91.
52. Gómez-Estaca J et al., 2014, Advances in antioxidant active food packaging. Trend Food Sci Tech. 35: 42-51.
53. Gou J et al., 2011, Enhancement of antioxidant and antimicrobial activities of Dianthus superbus, Polygonum aviculare, Sophora flavescens,and Lygodium japonicum by pressure-assisted water extraction. Food Sci Biotech 20: 283–287.
54. Grinberg VY, Tolstoguzov VB, 1997, Thermodynamic incompatibility of proteins and polysaccharides in solutions. Food Hydrocolloid 11: 145–158.
55. Guillard V et al., 2009, Food preservative content reduction by controlling sorbic acid release from a superficial coating. Inn Food Sci Emerg Tech 10: 108–115.
56. Han J et al., 2009, Electrospun shikonin-loaded PCL/PTMC composite fiber mats with potential biomedical applications. Int J Pharm 382: 215-221.
57. HarborneJ, Williams C, 2000, Advances in flavonoid research since 1992. Phytochemistry 55: 481-504.
58. Haslam E, 1996, Natural Polyphenols (Vegetable Tannins) as Drugs: Possible Modes of Action. J Nat Prod 59: 205-215.
59. He CL et al., 2006, Coaxial electrospun poly(L-lactic acid) ultrafine fibers for sustained drug delivery. J Macromol Sci B 45: 515-524.
60. Heikkila T et al., 2007, Evaluation of Mesoporous TCPSi, MCM-41, SBA-15, and TUD-1 Materials as API Carriers for Oral Drug Delivery. Drug Deliv 14: 337−347.
61. Heim K et al., 2002, Flavonoid antioxidants: chemistry, metabolism and structure-activity relationships. J Nutr Biochem 13: 572-584.
62. Hoffmann F et al., 2006, Silica-Based Mesoporous Organic-Inorganic Hybrid Materials. Angew Chem Int Ed Engl 45: 3216−3251.

63. Homayoni H et al., 2009, Electrospinning of chitosan nanofibers: processing optimization. Carbohyd Polym 77: 656-661.
64. Holst B, Williamson G, 2008, Nutrients and phytochemicals: from bioavailability to bioefficacy beyond antioxidants. Curr Opinion Biotechn, 19: 73-82.
65. Hsieh Y et al., 2002, Functional fibers for immobilization of biomolecules. Project M02-CD05. National Textile Center. Report.
66. Hu X et al., 2014, Electrospinning of polymeric nanofibers for drug delivery applications. J Control Release 185: 12–21.
67. Huang X, Brazel CS, 2001, On the importance and mechanisms of burst release in matrix-controlled drug delivery systems. J Control Release 73: 121 –136.
68. Ionescu LC et al., 2010, An anisotropic nanofiber/microsphere composite with controlled release of biomolecules for fibrous tissue engineering. Biomaterials 31: 4113–4120.
69. Islam MS, Karim MR, 2010, Fabrication and characterization of poly(vinyl alcohol)/alginate blend nanofibers by electrospinning method. Colloid Surface A 366: 135-140.
70. Ji HF et al., 2006, Proton dissociation is important to understanding structure–activity relationships of gallic acid antioxidants. Bioorga Med Chem Lett 16: 4095-4098.
71. Jiménez J. et al., 2008, Effects of grape antioxidant dietary fiber in cardiovascular disease risk factors Nutrition 24: 646–653.
72. Jones OG, McClements DJ, 2011, Recent progress in biopolymer nanoparticle and microparticle formation by heat treating electrostatic protein polysaccharide complexes. Adv Colloid Interface 167: 49-62.
73. Jug M et al., 2008, Cyclodextrin-based pharmaceuticals. Radiat Med Sci 499: 9–26.
74. Kayaci F et al., 2013, Enhanced thermal stability of eugenol by cyclodextrin inclusion complex encapsulated in electrospun polymeric nanofibers. J Agr Food Chem 61: 8156-8165.
75. Karami Z et al., 2013, Preparation and performance evaluations of electrospun poly(ε-caprolactone), poly(lactic acid), and their hybrid (50/50) nanofibrous mats containing thymol as an herbal drug for effective wound healing. J Appl Polym Sci 129: 756-766.
76. Karim MR et al., 2009, Preparation and characterization of electrospun pullulan/montmorillonite nanofiber mats in aqueous solution. Carbohyd Polym 78: 336–342.
77. Keating G J, O'Kennedy R. The chemistry and occurrence of coumarins, p. 348. In R. O'Kennedy and R. D. Thornes (ed.), Coumarins: biology, applications and mode of action. John Wiley & Sons, Inc., New York, N.Y. 1997
78. Kenawy ER et al., 2002, Release of tetracycline hydrochloride from electrospun poly(ethylene-covinylacetate), poly(lactic acid), and a blend. J Control Release 81: 57–64.
79. Kim J, et al., 2009, Antioxidant and antidiabetic activity of Dangyuja (Citrus grandis Osbeck) extract treated with Aspergillus saitoi. Food Chem 117: 35–41
80. Kong L, Ziegler GR, 2013, Quantitative relationship between electrospinning parameters and starch fiber diameter. Carbohyd Polym 92: 1416-1422.
81. Koontz JL et al.,2009, Cyclodextrin Inclusion Complex Formation and Solid-State Characterization of the Natural Antioxidants α-Tocopherol and Quercetin. J Agric Food Chem 57: 1162–1171.
82. Kost J, Langer R,2001, Responsive polymeric delivery systems. Adv Drug Delivery Rev 46: 125–148.
83. Kriegel C. et al., 2008, Fabrication, functionalization, and application of electrospun biopolymer nanofibers. Crit Rev Food Sci Nutrition 48: 775-797.
84. Kresge CT et al., 1992, Ordered Mesoporous Molecular Sieves Synthesized by a Liquid-Cristal Template Mechanism. Nature 359: 710−712.
85. Kriegel C et al., 2009, Nanofibers as carrier systems for antimicrobial microemulsions. Part I: Fabrication and characterization. Langmuir 25: 1154-1161.
86. Kuan CY et al., 2011, Physicochemical characterization of alkali treated fractions from corncob and wheat straw and the production of nanofibers. Food Res Int 44: 2822-2829.

87. Lesmes U, McClements DJ, 2009, Structure-function relationships to guide rational design and fabrication of particulate food delivery systems. Trend Food Sci Tech 20: 448-457.
88. Langer R. Peppas, N, 1983, Chemical and physical structure of polymers as carriers for controlled release of bioactive agents: a review. J Macromol Sci Rev in Macromol Chem Physic, 23: 61-126.
89. Larson R, 1988, The antioxidants of higher plants. Phytochemistry 27: 969-978.
90. Li Y et al., 2009, Electrospun zein fibers as carriers to stabilize (−)-epigallocatechin gallate. J Food Sci 74: C233-C240.
91. Liao I, 2006, Aligned core-shell nanofibers delivering bioactive proteins. Future Medicine 1: 465-471.
92. Liao Y et al., 2008, Preparation, characterization, and encapsulation/release studies of a composite nanofiber electrospun from an emulsion containing poly(lactic-co-glycolic acid). Polymer 49: 5294-5299.
93. Lin HY et al., 2012, Pectin-chitosan-PVA nanofibrous scaffold made by electrospinning and its potential use as a skin tissue scaffold. J Biomat Sci Polym Ed 24: 470-484.
94. Lopez-Rubio A, Lagaron JM, 2012, Whey protein capsules obtained through electrospraying for the encapsulation of bioactives. Inn Food Sci Emerg Tech 13: 200-206.
95. Lu JW et al., 2006, Electrospinning of sodium alginate with poly(ethylene oxide). Polymer, 47: 8026-8031.
96. Luykx D et al., 2008, A review of analytical methods for the identification and characterization of nano delivery systems in food. J Agr Food Chem 56: 8231-8247.
97. Loscertales IG et al., 2002, Micro/nano encapsulation via electrified coaxial liquid jets, Science 295: 1695-1698.
98. Luong-Van E et al., 2006, Controlled release of heparin from poly(epsilon-caprolactone) electrospun fibers, Biomaterials 27: 2042–2050.
99. Madhugiri S et al., 2003, Electrospun MEH-PPV/SBA-15 Composite Nanofibers Using a Dual Syringe Method. J Am Chem Soc 125: 14531−14538.
100. Ma Z, Ramakrishna S, 2008, Electrospun regenerated cellulose nanofiber affinity membrane functionalized with protein A/G for IgG purification. J Memb Sci, 319: 23-28.
101. Mal NK et al., 2003, Photocontrolled Reversible Release of Guest Molecules from Coumarin-Modified Mesoporous Silica. Nature 421: 350−353.
102. Manakker F et al., 2009, Cyclodextrin-based polymeric materials: Synthesis, properties, and pharmaceutical/biomedical applications. Biomacromolecules 10: 3157–3174.
103. Manasco JL et al., 2012, Cyclodextrin fibers via polymer-free electrospinning. RSC Adv 2: 3778-3784.
104. Martin HJ et al., 2003, The inhibitory effects of flavonoids and antiestrogens on the Glut1 glucose transporter in human erythrocytes. Chem-Biol Interact 146: 225–235.
105. Martins A et al., 2010, Osteogenic induction of hBMSCs by electrospun scaffolds with dexamethasone release functionality. Biomater 31: 5875-5885.
106. Mason TL, Wasserman BP, 1987, Inactivation of red beet betaglucan synthase by native and oxidized phenolic compounds. Phytochemistry 26:2197–2202.
107. Meinel AJ et al., 2012, Electrospun matrices for localized drug delivery: Current technologies and selected biomedical applications. Eur J Pharm Biopharm 81: 1–13.
108. Mickova A et al., 2012, Core/shell nanofibers with embedded liposomes as a drug delivery system. Biomacromolecules, 13: 952-962.
109. McClements DJ, 1998, Food emulsions: principles, practice, and techniques. CRC press.
110. Munin A, Edwards-Lévy F, 2011, Encapsulation of natural poly-phenolic compounds: A review. Pharmaceutics 3: 793–829.
111. Natella F et al., 199, Benzoic and cinnamic acid derivatives as antioxidants: structure–activity relation. J Agr Food Chem 47:1453–1459
112. Natu MV et al., 2010, Effects of drug solubility, state and loading on controlled release in

bicomponent electrospun fibers. Int J Pharm 397: 50-58.
113. Neo YP et al., 2012, Influence of solution and processing parameters towards the fabrication of electrospun zein fibers with sub-micron diameter. J Food Eng 109: 645-651.
114. Neo YP et al., 2013a, Evaluation of gallic acid loaded zein submicron electrospun fiber mats as novel active packaging materials. Food Chem 141: 3192-3200.
115. Neo YP et al., 2013b, Encapsulation of food grade antioxidant in natural biopolymer by electrospinning technique: a physicochemical study based on zein-gallic acid system. Food Chem 136: 1013-1021.
116. Nijveldt R, 2001, Flavonoids: a review of probable mechanisms of action and potential applications. Am J Clin Nutr, 74: 418-425.
117. Okutan N et al., 2014, Affecting parameters on electrospinning process and characterization of electrospun gelatin nanofibers. Food Hydrocolloid 39: 19-26.
118. Opanasopit P et al., 2009, Electrospun poly (vinyl alcohol) fiber mats as carriers for extracts from the fruit hull of mangosteen. Int J Cosmetic Sci 31, 233-242.
119. Park C et al., 2009, Enzyme Responsive Nanocontainers with Cyclodextrin Gatekeepers and Synergistic Effects in Release of Guests. J Am Chem Soc 131: 16614−16615.
120. Park CH, Lee J, 2010, One-step immobilization of protein-encapsulated core/shell particles onto nanofibers, Macromol Mater Eng 295: 544–550.
121. Parvathy K et al., 2009, Antioxidant, antimutagenic and antibacterial activities of curcumin-β-diglusoside. Food Chem, 115: 265–271
122. Piazza L, Benedetti S, 2010, Investigation on the rheological properties of agar gels and their role on aroma release in agar/limonene solid emulsions. Food Res Int, 43: 269-276.
123. Pérez-Esteve E et al., 2014, Incorporation of Mesoporous Silica Particles in Gelatine Gels: Effect of Particle Type and Surface Modification on Physical Properties. Langmuir 30: 6970−6979.
124. Perez-Masia R et al., 2013, Development of zein-based heat-management structures for smart food packaging. Food Hydrocolloid 30: 182-191.
125. Perrett S et al., 1995, The plant molluscicide Millettia thonningii (Leguminosae) as a topical antischistosomal agent. J. Ethnopharmacol 47: 49–54.
126. Phillips RL et al., 1985, Elevated protein-bound methionine in seeds of a maize line resistant to lysine plus threonine. Cereal Chem 62: 213-218.
127. Pinho E et al., 2014, Cyclodextrins as encapsulation agents for plant bioactive compounds. Carbohyd Polym 101: 121– 135.
128. Pothakamury UR, Barbosa-Canovas GV, 1995, Fundamental aspects of controlled release in foods. Trends Food Sci Tech 6: 397-406.
129. Qi H et al., 2006, Encapsulation of drug reservoirs in fiber by emulsion electrospinning. Morphology characterization and preliminary release assessment. Biomacromolecules 7: 2327-2330.
130. Recourt K et al., 1989, Accumulation of a nod gene inducer, the flavonoid naringenin, in the cytoplasmic membrane of Rhizobium leguminosarum biovar viciae is caused by the pH-dependent hydrophobicity of naringenin. J Bact 171: 4370-4377.
131. Rooney, M. L. (1995). Overview of active food packaging. In Active food packaging (pp. 1e37). US: Springer.
132. Safi S et al., 2007, Study of electrospinning of sodium alginate, blended solutions of sodium alginate/poly(vinyl alcohol) and sodium alginate/poly(ethylene oxide). J Appl Polym Sci 104: 3245-3255.
133. Sakai S et al., 2009, Surface immobilization of poly(ethyleneimine) and plasmid DNA on electrospun poly(L-lactic acid) fibrous mats using a layer-by-layer approach for gene delivery. J Biomed Mater Res A 88A: 281-287.
134. Sen R. et al., 2004, Preparation of single-walled carbon nanotube reinforced polystyrene and polyurethane nanofibers and membranes by electrospinning. Nano Letters: 459-464.

135. Schiffman JD, Schauer CL, 2008, A review: Electrospinning of biopolymer nanofibers and their applications. Polym Rev 48: 317-352.
136. Schiraldi A et al., 2012, Water Activity in Biological Systems – A Review. Polym J Food Nutr Sci 62: 5-13.
137. Serizawa T et al., 2002, Thermoresponsive ultrathin hydrogels prepared by sequential chemical reactions. Macromolecules 35: 2184-2189.
138. Shen X et al., 2011, Electrospun diclofenac sodium loaded Eudragit® L 100-55 nanofibers for colon-targeted drug delivery. Int J Pharm 408: 200-207.
139. Shulman M et al., 2011, Enhancement of naringenin bioavailability by com-plexation with hydroxypropoyl-β-cyclodextrin. Plos One 6: e18033.
140. Shutava TG et al., 2009, (−)-Epigallocatechin gallate/gelatin layer-by-layer assembled films and microcapsules. J Colloid Interf Sci 330: 276-283.
141. Siepmann J, Siepmann F, 2008, Mathematical modeling of drug delivery. Int J Pharm 364: 328-343.
142. Sikareepaisan P et al., 2008, Electrospun gelatin fiber mats containing a herbal -Centella asiatica- extract and release characteristic of asiaticoside. Nanotechnology 19: 015102-015111.
143. Silva F et al., 2000, Phenolic acids and derivatives: studies on the relationship among structure, radical scavenging activity and physicochemical parameters. J Agr Food Chem 48:2122–2126.
144. Slabbert N, 1977, Ionisation of some flavanols and dihydroflavonols. Tetrahedron 33: 821-824.
145. Stijnman AC et al., 2011, Electrospinning of food-grade polysaccharides. Food Hydrocolloid 25: 1393-1398.
146. Stockton WB, Rubner MF, 1997, Molecular-level processing of conjugated polymers. 4. Layer-by-layer manipulation of polyaniline via hydrogen-bonding interactions. Macromolecules, 30: 2717-2725.
147. Stoiljkovic A, et al., 2007, Preparation of water-stable submicron fibers from aqueous latex dispersion of water-insoluble polymers by electrospinning. Polymer, 48: 3974-3981.
148. Such GK et al., 2006, Assembly of ultrathin polymer multilayer films by click chemistry, J Am Chem Soc 128: 9318-9319.
149. Sullivan ST et al., 2014, Electrospinning and heat treatment of whey protein nanofibers. Food Hydrocolloid 35: 36-50.
150. Sun XZ et al., 2013, Electrospun curcumin-loaded fibers with potential biomedical applications. Carbohyd Polym 94: 147-153.
151. Szejtli J, 2003. Cyclodextrins in the textile industry. Starch–Starke, 55: 191–196.
152. Thammachat T et al., 2011, Preparation and Characterization of Shellac Fiber as a Novel Material for Controlled Drug Release. Advance Mat Res, 152: 1232-1235.
153. Tang F et al., 2012, Mesoporous Silica Nanoparticles: Synthesis, Biocompatibility and Drug Delivery. Adv Mater 24: 1504−1534.
154. Toda M et al., 1992, The protective activity of tea catechins against experimental infection by Vibrio cholerae O1. Microbiol Immunol 36: 999–1001.
155. Tommasini S et al., 2004, Improvement in solubility and dissolution rate of flavonoids by complexation with β-cyclodextrin. J Pharm Biomed Anal 35: 379-387.
156. Uyar T et al., 2009, Electrospun polystyrene fibers containing high temperature stable volatile fragrance/flavor facilitated by cyclodextrin inclusion complexes. React Funct Polym 69: 145-150.
157. Uyar T et al., 2009, Electrospinning of cyclodextrin functionalized poly(methyl methacrylate)(PMMA) nanofibers. Polymer, 50: 475-480.
158. Vega-Lugo AC, Lim LT, 2009, Controlled release of allyl isothiocyanate using soy protein and poly (lactic acid) electrospun fibers. Food Res Int 42: 933-940.

159. Wang B et al., 2010a, Applications of electrospinning technique in drug delivery. Chem Eng Commun 197: 1315-1338.
160. Wang S et al., 2013, Electrospun soy protein isolate-based fibre fortified with anthocyanin-rich red raspberry (Rubus strigosus) extracts. Food Res Int 52: 467-472.
161. Wang C et al., 2012, Conventional electrospinning vs. emulsion electrospinning: a comparative study on the development of nanofibrous drug/biomolecule delivery vehicles. Adv Mat Res 410: 118-121.
162. Wang X, Zhao J, 2013, Encapsulation of the herbicide picloram by using polyelectrolyte biopolymers as layer-by-layer materials. J Agr Food Chem 61: 3789-3796.
163. Wang Y et al., 2010b, A novel controlled release drug delivery system for multiple drugs based on electrospun nanofibers containing nanoparticles: J Pharm Sci99: 4805-4811.
164. Wildman, RE, 2006, Handbook of nutraceuticals and functional foods. CRC press.
165. Wongsasulak S et al., 2007, The effect of solution properties on the morphology of ultrafine electrospun egg albumen-PEO composite fibers. Polymer 48: 448-457.
166. Wongsasulak S et al., 2010, Electrospinning of food-grade nanofibers from cellulose acetate and egg albumen blends. J Food Eng 98: 370-376.
167. Wongsasulak S et al., 2014, Effect of entrapped α-tocopherol on mucoadhesivity and evaluation of the release, degradation, and swelling characteristics of zeinechitosan composite electrospun fibers. Journal of Food Engineering, 120, 110-117.
168. Xie J, Hsieh YL, 2003, Ultra-high surface fibrous membranes from electrospinning of natural proteins: casein and lipase enzyme. J Mat Sci 38: 2125-2133.
169. Xu X et al., 2006, Preparation of core-sheath composite nanofibers by emulsion electrospinning. Macromol Rapid Comm 27: 1637-1642.
170. Yang D et al., 2007, Preparation of gelatin/PVA nanofibers and their potential application in controlled release of drugs. Carbohyd Polym 69: 538-543.
171. Yao C et al., 2007, Electrospinning and crosslinking of zein nanofiber mats. J Appl Polym Sci 103: 380-385.
172. Yarin AL, 2011, Coaxial electrospinning and emulsion electrospinning of core–shell fibers. Polym Advance Tech, 22: 310-317.
173. Yoo HS et al., 200, Surface-functionalized electrospun nanofibers for tissue engineering and drug delivery. Adv Drug Deliver Rev 61: 1033-1042.
174. Yu DG et al., 2009, Oral fast-dissolving drug delivery membranes prepared from electrospun polyvinylpyrrolidone ultrafine fibers. Nanotechnology 20: 055104-0055112.
175. Zamani M et al, 2013, Advances in drug delivery via electrospun and electrosprayed nanomaterials. Int J Nanomed 8: 2997–3017.
176. Zeng J et al., 2005, Influence of the drug compatibility with polymer solution on the release kinetics of electrospun fiber formulation. J Control Release 105, 43-51.
177. Zhang P et al., 2013, Solubility of Naringenin in Ethanol and Water Mixtures. J Chem Eng Data, 58: 2402-2404.
178. Zhang YZ et al., 2005, Recent development of polymer nanofibers for biomedical and biotechnological applications, J Mater Sci - Mater M 16:933–946.
179. Zhao D et al., 1998, Nonionic triblock and star diblock copolymer and oligomeric surfactant syntheses of highly ordered, hydrothermally stable, mesoporous silica structures. J Am Chem Soc 120: 6024−6036.
180. Zuidam, N.J. & Shimoni, E. (2007). Overview of Microencapsulates for Use in Food Products or Processes and Methods to Make Them. In NJ Zuidam & VA Nedovic (Eds.), Encapsulation Technologies for Active Food Ingredients and Food Processing, (pp 3-29). New York: Springer (Chapter 4).

3
NANOFIBROUS MEMBRANES AS BEVERAGE FILTRATION DEVICES

3.1 INTRODUCTION

Filtration is one of the most important unit operation common to the food and beverage industry which can be used to clarify, stabilize, depectinize and/or concentrate liquids (such as juices, wine, beer, oils and syrups) by the removal of small amounts of solid particles. Polymeric membranes are widely used in the beverage industry for microfiltration, ultrafiltration and reverse osmosis operations, in clarification and/or purification processes of a myriad of plants dedicated to the beverage production, from bottled water, to wine-making, brewery, to fruit juices. In most of the cases such filtration processes substitute other separation methods as they offer advantages such as enhanced mechanical, thermal and chemical resistance as well as desirable threshold molecular cutoffs (Scott, 1998).

Fabrication of membranes is typically made by conventional methods such as vapor or temperature-induced phase separation, stretching of melt-processed semi-crystalline polymer films, irradiation, extrusion, amongst others. (Pinnau & Freeman, 2000).

Electrospinning is an alternative technique for producing polymeric nanofibrpus membranes with good mechanical properties, large surface-to-mass ratio and relatively small pore sizes with an interconnected structure (Frenot & Chronakis, 2003; Barhate & Ramakrishna, 2007), all of them desirable characteristics of filtration membranes. Moreover, the as-electrospun polymers feature low density in comparison with their similar when manufactured in different ways, which represents a clear advantage from the point of view of the material economy. This technique has gained much attention especially because its simplicity and the fact that the large surface-to-mass ratio opens a wide range of potential applications as it makes the electrospun fibers an ideal material for sensors, controlled release systems, biomolecules and cells immobilization and tissue engineering applications (Huang *et al*., 2003).

The implementation of novel nanostructured filters can offer several advantages respect the current state of the art. For instance, nanofibrous membranes characterized by a great surface to volume ratio allow to develop 'one-step' clarification processes, reducing the need of filtering aids, enzymatic treatments. In spite of the fact that these same features (i.e., large contact areas, small pore sizes, resistance) make them also attractive in both gas and liquid filtration, there is very little information about their use in beverages (Veleirinho & Lopes-da-Silva, 2009; Zhang *et al.*, 2010) and even less on the issue of selective adsorption of molecules, as polyphenolic compounds (Scampicchio *et al.*, 2008), that are relevant for the biochemical and sensory stability of the beverages during shelf life. Moreover, according to Veleirinho and Lopes-da-Silva (2009) in liquid filtrations the electrospun nanofibrous membranes are expected to overcome some of the drawbacks related to the porous polymeric membranes manufactured by traditional methods, e.g., low-flux and high-fouling performance.

In this part of the thesis nylon-6 nanofibrous membranes (NFM) are studied in connection with the clarification of apple juice achieved by a dead-end filtration system operating at different trans-membrane pressures. Relevant morphological, structural and transport characteristics of electrospun nylon-6 membranes as potential filtration devices have been explored and compared to those of commercial polymeric filtration membranes. The results will demonstrate that NF membranes have much greater initial reactivity respect conventional membranes and a greater capacity for adsorb bitter polyphenols even after membrane fouling[2].

3.2 MATERIALS AND METHODS

3.2.1 Chemicals

All chemicals and solvents were of analytical reagent grade and were used without any further purification. Formic acid was purchased from Fluka, Sigma-Aldrich (Steinham, Germany). Ethanol,

[2] This part of the work was done under the tutorship of Pr. Matteo Scampiccio. Faculty of Science and Technology. Free University of Bozen – Bolzano, Italy.

methanol, nylon-6, 2,2-diphenyl-1-picrylhydrazyl (DPPH·), 2,2'-azobis(2-amidinopropane) dihydrochloride (AAPH), Folin-Ciocalteau reagent, 6-hydroxy-2,5,7,8-tetramethylchroman-2-carboxylic acid (Trolox), boric acid, sodium carbonate, citric acid and standards of gallic acid, caffeic acid, tannic acid, D-glucose, D-fructose, sucrose and L-malic acid were purchased from Sigma-Aldrich (St. Louis, MO). All the solutions were prepared using distilled deionized water obtained with a Mili-Q system (Millipore, Bedford, MA).

3.2.2 Turbid apple juice

Monovarietal apple juices were purchased from a local store (McIntosh and Red Delicious apples).

3.2.3 Commercial membranes

Whatman polyamide membranes with nominal pore sizes of 0.45 μm (W-PA1) and 0.2 μm (W-PA2), respectively (Whatman, Springfield Mill, UK) and Millipore HAWG047S3 (mix of cellulose acetate and cellulose nitrate) with a nominal pore size of 0.45 μm (M-CM).

3.2.4 Preparation of membranes by electrospinning

Nylon-6 membranes were prepared as described by Scampicchio *et al.* (2009) with some modifications. Briefly, a 23 % (w/w) solution of nylon-6 was prepared in formic acid. Plastic syringes (10 mL) fitted with a metallic needle (Hamilton) were filled with the polymeric solution and placed in a KDS100 syringe pump (KD-Scientific, New Hope, PA) at a flow rate of 0.15 mL h^{-1}. The needle of the syringe was linked to a Spellman SL150 high voltage power supply by an alligator clip. A foil-covered copper tray, positioned at 11 cm in front of the needle, was used as collector and grounded. For the electrospinning, the electrical potential was set at 25 kV. At the end of the electrospinning runs, the membranes were peeled-off. Membranes with different thicknesses were obtained by stopping the collection after different times (from 5 min to 60 min).

3.2.5 Scanning electron microscopy

A field emission JEOL (FEG-SEM) scanning electron microscope was used to observe the morphology of the nanofibers. Conditions were: accelerating 5 kV voltage and 6 mm working distance, with a 30 μm width slit. The samples were first gold sputtered (Sputtering Polaron E 5100) for 30 s (rate 1 nm s^{-1}) using argon and 18 mA current intensity. From each image, 100 segments were randomly selected and diameters measured with the ImageJ 1.4 software.

3.2.6 Thickness, density and porosity

Thickness was measured by a micrometer. Apparent density was measured by weighting 1 cm2 of each membrane. Porosity (π) was calculated using the following equation (Ma *et al*., 2005):

$$\pi = \left[1 - \left(\frac{\delta_a}{\delta_b}\right)\right] \bullet 100\% \quad (1)$$

where δa is the apparent density of the membrane and δb is the nylon-6 bulk density.

3.2.7 Mechanical properties

Mechanical properties were evaluated by a simple puncture test using a TA.XT Plus texture analyzer (Stable Micro Systems, Godalming, UK). Film specimens were mounted on a film holder. The puncture probe (spherical end: 3 mm diameter) was fixed on the load cell (50 kg) and driven downward with a cross-head speed of 0.1 mm s^{-1} to the center of the film holder's hole. Load versus displacement curves were recorded until rupture of the films and used to determine the force at break (F_{break}), the work at break (W_{break}) and the slope of the curve within the linear region or force-to-displacement ratio (*dF/dx*) (Siepmann *et al*., 2006).

3.2.8 Filtration set-up

The small scale filterability studies were performed with the FilterTec system (SciLog Inc, USA) using a Tandem 1081 peristaltic pump head driven by a 160-RPM motor (Schick, 2003). Tygon tubing (#16) was used for pump rates of 35-100 mL min^{-1}. The system was able to run dead-end filtration system in either constant-flow or constant-pressure modes. Operative pressures ranged from 69 to 345 kPa. The system was connected with a pressure transducer and a electronic balance, as shown in Figure 3.1. All filtration experiments were repeated in double. A new membrane was used for every filtration experiment.

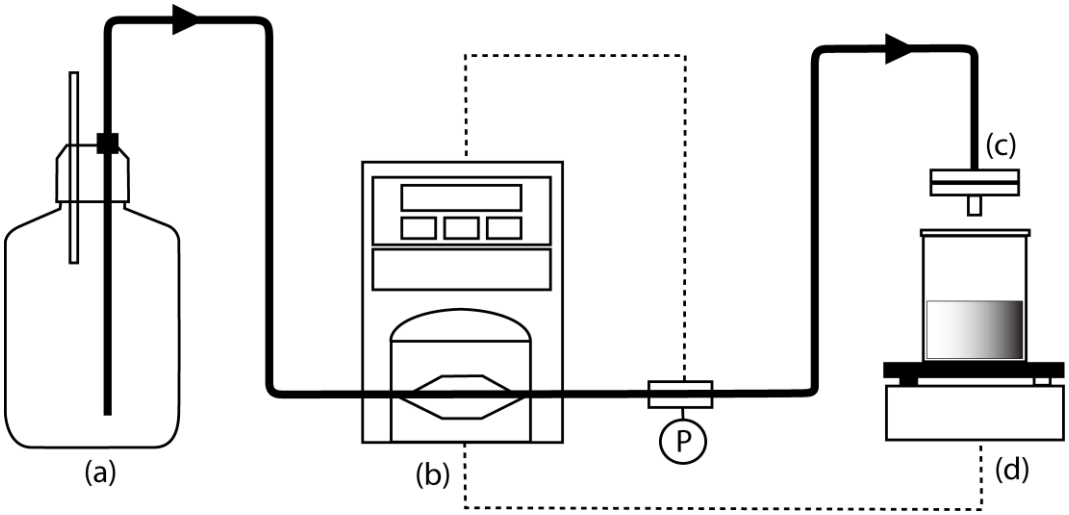

Figure 3.1. Experimental set-up for dead-end filtration. Legend: (a) Sample container; (b) peristaltic pump; (c) filter holder; (d) balance; (P) pressure transducer. Dotted lines indicate remote communications between the pump, the balance and the pressure transducer. (Schick, 2003)

3.2.9 Chemical and physicochemical analysis of the juice

Turbidity, color, soluble solids, total solids, pH and total acidity were measured before and after the filtration of the juice. Briefly, turbidity and color (brown) were measured by UV-VIS: turbidity is expressed as percentage of transmittance at 650 nm (Gökmen *et al.*, 2001). Color is expressed as percentage of transmittance at 440 nm (He *et al.*, 2007). Soluble solids were measured with a Brix-meter (N-1 alpha, ATAGO, Japan). Total solids were determined by weight after drying the juice in oven for 24 h at 70°C (AOAC, 1984). Total acidity was determined by titration with 0.1 M NaOH to pH 8.1 and the result expressed as malic acid equivalent.

3.2.10 Sugars and organics acids

Fructose, glucose, sucrose were measured by HPLC with a reverse phase column (YMC-Pack polyamine II S-5um column (250 mm × 4.6 mm)) and a refractive index detectors. Mobile phase was acetonitrile/water (75:25) at 1.5 mL min^{-1}. Malic acid was quantified by HPLC using a diode array detector (210 nm) with an Aminex Ion Exclusion HPX-87H column (300 mm × 47.8 mm). Isocratic elution was carried out at 40 °C using 5 mmol/L sulphuric acid at 0.6 mL/min as the mobile phase.

3.2.11 Phenols and antioxidants

Total phenols were measured by the Folin Ciocalteau assay (Ribéreau-Gayon *et al.*, 2000). Radical scavenging capacity was measured by the ORAC assay and DPPH radical scavenging capacity. The ORAC assay using fluorescein as fluorescent probe (ORACFL) was carried out on juice samples

diluted 1000-fold in phosphate buffer (pH 7.0) (Prior *et al.*, 2003). DPPH was measured as described by Buratti *et al.* (2008). Briefly, 5 mL of DPPH• methanolic solution ($7.6 \bullet 10^{-5}$ M) were mixed with 0.2 mL of a methanol:water:formic acid solution (in the ratio 70:29:1) and 0.8 mL of sample. The mix was incubated at 35 °C for 5 min. The discoloration reaction was followed by measuring the absorbance at 515 nm.

3.3 RESULTS AND DISCUSSION

3.3.1 Characterization of the electrospun nanofibrous membranes

Membranes of nylon-6 were electrospun for different collection times (from 5 to 60 min). The membranes thickened at a rate of 2.3 μm min^{-1} (r^2=0.98), resulting in thickness between 10 to 125 μm, as shown in Figure 3.2.

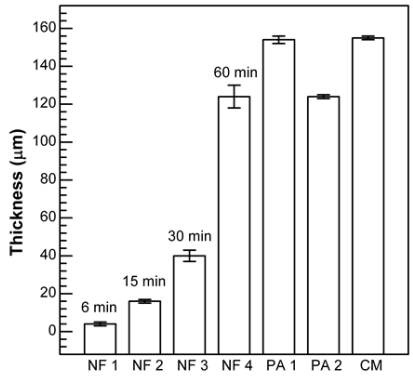

Figure 3.2 Thickness of nylon-6 nanofibrous membranes at various collection times (NF 1-4), commercial polyamide membranes (PA 1-2) and commercial cellulose membranes (CM).

Figure 3.3 shows field-emission scanning electron microscope (FESEM) images of electrospun fibers that exhibit a randomly oriented and interconnected arrangement which results in membranes with a pseudo-porous structure. Nanofibers with a thickness of 95 ± 25 nm (n = 100) are formed because of chain entanglements in the charged solution that stabilize the electrospinning jet and prevent its breakup or the formation of droplets (McKee *et al.*, 2006).

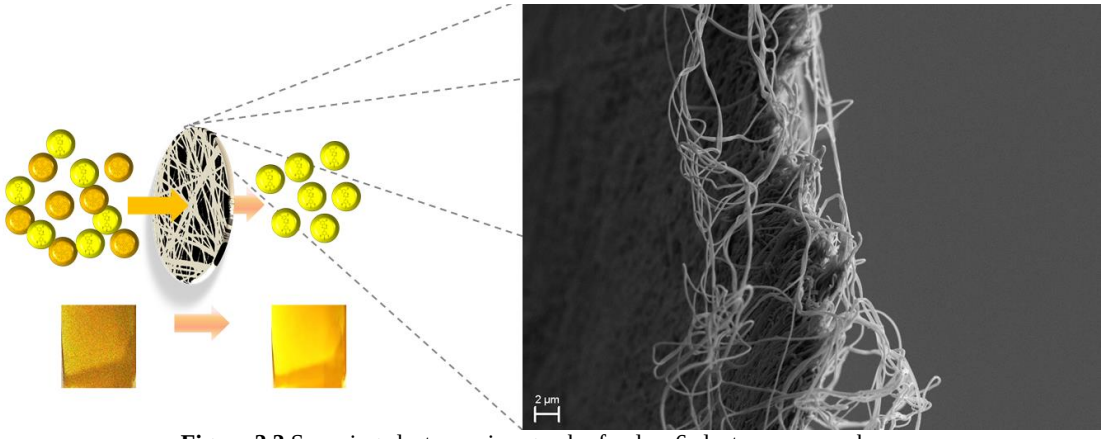

Figure 3.3 Scanning electron micrograph of nylon-6 electrospun membrane.

Physical characteristics of nylon-6 (nanofibrous) and commercial (non-fibrous) membranes were compared (Table 3.1). Electrospun membranes have lower average density (75 kg m^{-3}) and higher

porosity (94%) than the commercial polyamide membranes (350 kg m^{-3} and 70%, respectively, for W-PA2), resulting in materials with lower costs and higher permeability. Considering the differences found with the polyamidic membranes, these results show that the structure of the membranes at the sub-micron scale greatly affects their physical properties.

Table 3.1. General characteristics of the electrospun nylon-6 (NFM 1-4) and commercial polymeric membranes

Membrane	Collection time (min)	Thickness ($m \cdot 10^{-6}$)	Density (kg m^{-3})	Porosity (%)	Force at break (N)	Elasticity (N m)	Work at break (N m^{-1})
NFM 1	6	4 ± 1	101 ± 13	91 ± 1	n.d.	n.d.	n.d.
NFM 2	15	16 ± 1	61 ± 11	94 ± 2	5.1 ± 0.7	9.6 ± 2.2	1.3 ± 0.2
NFM 3	30	40 ± 3	73 ± 10	93 ± 1	13.0 ± 0.1	23.8 ± 2.7	4.0 ± 0.3
NFM 4	60	124 ± 6	67 ± 18	95 ± 1	13.5 ± 0.8	28.2 ± 3.3	4.1 ± 0.3
W-PA 1	-	154 ± 2	299 ± 3	75 ± 1	3.3 ± 0.1	2.6 ± 0.1	2.2 ± 0.1
W-PA 2	-	124 ± 1	353 ± 3	70 ± 1	4.0 ± 0.1	3.4 ± 0.2	2.5 ± 0.0
M-CM	-	155 ± 1	314 ± 2	81 ±1	2.3 ± 0.4	1.2 ± 0.3	2.7 ± 0.2

The membranes show also a good mechanical resistance. As the thickness increases from 16 to 124 μm, then the force-to-displacement ratio (dF/dx), force at break (F_{break}) and work at break (W_{break}) increased until a plateau was reached. For thickness of 124 μm, the electrospun membranes have greater (a) force at break; (b) force-to-displacement ratio; and (c) work at break than commercial polyamide membranes (Table 3.1).

3.3.2 Dead-end filtration

Apple juice was filtered at constant pressures commonly found in microfiltration processes, namely 207, 276 and 345 kPa (30, 40 and 50 psi) while the flow-rate was continuously measured by recording the mass change of the permeate with a balance connected to a PC (Figure 3.1). The typical behavior of the filtration process with a NFM of 124 μm thickness is shown in Figure 3.4. The maximum flow rate (0.67 mL min^{-1} at a constant 345 kPa) was achieved during the first part of the experiment. Then, the flow rate slowly decreased. This indicated that the adsorption of organic species and particles caused a progressive fouling, leading to a decrease of the permeate flux through the membrane. After 20 min, the flow rate dropped below 0.15 mL min^{-1} and the collected filtrate was 5 g (20 mg cm^{-2}).

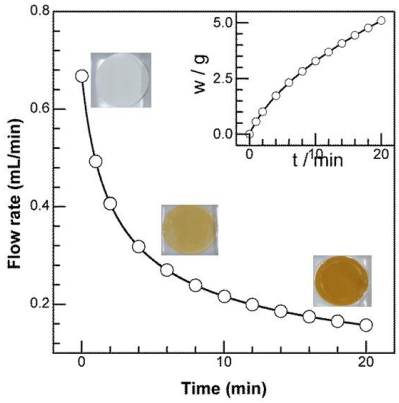

Figure 3.4 . Filtrate flow rate in a typical apple juice filtration experiment with the characteristic aspect of membranes at the different stages of the process. In the box, cumulative collected weight of filtrate. NFM 124 μm; ΔP = 345 kPa (50 psi)

3.3.3 Filter medium resistance

The mechanism for the observed filtration behavior can be explained with a model based on three resistances in series, respectively, the initial filter resistance, the polarization resistance and the cake resistance. This method corresponds to a simplification of the model proposed by Jiraratananon & Chanachai (1996). The initial filter resistance, R_m, is described by the Darcy's law in experiment using distilled water as the liquid flowing through the membrane and calculated by using the following equation:

$$\mathrm{R_m} = \frac{dt}{dV} \cdot \frac{\Delta P \cdot A}{\eta} \qquad (2)$$

Where V is the filtrate volume in time t; ΔP is the pressure drop; A is the wet surface area of the membrane and η is the viscosity of the fluid at operating temperature (in this case, of distilled water at 20 °C). The resulting flow rate (dV/dt) was measured at different constant pressures (ΔP, 207, 276 and 345 kPa). Electrospun membranes have R_m values from 2 to $54 \cdot 10^{10}$ m^{-1}, depending on the thickness. This confirms the good permeability to water flow of the nanofibrous membranes.

3.3.4 Polarization resistance

The second resistance is due to the concentration polarization R_p. This accumulation of solute at the membrane interface can limit the flux, leading to charged chemical species promoting local aggregation and cohesiveness of the fouling layer. To measure R_p, apple juices were used. The resistance was determined by the integral solution of the Sperry equation in the case of constant pressure (Orr, et al., 1977; Suki et al., 1984). The inverse of the flow rate (t/V) as a function of the volume of filtrate (V) provide access to an overall membrane resistance which include the initial filter resistance, R_m, and the polarization resistance, R_p (Yu and Lencki, 2004):

$$\frac{t}{V} = \frac{\eta \cdot (R_p + R_m)}{A \cdot \Delta P} + \frac{\eta \cdot \alpha \cdot C}{2 \cdot A^2 \cdot \Delta P} \cdot V \qquad (3)$$

where α is the specific resistances of the deposit or cake and C is the concentration of total suspended solids in the juice. Table 3.2 shows that R_p values of the electrospun membranes vary from 2.6 to 3.5 10^{13} m^{-1} as a function of the pressure drop used (207, 276 or 345 kPa). As expected, these values are of three orders of magnitude higher than of R_m, which may be neglected or, in case, used for quality control and checking of the membrane cleanliness and aging.

Commercial polyamide membranes show R_p values in the range between 1.1 and $2.0 \cdot 10^{13}$ m^{-1} for W-PA1 or 2.5 and $3.1 \cdot 10^{13}$ m^{-1} for W-PA2. Interestingly, as the pressure drop increases, the R_p value for the electrospun membranes decreases, whereas, for the commercial membranes, it increases. The specific behavior of NFM can be explained considering their specific adsorption capacity (Scampicchio et al. 2008). Apparently, at higher pressures, the adsorption of fouling species on the fibers is enhanced. This remove foulants on the fiber surface and, in turn, reduces the resistance to flow of the membrane. The adsorption behavior of NMF was also observed in separate experiments described in sections 3.6 and 3.7.

3.3.5 Cake resistance

The last contribution to the membrane resistance is attributed to the cake formed during apple juice filtration. Specific resistances of the deposit or cake (α, m/kg) were obtained by the slope of equation 3. Table 3.2 shows values ranging from 0.7 to $1.7 \cdot 10^{15}$ m/kg , depending on the pressure drop applied rather than on the membrane used. This is expected as the cake resistance is function of the solids contained in the fluid and not on the filter medium used.

Table 3.2. Initial filter (Rm), polarization (Rp) and cake (α) resistance of nanofibrous (thickness 124 μm) and commercial polyamide membranes in apple juice filtration experiments at different pressure drops

	ΔP		Rm	R^{2*}	Rp	α	R^{2**}
Membrane	*psi*	*kPa*	*x 10^{10} m^{-1}*		*10^{13} m^{-1}*	*10^{15} $m{\cdot}kg^{-1}$*	
NFM	30	207	53.9 ± 4.5	1.00	3.1 ± 0.5	1.7 ± 0.4	0.99
	40	276			3.4 ± 0.3	1.6 ± 0.3	0.90
	50	345			2.6 ± 0.2	1.3 ± 0.2	0.99
W-PA 1	30	207	3.7± 0.2	1.00	1.1 ± 0.2	0.7 ± 0.3	0.97
	40	276			1.7 ± 0.3	1.0 ± 0.3	0.99
	50	345			2.0 ± 0.2	1.3 ± 0.5	0.98
W-PA 2	30	207	4.9± 0.1	0.99	2.5 ± 0.2	1.0 ± 0.2	0.99
	40	276			2.8 ± 0.3	1.4 ± 0.4	0.99
	50	345			3.1 ± 0.1	1.6 ± 0.3	0.99

*R^2 is the linear correlation coefficient obtained when plotting the flux *dV/dt* vs *V*, indicating the goodness of the experimental data's fit to equation 2. **R^2 is the linear correlation coefficient obtained when plotting *t/V* vs *V*, indicating the goodness of the experimental data's fit to equation 3. Results are expressed as average of 2 measurements +/- the standard deviation

3.3.6 Apple juice clarification

Nanofibrous membranes have been compared with commercial ones to test their clarification capability. Two of the main parameters used to monitor the efficacy of the clarification process are the color (transmittance value at 660 nm) and turbidity (transmittance value at 440 nm). Figure 3.5 shows that as the membranes thickness increased, the turbidity loss became greater. NFM of 4 μm resulted in quick filtration cycles (1.5 min for 5 mL of filtrate) and low turbidity reduction (~ 20%). Membranes of 40 μm yielded juice turbidity similar to the commercial juices. Membranes with thickness of 124 μm resulted in the clearest juice, with turbidity loss of 98%.

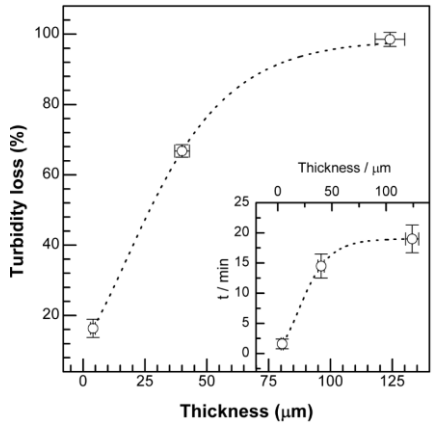

Figure 3.5. Turbidity reduction in apple juice filtration using NFM of various thickness. In the box, 5·10-3 L filtration cycle-time. Vertical error bars correspond to standard deviations of n=3 repetitions. Horizontal error bars indicate standard deviation of the thickness value for the various NFM (n=20).

Apple juice samples were filtered in a dead-end filtration system at constant pressure (50 psi). Changes in turbidity and color are reported in Table 3.3. In all the cases regarding turbidity and color, nanofibrous membranes showed similar or superior performances in comparison to commercial polyamide or cellulose membranes.

Table 3.3. Effect of filtration (ΔP = 50 psi) with nanofibrous (thickness 124 μm) and commercial membranes on apple juice turbidity (transmittance value at 660 nm) and color (transmittance value at 440 nm)

		Turbidity (660 nm)		**Color (440 nm)**	
Juice	*Filter*	*initial*	*after filtration*	*Initial*	*after filtration*
	NFM		2 ± 1		30 ± 1
AJ1	W-PA1	78 ± 0.1	6 ± 1	95 ± 0.1	28 ± 2
	M-CM		4 ± 1		48 ± 1
	NFM		1 ± 1		21 ± 1
AJ2	W-PA1	57 ± 0.1	2 ± 1	94 ± 0.1	19 ± 1
	M-CM		4 ± 1		51 ± 1
	NFM		1 ± 1		4 ± 2
AJ3	W-PA1	53 ± 0.1	3 ± 1	93 ± 0.1	14 ± 2
	M-CM		4 ± 1		50 ± 1

*NFM: nanofibrous membrane; W-PA: Whatman polyamide membranes with nominal pore sizes of 0.45 μm; M-CA: Millipore membranes of cellulose acetate and cellulose nitrate with a nominal pore size of 0.45 μm. Results are expressed as average values ± standard deviation of n=3 repeatitions.

Turbidity loss was also measured as a function of transmembrane pressure since it affects membrane performance (Persson *et al*., 1995). Figure 3.6 shows the effect on turbidity loss of dead-end filtration process performed at increasing pressures for the electrospun membrane and a commercial polymeric membrane. As the pressure increases, NFM enhance their ability to reduce the juice turbidity. Instead, polyamide commercial membranes behave opposite and they reduce their capability to reduce the juice turbidity. This behavior can be explained considering that nanofibrous membranes are compressible, and at higher pressure result in smaller thickness, pore size and cut-off. This behavior is not present in commercial polyamide membranes.

3.3.7 Selective adsorption of soluble nutrients

A further special feature of NFM is their capability to adsorb hydrophobic species, like phenols (Scampicchio *et al*., 2008). The capability to remove phenols from the juice is relevant for the beverage industry as the interactions between polyphenols and proteins are responsible of juice browning and sedimentation (Johnson *et al*., 1968). Thus, adsorption behavior of the membranes towards phenol-like compounds present in apple juice was next monitored.

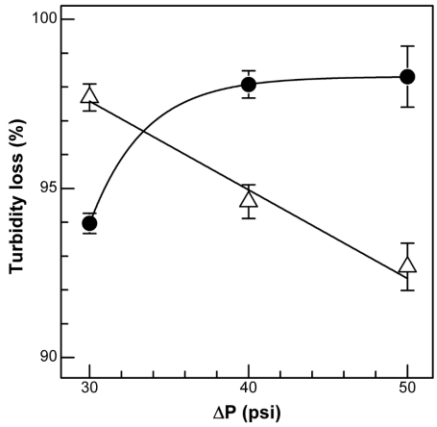

Figure 3.6 .Effect of different transmembrane pressures on turbidity reduction of apple juice, using nanofibrous (•) and commercial polyamide (Δ) membranes Error bars correspond to standard deviations of n=3 repetitions

Results are shown in Figure 3.7. During the initial minutes of filtration with the electrospun membranes, the measured values of total phenols is minimum at the beginning (phase A). Then, the total phenol value rapidly increases, until it reaches a similar adsorption behavior of commercial polyamide membranes (phase B). In phase A, the electrospun membranes are far more effective than polyamide membranes to adsorb phenols. However as the membranes become fouled, the membranes behavior overlap and the type of membranes show similar behavior. This trend is specific for phenols compounds only. For comparison, organic acid (such as malic acid) and the main sugars (such as fructose, glucose and sucrose) have been measured during the filtration process. Results show that their adsorption is almost negligible (Table3.4).

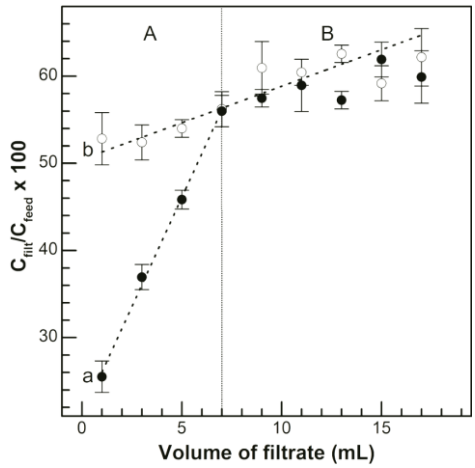

Figure 3.7. Change of remaining phenolic compounds in the filtrate during apple juice filtration (% of the concentration in unfiltered juice) with (a) nylon-6 nanofibrous and (b) commercial polyamide membranes. Error bars correspond to standard deviations of *n*=3 repetitions.

Furthermore, NFM adsorb only those phenols that are in their undissociated state, or in other words, that have pKa more basic than the pH of the apple juice. To prove it, standard solution of caffeic acid (pKa ~ 4.5) and tannic acid (pKa ~ 10) dissolved in a buffer at pH 3.5 were filtrated and the resulting permeate monitored by chrono-amperometry. Figure 3.8 shows that the nanofibrous

membranes are weak to remove caffeic acid (C), but efficient to adsorb tannic acid (A and B). This can be explained considering that undissociated phenols (like tannins) have more affinity to the nylon membrane than to water. Instead, the hydrophobicity of the membrane limits the adsorption of caffeic acid, which is partially dissociated at the pH of the juice.

Table 3.4. Effect of filtration (ΔP = 50 psi) with nylon-6 nanofibrous membrane (thickness 124 μm) and a commercial polyamide membrane (W-PA 1) on pH, malic acid, sugars, total phenolic compounds and antioxidant activity of apple juice. Results are expressed as average values ± standard deviation of n=3 repetitions

		Filtered juice	
	Unfiltered juice	**Nanofibrous**	**Commercial**
pH	3.40 ± 0.1	3.40 ± 0.1	3.40 ± 0.1
Malic acid (mM)	65.4 ± 0.7	58.8 ± 1.3	61.7 ± 2.0
Fructose (wt%)	9.47 ± 0.10	7.14 ± 0.41	7.34 ± 0.59
Glucose (wt%)	2.65 ± 0.04	2.19 ± 0.12	2.26 ± 0.10
Sucrose (wt%)	2.53 ± 0.04	1.89 ± 0.11	1.93 ± 0.17
Total phenols (ppm gallic acid)	326.7 ± 2.5	83.4 ± 3.1	149.7 ± 4.7
ORAC (μM Trolox eq.)	39.5 ± 0.5	16.6 ± 2.0	17.6 ± 0.9

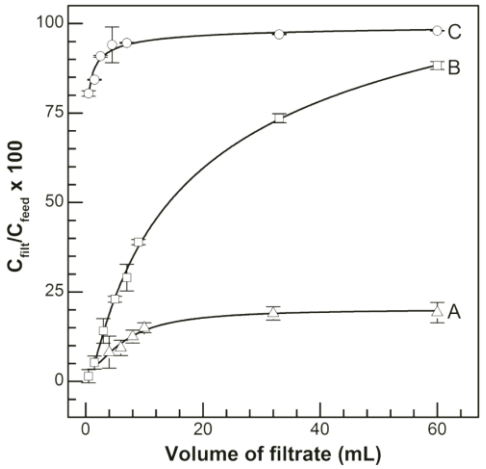

Figure 3.8. Change in phenolic concentration of different polyphenols standard solutions during filtration with nylon-6 nanofibrous membrane. 8 ppm (A) and 800 ppm (B) tannic acid and 800 ppm caffeic acid (C). Error bars correspond to standard deviations of n=3 repetitions.

A practical implication of this finding is that the filtrations with nylon nanofibrous membranes do not affect the antioxidant activity of the apple juice. The ORAC assay was performed before and after the filtration of the same apple juice with commercial and electrospun membranes. The results reported in Table 3.4 show that the electrospun nanofibers caused a great decrease of total phenols but not antioxidant capacity, which remains comparable to those of the commercial polyamide membranes. The capability to maintain the maximum antioxidant capacity of the juice, and at the same time, to enhance the removal of phenols, is a desirable feature as it can contribute to enhance the nutritional appealing of the product, its stability and shelf-life (Herrmann, 1990).

In conclusion, nylon-6 nanofibrous membranes, with fibers of diameter around 95 nm, display structural, mechanical and transport features that make them ideal devices for filtering purposes, namely, interconnected and pseudo-porous structure, very high porosity (94%), remarkable resistance

to transversal stress and good permeability to water. Their fabrication by electrospinning of nylon-6 acidic solutions is straightforward and cheap. Furthermore, this technique allows for easily adjusting relevant variables, such as membrane thickness, which in turn permits to modulate processing characteristics and filtrate quality. In this work, the membranes were successfully applied in apple juice filtration. NFM with thickness around 124 μm, operating at a transmembrane pressure of 345 kPa (50 psi), produced apple juice with optical characteristics similar to commercial clarified juices. Their capacity to remove turbidity and color was superior compared to commercial polymeric membranes. Increasing pressure enhances the NFM ability to reduce turbidity whereas conventional polyamide membranes show the opposite behavior. Nanofibrous membranes showed a higher adsorption capacity towards undissociated polyphenols rather than to lighter phenolics like caffeic acid, which results in the selective removal of bitter polyphenols at the pH of apple juice (3.5).

Although further scale-up studies are necessary as they will permit to better describe the performance of nanofibrous membranes on a large scale, the results of this work demonstrate that NFM are promising materials for the industry of beverage processing. In particular, their application in apple juice filtration allows for obtaining a high quality product with no use of clarification aids or additional clarification steps. Moreover, NFM enable the combination of the conventional sieving mechanisms, typical of microporous filters, with the ability of affinity membranes to remove specific compounds.

3.4 REFERENCES

1. Barhate RS, Ramakrishna S, 2007, Nanofibrous filtering media: Filtration problems and solutions from tiny materials. J Membr Sci 296: 1-8.
2. Buratti S et al., 2008, A low-cost and low-tech electrochemical flow system for the evaluation of total phenolic content and antioxidant power of tea infusions. Talanta 75: 312-316.
3. Frenot A, Chronakis IS, 2003, Polymer nanofibers assembled by electrospinning. Curr Opin Colloid Interface Sci 8: 64-75.
4. Gökmen V et al., 2001, Effects of various clarification treatments on patulin, phenolic compound and organic acid compositions of apple juice. Eur Food Res Technol 213: 194-199.
5. He Y et al., 2007, Effective clarification of apple juice using membrane filtration without enzyme and pasteurization pretreatment. Sep Purif Technol 57: 366-373.
6. Herrmann K, 1990, Significance of hydroxycinnamic acid compounds in Food. I. Antioxidant activity-effect on the use, digestibility, and microbial spoilage of food. Chem Mikr Tech Lebensmittel 12: 137-144.
7. Huang ZM et al., 2003, A review on polymer fibers by electrospinning and their applications in nanocomposites. Compos Sci Technol 63: 2223–2253.
8. Jiraratananon R, Chanachai A, 1996, A study of fouling in the ultrafiltration of passion fruit juice. J Membr Sci 111: 39-48.
9. Johnson G et al., 1968, The chemical nature and precursors of clarified apple juice sediment. J Food Sci 33: 254-257.
10. Ma Z et al., 2005, Surface engineering of electrospun polyethylene terephthalate (PET) nanofibers towards development of a new material for blood vessel engineering. Biomaterials 26: 2527–2536.
11. McKee MG et al., 2006, Phospholipid Nonwoven Electrospun Membranes. Science 311: 353.
12. Orr C, Filtration principles and practice. Marcel-Dekker, New York, 1977.
13. Persson KM et al., 1995, Study of membrane compaction and its influence on ultrafiltration water permeability. J Membr Sci 100: 155-162.
14. Pinnau I., Freeman BD, Formation and modification of polymeric membranes: overview. In I. Pinnau, (Eds.), Membrane Formation and Modification (pp. 1-22). ACS Symposium Series: American Chemical Society. Washington, DC, 2000.

15. Prior RL et al., 2003, Assays for hydrophilic and lipophilic antioxidant capacity (oxygen radical absorbance capacity (ORACFL) of plasma and other biological and food samples. J Agr Food Chem 51: 3273–3279.
16. Ribéreau-Gayon P et al. Handbook of Enology. The chemistry of wine stabilization and treatments. John Wiley and Sons Ltd., 2000, vol. 2, pp. 157–162.
17. Scampicchio M et al., 2008, Electrospun nanofibers as selective barrier to the electrochemical polyphenol oxidation. Electrochem Commun 10: 991-994.
18. Scampicchio M et al., 2009, Optical nanoprobes based on gold nanoparticles for sugar sensing. Nanotechnology 20: 1-5.
19. Schick K, 2003, Enhancing dead end filtration throughput using a non-traditional liquid handling procedure. Filtr Separat 40: 30-33.
20. Scott K. Handbook of Industrial Membranes, Elsevier Science Ltd., 1st ed, 1998, pp 145-753.
21. Siepmann F et al., 2006, Drugs acting as plasticizers in polymeric systems: A quantitative treatment. J Controlled Release 115: 298-306.
22. Suki A et al., 1984, Flux decline in protein ultrafiltration. J Membr Sci 21: 269−283.
23. Veleirinho B, Lopes-da-Silva JA, 2009, Application of electrospun PET nanofiber mat to apple juice clarification. Process Biochem 44: 353-356.
24. Yu J, Lencki RW, 2004, Effect of enzyme treatments on the fouling behavior of apple juice during microfiltration. J Food Eng 63: 413-423.
25. Zhang, H., Nie, H., Yu, D., Wu, C., Zhang, Y., & White, C.J.B. (2010). Surface modification of electrospun PAN nanofiber towards developing a membrane for bromelain adsorption. Desalination 256, 141-147.

4
CONCLUSIONS

CONCLUSIONS

Nanofibrous materials combine the advantages of particulate nanomaterials, namely large surface areas, high porosity and high responsive capacity to environmental stimuli, with the advantages of polymeric laminate materials like films or membranes, namely mechanical resistance, handling versatility, elasticity and permeability. Electrospinning of polymeric or polymeric blend solutions, dispersions or emulsions is straightforward and allow for the fast production of nanofibrous materials with minimum harmful effects on the materials involved in the electrospinning process.

In this thesis, we proved the potentialities of a single kind of materials, non-woven electrospun nanofibers, for solving very specific issues of the food and beverage industry in three spheres: (i) food electrochemical sensing for quality control, (ii) as encapsulation systems for the controlled release of bioactives, to be used as functional ingredients or active packaging materials and (iii) as separation membranes for highly selective and energy-reduced beverage clarification. This kind of materials allow for the design of customised solutions for the food industry in a remarkably transversal way.

In detail, with regard to the **first sphere (food sensing)**:

(1) The applicability of a novel sensing unit based on a disposable screen printed carbon electrode (SP) coated by a electrospun nylon-6 nanofibrous membrane was demonstrated for the in-situ determination of AA in both standard solution and real fruit samples. The sensor displays high sensitivity, reproducibility and selectivity towards AA with a good stability and a fast response. Due to the simplicity of the apparatus, it could be used like a portable device to be applied in the field. (**2)** The immobilization of xanthine oxidase onto nanofibrous membranes through a very simple methodology and its use as coating of rhodium-carbon home-made electrodes operating at low potentials, allow for a very specific amperometric detection of purines (i.e., xanthine), an important chemical marker of the freshness of meat products, specially fish. The increase in current was attributed to the reduction of hydrogen peroxide on the electrode surface, constantly regenerated by the enzyme through the oxidation of xanthine to uric acid. The rate of increase of redox amperometric signals ($-\mu A\ s^{-1}$) was considered as a measurement of the reaction rate, and therefore of the analyte concentration, the results indicated that this device can be a valid alternative for the selective detection of xanthine or other purines. More active enzymes or improved polymer blends are needed in order to ameliorate the response times of the sensor and be able to quantify xanthine concentration.

With regard to the **second sphere (encapsulation and controlled release of bioactives)**:

(1) Two types of highly antioxidant phenolic compounds of very different hydrophobicity, namely **gallic acid (GA)** and **naringenin (NAR)** were succesfully encapsulated by blend electrospinning in ultrafine fibers made of two different edible biopolymers, namely **zein** (a hydrophobic protein extracted from corn maize) and **pullulan** (a water-soluble linear polysaccharide). Aditionally, the single-step electrospinning formation of **pullulan/β-CD** inclusion complex composites, was explored as an alternative for improving the naringenin low water-solubility. The nanoencapsulation systems proved to be stable for months and each one of these systems offered different release behaviours depending both on the cargo and on the carrier, meaning a broad range of potential applications. (**2)** Mesoporous silica particles were synthesized and used for entrapping naringenin, and a pH-responsive linear polyamine (N3) was anchored covalently to the pore outlets of the loaded silica particles. The resulting solids (MSP) were re-dispersed and successfully incorporated in electrospun pullulan producing nanofibrous NF-MSP composites. The release of the antioxidant from the NF-MSP composite material to the medium was pH-dependent, MSP-dependent and sustained for 3 – 5 hours. The incorporation of the material implied no delay in the release process with respect to the functionalized MSP. These systems can be claimed to be "self-dispersing"- pH controlled release devices in aqueous media. (**3)** A system that is produced by a single-step electrospinning process in which β-cyclodextrin crystals encapsulate aroma compounds (limonene and perillaldehyde are used as model volatile bioactives) as they are simultaneously fixed to the meshes of edible pullulan nanofibers. The retentive capacity of the edible nanofibrous system was found to be optimal and the system is

stable during months without significant loss when kept. in relatively dry conditions, even at high temperatures (up to 260 °C). The release of the volatile from the membranes is triggered by relative humidity changes, taking place at $a_w \geq 0.9$. This system can be potentially used in active packaging, in particular of fresh foods, for which the risk of microbial degradation increases at high a_w conditions, and therefore demand special protection

With regard to the **third sphere (beverage filtration)**:

(1) nylon-6 nanofibrous membranes display structural, mechanical and transport features ideal for filtering purposes. Electrospinning allows for easily adjusting relevant variables, such as membrane thickness, which in turn permits to modulate processing characteristics and filtrate quality. Membranes were successfully applied in apple juice filtration. NFM operating at a transmembrane pressure of 345 kPa, produced apple juice with optical characteristics similar to or better than commercial clarified juices. Their capacity to remove turbidity and color was superior compared to commercial polymeric membranes. Increasing pressure enhanced the NFM ability to reduce turbidity, whereas conventional polyamide membranes show the opposite behavior. **(2)** In apple juice clarification, nanofibrous membranes showed a higher adsorption capacity towards undissociated polyphenols rather than to lighter phenolics like caffeic acid, which results in the selective removal of bitter polyphenols at the pH of apple juice (3.5). The results demonstrate that NFM are promising materials for the industry of beverage processing. In particular, their application in apple juice filtration allows for obtaining a high quality product with no use of clarification aids or additional clarification steps, enabling the combination of the conventional sieving mechanisms, typical of microporous filters, with the ability of affinity membranes to remove specific compounds.

ACKNOWLEDGMENTS

The financial support of this PhD was provided by the Colombian government through the International PhD Training Program (*Generación del Bicentenario, Becas Francisco José de Caldas*) of the Administrative Department of Science, Technology and Innovation (*COLCIENCIAS*). Thanks to the University of Milan, to the DeFENS, to Fondazione Feltrinelli and EXPO Milan 2015, to the Filarete Foundation, to the National University of Colombia (in particular to ICTA), since all these institutions contributed also partially to the realization of this thesis work. To the University of Bolzano Bozen and the Universidad Politécnico de Valencia (Spain), institutions that received me and embraced me to carry out parts of my research. The completion of the PhD in any case was made possible by a never ending of relatives, friends, colleagues and tutors who lent me their hands, hugs, coffees, cigarettes, scientific advice, smiles, money, car-rides, bike-rides, phone-calls, cell-phones, lab-keys, reagents, solvents, facilities, food and hearts, whenever I needed.

Since I have just a couple of hours to upload the thesis, I just couldn't finish a proper thankfulness word for each one of you. But if you ever read this, please excuse me, and know that I thank you for opening the doors of your house, intelligence and kind to me. For free, for no reason at all.

Thank you God, mami, tía M, tía Ch, tía M2, Luisca, cugino Carlos, Carlos R. Thank you so much to the CANT group, thank you Tommy, Ale, Nabil, Harsha, Vale, Vero, Silvietta, Li Fei, Ilke, Marco M, Marthi, Loris, Davide, Manu, Jib, Loris, Silvia, Buddy, Solomon, Marghe. Thank you Stella, Matteo, Simo, Erika, Su, Prof. Mannino, Prof. Schiraldi, Profssa. Sorlini, Marco S, Prof. Piergiovanni, Davide (Filarete). Thank you, Gaetano, Valeria, Danny, Ilaria, Fra, Bimba, Big Andrew, Justine, Zoé, Mara, Mirco and all the kids that passed by our labs. Thanks to my family in Novara. Thank you Carlos Z, Pr. Consuelo, Pr. Judith F., Carito, Édgar, María, Mar, Cris, Yun, Loles Marcos, José Barat, Ramón Martínez Máñez, Félix S, Q-Yis, Rafa Gavara, Pilar H, Virgnia, Josep. Thanks to my *sensei*, Prof. Martha Quicazán for believing in me and guiding me. Thank you Sara. Thank you Pekso. Thank you, Renato.

I am sure that when I will read this list my heart will stop because I forget several names here, so again, please excuse me.

Finally thanks to all the scientists whose work I ever read (at least a paragraph) or whose work was read by the scientists whose work I read. Thanks to all the science community, for their work, for providing their sacrifice to us to be standing on the shoulders of giants.

APPENDIX 1: LIST OF PAPER, ORAL COMMUNICATIONS AND POSTERS

Peer-reviewed publications

1. Fuenmayor C.A. (2014). Nanotechnology and sustainability challenges of the agri-food system, a scientific review. Keywords on Lab Expo Milano 2015. Fondazione Feltrinelli (*Accepted for publication*).
2. Fuenmayor, C. A., Benedetti, S., Pellicanò, A., Cosio, M. S., & Mannino, S. (2014). direct in situ determination of ascorbic acid in fruits by screen-printed carbon electrodes modified with nylon-6 nanofibers. Electroanalysis, 26(4), 704-710.
3. Fuenmayor, C. A., Lemma, S. M., Mannino, S., Mimmo, T., & Scampicchio, M. (2014). Filtration of apple juice by nylon nanofibrous membranes. Journal of Food Engineering, 122, 110-116.
4. Acosta, C., Pérez-Esteve, E., Fuenmayor, C. A., Benedetti, S., Cosio, M. S., Soto, J. & Martínez-Máñez, R., 2014, Polymer composites containing gated mesoporous materials for on-command controlled release. ACS applied materials & interfaces, 6(9), 6453-6460.
5. Fuenmayor, C., Zuluaga, C., Díaz, C., Cosio, M., & Mannino, S. (2014). Evaluation of the physicochemical and functional properties of Colombian bee pollen. Rev. MVZ Córdoba, 19(1), 4003-4014.
6. Fuenmayor, C. A., Mascheroni, E., Cosio, M. S., Piergiovanni, L., Benedetti, S., Ortenzi, M., Schiraldi A. & Mannino, S. (2013). Encapsulation of R-(+)-Limonene in Edible Electrospun Nanofibers. Chemical Engineering Transactions, 32, 1771-1776.
7. Mascheroni, E., Fuenmayor, C. A., Cosio, M. S., Di Silvestro, G., Piergiovanni, L., Mannino, S., & Schiraldi, A. (2013). Encapsulation of volatiles in nanofibrous polysaccharide membranes for humidity-triggered release. Carbohydrate polymers, 98(1), 17-25.
8. Fuenmayor, C. A., Díaz-Moreno, A. C., Zuluaga-Domínguez, C. M., & Quicazán, M. C. (2013). Honey of Colombian stingless bees: Nutritional characteristics and physicochemical quality indicators. In Pot-Honey (pp. 383-394). Springer New York.
9. Zuluaga-Domínguez, C. M., Díaz-Moreno, A. C., Fuenmayor, C. A., & Quicazán, M. C. (2013). An Electronic Nose and Physicochemical Analysis to Differentiate Colombian Stingless Bee Pot-Honey. In Pot-Honey (pp. 417-427). Springer New York.
10. Fuenmayor, C. A., Díaz-Moreno, A. C., Zuluaga-Domínguez, C. M., & Quicazán, M. C. (2013). Miel de angelita: nutritional composition and physicochemical properties of *Tetragonisca angustula* honey. Interciencia, 37, 142-147

Posters and oral communications in scientific congresses

1. *Determinación directa de ácido ascórbico en frutas por medio de eléctrodos serigrafiados de carbono modificados con nanofibras de nylon*. **2014**. VII International Workshop on Sensors and Molecular Recognition. 3-4 July. Burjassot, Spain.(**Oral**)
2. *Composites de nanofibras biopoliméricas y partículas de sílica mesoporosa funcionalizadas para la encapsulación y liberación controlada de bioactivos*. **2014**. VII International Workshop on Sensors and Molecular Recognition. 3-4 July. Burjassot, Spain.(**Oral**)
3. *Bee-bread of Colombian stingless bees and Apis mellifera: nutritional characteristics and physicochemical quality indicators*. **2013**. XXXXIII International Apicultural Congress - Apimondia. 29 Sept – 4 Oct. Kiev, Ucrania. (**Oral**).
4. *Encapsulation of a volatile bioactive compound in edible nanofibers.* **2013**. International Conference on Chemical & Process Engineering. 2-5 Junio, Milan, Italy. (**Oral**).
5. *Nanotechnology for encapsulation and release of bioactive compounds*. **2013**. 2nd North and East European Congress on Food. 26-29 Mayo, Kiev, Ucrania. (**Oral**).

Appendix 1

6. *Nylon-6/pullulan/β-cyclodextrin composite nanofibrous membranes for encapsulation and release of bioactive volatile compounds*. 2013. Agorà – Incontro Nazionale sul Food Packaging. **2013**. 17-18 Oct, Monza, Italy. (**Poster-presented by co-author**)
7. *Electrospun nanofibrous membranes for filtration of selected beverage*s. **2012**. XVII Workshop on the Developments in the Italian PhD Research on Food Science, Technology and Biotechnology. 9-21 Sept, Cesena, Italy. (**Poster**)
8. *Solid state fermentation of bee-collected pollen induced by lactic acid starter cultures with probiotic bacteria*. **2012**. II International Symposium on Bee Products. 9-12 Sept, Braganza, Portugal. (**Oral**)
9. *Nanoemulsions for the determination of antioxidant capacity of oils by an electrochemical method"*. 14th International Conference on Electroanalysis. **2012**. 3-7 Jun, Portoroz, Slovenia. (**Poster**).
10. *Development of edible electrospun nanofibers for controlled release of aroma compounds.* **2012**. Congreso en Investigación en ciencia y tecnología de alimentos IICTA. 13-15 Jun, Bogotá, Colombia. (**Poster**)
11. *Sistemi biopolimerici attivi per l'industria alimentare*. **2012**. La ricerca italiana sugli imbalaggi attivi con particolari focus all'utilizzo dei nanomateriali. 9 May, Milán, Italia (**Oral-presented by co-author**).